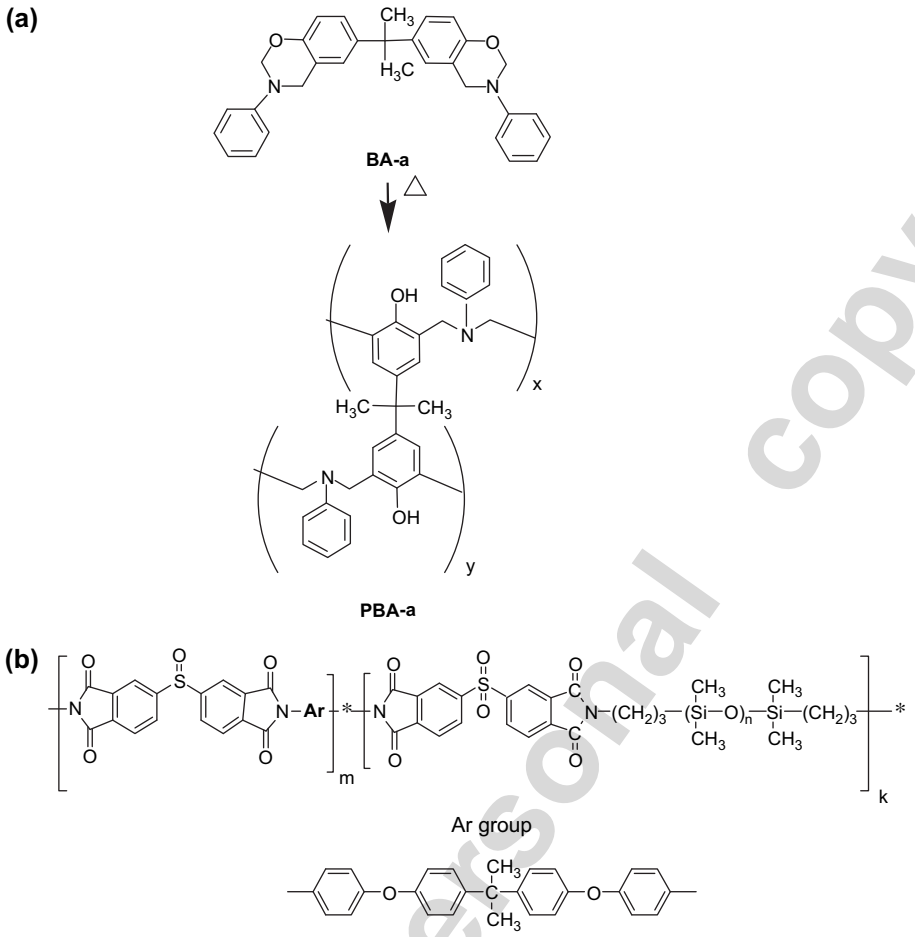

Fig. 1. (a) Benzoxazine monomer and polybenzoxazine; (b) polysiloxane-*block*-polyimide (SPI).

4. Measurements

4.1. Thermal analysis

Differential Scanning Calorimeter (DSC) of TA instruments (model DSC2910), calibrated with Indium standard, was used. A sample of about 10 mg was used for each test. In order to erase any thermal history, the samples were heated at 10 °C/min. Then, they were cooled to the ambient temperature, and scanned again using the same heating rate as before.

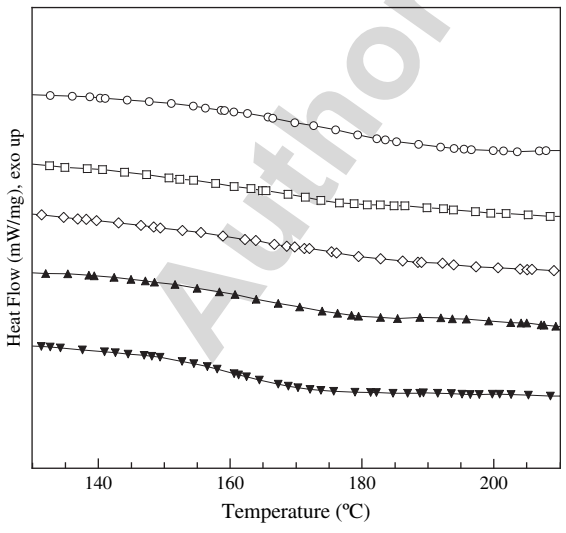

Fig. 2. DSC thermograms of PBA-a, SPI and their blends at various SPI contents: (○) SPI, (□) 75 wt%, (◇) 50 wt%, (▲) 25 wt%, and (▼) PBA-a.

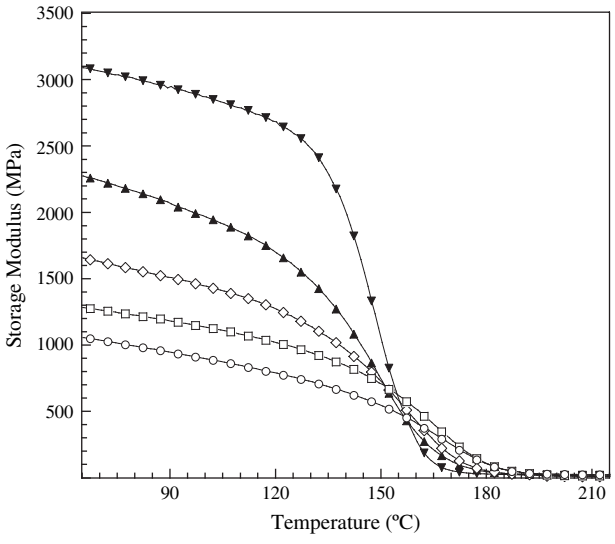

Fig. 3. Storage moduli of PBA-a, SPI and their blends at various SPI contents: (○) SPI, (□) 75 wt%, (◇) 50 wt%, (▲) 25 wt%, and (▼) PBA-a.

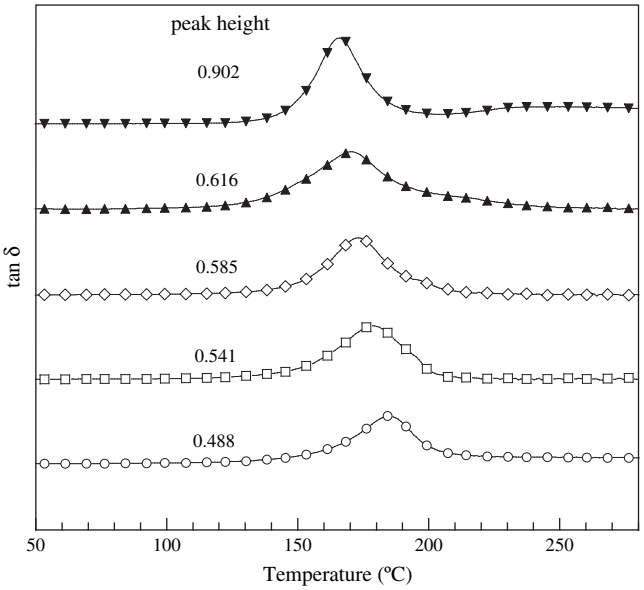

Fig. 4. Loss tangent of PBA-a, SPI and their blends at various SPI contents: (○) SPI, (□) 75 wt%, (◇) 50 wt%, (▲) 25 wt%, and (▼) PBA-a.

The glass-transition temperatures (T_g) of the blends were measured.

Dynamic mechanical properties of the blends were tested using the NETZSCH Model DMA242. The experiment is done in a tension mode using the dimension of the specimens of approximately 23.7 mm (length) × 5 mm (width) × 0.5 mm (thickness). The applied strain amplitude was 0.3% at the deformation frequency of 1 Hz. The specimens were heated using a temperature ramp rate of 3 °C/min from 40 to 250 °C.

4.2. Thermal gravimetric analysis (TGA)

The decomposition temperature (T_d) and char yield of the blends were studied using TGA Instruments (model TGA/SDTA 851ᵉ). The experiments were performed using a heating rate of 20 °C/min from 40 to 1000 °C under nitrogen atmosphere. The flow of purging nitrogen was kept at 80 ml/min. The sample mass was approximately 20 mg.

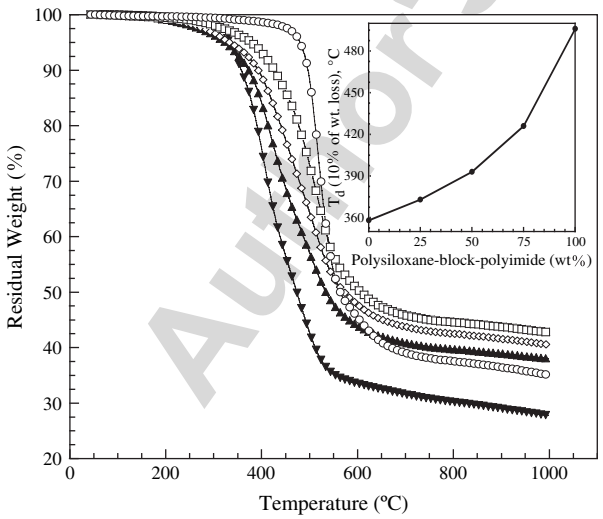

Fig. 5. Thermogravimetric curves of PBA-a, SPI and their blends at various SPI contents: (○) SPI, (□) 75 wt%, (◇) 50 wt%, (▲) 25 wt%, and (▼) PBA-a. Inset: decomposition temperatures (T_d at 10% weight loss) at various SPI contents.

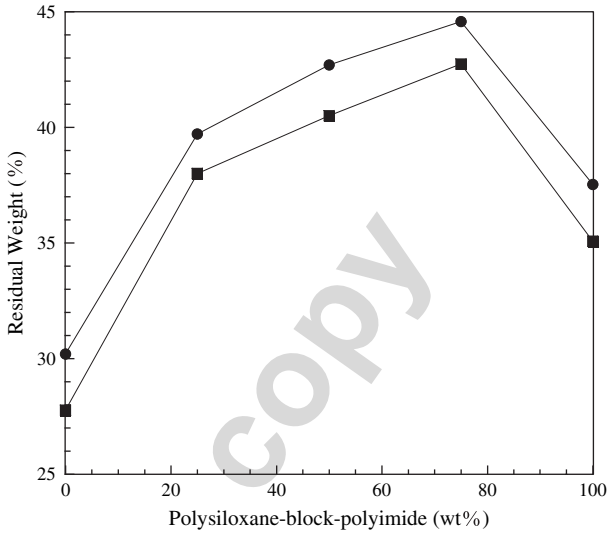

Fig. 6. Char yield of PBA-a, SPI and their blends at various temperatures: (●) 1000 °C, (■) 800 °C.

Kinetics analysis via Kissinger method, Flynn–Wall–Ozawa method, and Coats–Redfern method was carried out at various heating rates, i.e. 5, 10, 20, and 25 °C/min.

5. Results and discussion

5.1. Effect of SPI content on glass-transition temperature

Fig. 2 shows the DSC thermograms depicting the glass-transition temperature (T_g) of PBA-a, SPI, and their blends. At heating rate of 10 °C/min, the T_g of the neat polybenzoxazine (PBA-a) was determined to be 160 °C. The T_gs of all blends were slightly higher than that of neat PBA-a ranging from 163 to 169 °C, while the T_g of the SPI was 173 °C. It is found that SPI was able to elevate the T_gs of the blends. In these systems, there was only one broad T_g in all blend compositions. However, the systems exhibit partial miscibility [26] as evidenced by a transformation of transparent PBA-a and SPI to opaque appearance with orange color of the blends.

Storage moduli of the PBA-a, SPI, and their blends in the temperature range of 40–220 °C are illustrated in Fig. 3. The thermograms revealed the glassy state moduli, reported at 40 °C of PBA-a to be approximately 3.1 GPa and that of SPI to be around 1.1 GPa. Therefore, the SPI is much less stiff than PBA-a due to the presence soft silicone segments in its molecular structure. The stability of the polymer can be seen from the slope of the glassy state moduli in the DMA thermograms. The lower the slope of the glassy state modulus, the greater is the thermal stability of the polymer. As a result, DMA thermograms suggested that SPI was more thermally stable than PBA-a. The presence of the SPI fraction thus helps improving thermal stability of the resulting blends.

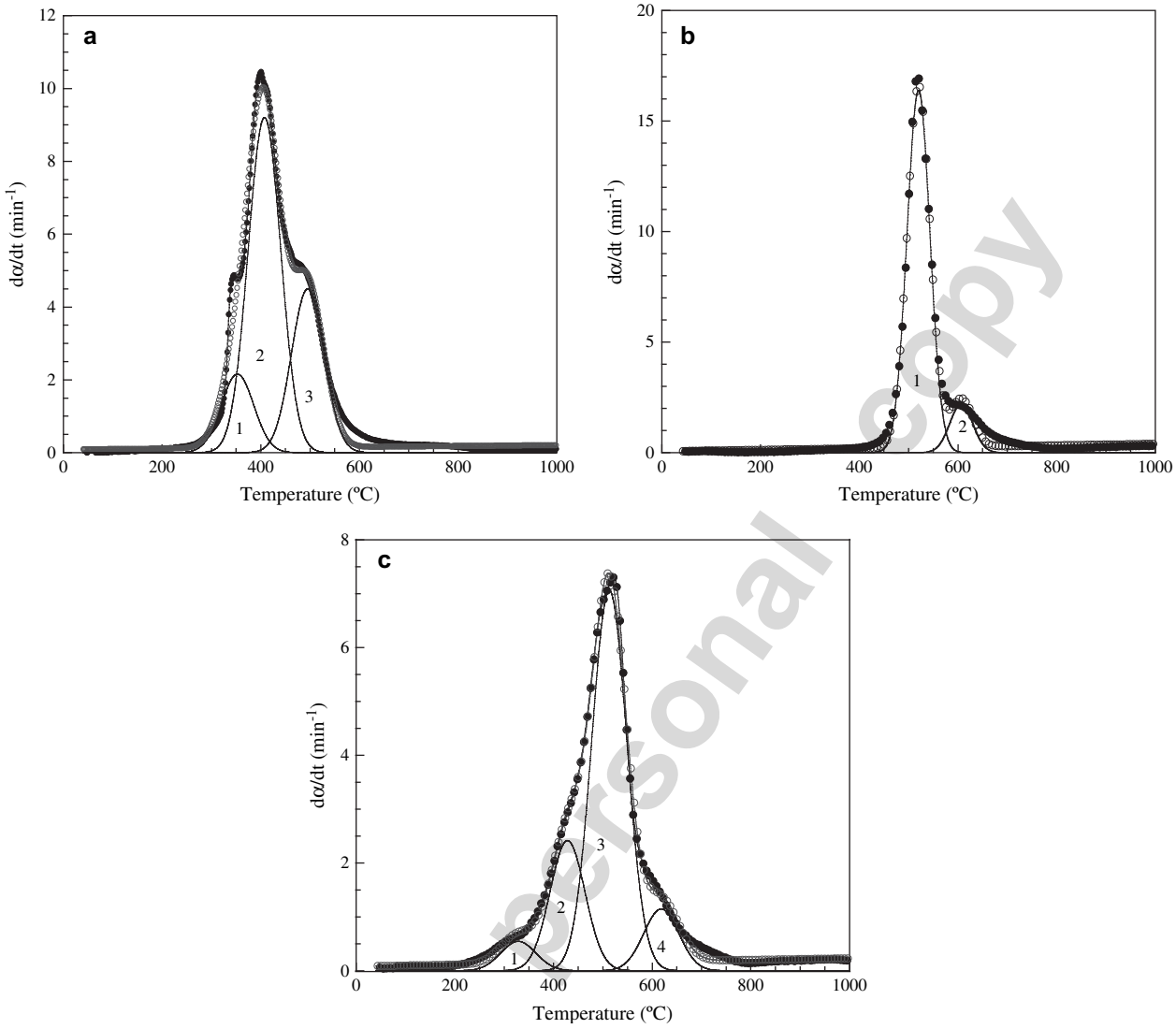

Fig. 7. DTG curve and individual contributions of (a) PBA-a (20 °C/min), $R^2 = 0.9918$; (b) SPI (20 °C/min), $R^2 = 0.9958$; (c) blends with 75 wt% of SPI (20 °C/min), $R^2 = 0.9968$; (●) experimental data, (○) simulated curve.

In addition, the tan δ of the polyimides and their blends is depicted in Fig. 4. Generally, the magnitude of tan δ peaks reflects the large scale mobility associated with α relaxation process, whereas the width of the tan δ relates to the homogeneity of the materials. The peak at lower temperature of 166 °C could be attributed to that of PBA-a and the peak at higher temperature of 184 °C was attributed to that of SPI. It can be noticed that only one single and broad peak was observed in all blend systems. Furthermore, the peaks of the blends were found to shift to higher temperature with increasing SPI content, which corresponds to the DSC results.

5.2. Thermogravimetric analysis of the blends and degradation kinetics

TGA thermograms of PBA-a, SPI, and their blends at various weight ratios of SPI are presented in Fig. 5. From the figure, it can be observed that the addition of SPI was able to enhance the decomposition temperature of the PBA-a. The inset of Fig. 5 explains the relationship between the decomposition temperatures at 10% weight loss and the SPI content in the blends. It clearly shows that the decomposition temperatures of the blends increase from about 360 °C (for 0 wt% of SPI) to about 500 °C (for 100 wt% of SPI) with the increase of the SPI fraction.

Interestingly, the char yields of the blended systems exhibited the synergistic behavior as shown in Fig. 6. The char yields of the blends were higher than those of neat PBA-a and SPI. The highest char value at 800 °C of about 45% was found at 75 wt% of the SPI fraction, while the value of pure PBA-a was only 30%. Theoretically, the possible reason for synergism in the char formation is due to a large amount of aromatic ring in the blends with some additional chemical bonding between the PBA-a and the SPI. This synergy in the char formation was also observed in the systems of polybenzoxazine alloyed with other types of polyimides [27].

From these results, we selected the blend at 75 wt% of SPI for further kinetic studies of the blending systems since it

Table 2
Initial temperature, final temperature, and peak temperature of small curves for polybenzoxazine, SPI and their blends at 20 °C/min in N_2 atmosphere

Polysiloxane-*block*-polyimide (wt% in PBA-a)										
		0			25	50	75			100
Stage 1	T_i	280	Stage 1	T_i	213	198	227	Stage 1	T_i	422
	T_{peak}	353		T_{peak}	323	313	328		T_{peak}	521
	T_f	426		T_f	432	427	429		T_f	618
	% Area	14		% Area	9	8	5		% Area	88
Stage 2	T_i	316	Stage 2	T_i	292	294	310	Stage 2	T_i	521
	T_{peak}	408		T_{peak}	420	429	428		T_{peak}	607
	T_f	499		T_f	548	563	546		T_f	694
	% Area	58		% Area	51	40	22		% Area	12
Stage 3	T_i	413	Stage 3	T_i	386	375	384	R^2		0.9958
	T_{peak}	496		T_{peak}	509	511	513			
	T_f	577		T_f	634	645	642			
	% Area	28		% Area	34	44	63			
R^2		0.9918	Stage 4	T_i	504	501	508			
				T_{peak}	609	616	618			
				T_f	714	730	728			
				% Area	6	8	10			
			R^2		0.9976	0.9974	0.9968			

Note: T_i = initial temperature and T_f = final temperature.

provides maximum char yield. After obtaining the TGA and DTG curves, we used Peakfit program to separate the DTG curves of the blends at 0 wt%, 75 wt%, and 100 wt%. After resolving the curves by using the computer software, it can be noticed that the DTG curve of the PBA-a, presented in Fig. 7a, composes of a three-stage weight-loss process. This result is in good agreement with the study of Hemvichian et al., which reports that this degradation process was observed with the middle peak having the highest maximum rate of weight loss. In addition, the degradation products were identified into eight categories as follows: benzene derivatives, amines, phenolic compounds, 2,3-benzofuran derivatives, iso-quinoline derivatives, biphenyl compounds, Mannich base compounds, and phenanthridine derivatives [3]. Moreover for the pure SPI, the DTG curve can also be resolved into two main loss processes as shown in Fig. 7b. These results correspond to the degradation study in the system of siloxane-containing polyimide with the molecular weight of 1300 [28], which reported at least two overlapping stages. Moreover, our results also reveal the same phenomenon as found in the similar system of polydimethylsiloxane (PDMS). It is well known that the thermal degradation of PDMS in nitrogen atmosphere results in depolymerization over the range of 400–650 °C to produce cyclic oligomers [29,30]. In the degradation of PDMS, the most abundant product is reported to be the trimer of hexamethylcyclotrisiloxane with decreasing amounts of tetramer, and higher oligomers [29]. For the blend system with 75 wt% of SPI as shown in Fig. 7c, the DTG can be resolved into four curves, which represent the four main stages of degradation in the blend. The determination of the areas under the resolved peaks (% area) and the peak positions (T_{peak}) was useful to make us understand more about the degradation process of the blend system. All these data including initial decomposition temperatures (T_i) and final decomposition temperatures (T_f) of pure PBA-a, SPI, and their blends are exhibited in Table 2. In comparison of peak positions, it can be observed that the T_{peak}s of stage 1 and stage 2 in the blends for all SPI compositions are similar to that of stage 1 in pure PBA-a, while the T_{peak}s of stage 4 in the blends for are close to that of stage 2 in pure SPI. Additionally, the T_{peak}s of stage 3 in the blends are the values between the T_{peak} of stage 3 in pure PBA-a and that of stage 1 in pure SPI. In the determination of the areas

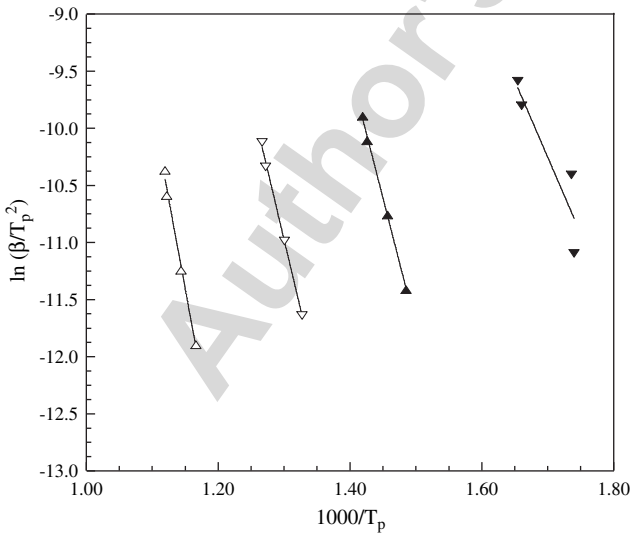

Fig. 8. Plots of ln β/T_p^2 versus $1000/T_p$ at different heating rates according to Kissinger method for the blends (75 wt% of SPI): (▼) peak 1, (▲) peak 2, (□) peak 3, (△) peak 4.

Table 3
Activation energies obtained by using Kissinger method for the blend (75 wt% of SPI)

Peak 1		Peak 2		Peak 3		Peak 4	
E_a (kJ/mol)	R^{2a}	E_a (kJ/mol)	R^{2a}	E_a (kJ/mol)	R^{2a}	E_a (kJ/mol)	R^{2a}
111	0.9204	187	0.9983	202	0.9972	260	0.9919

[a] Correlation coefficient.

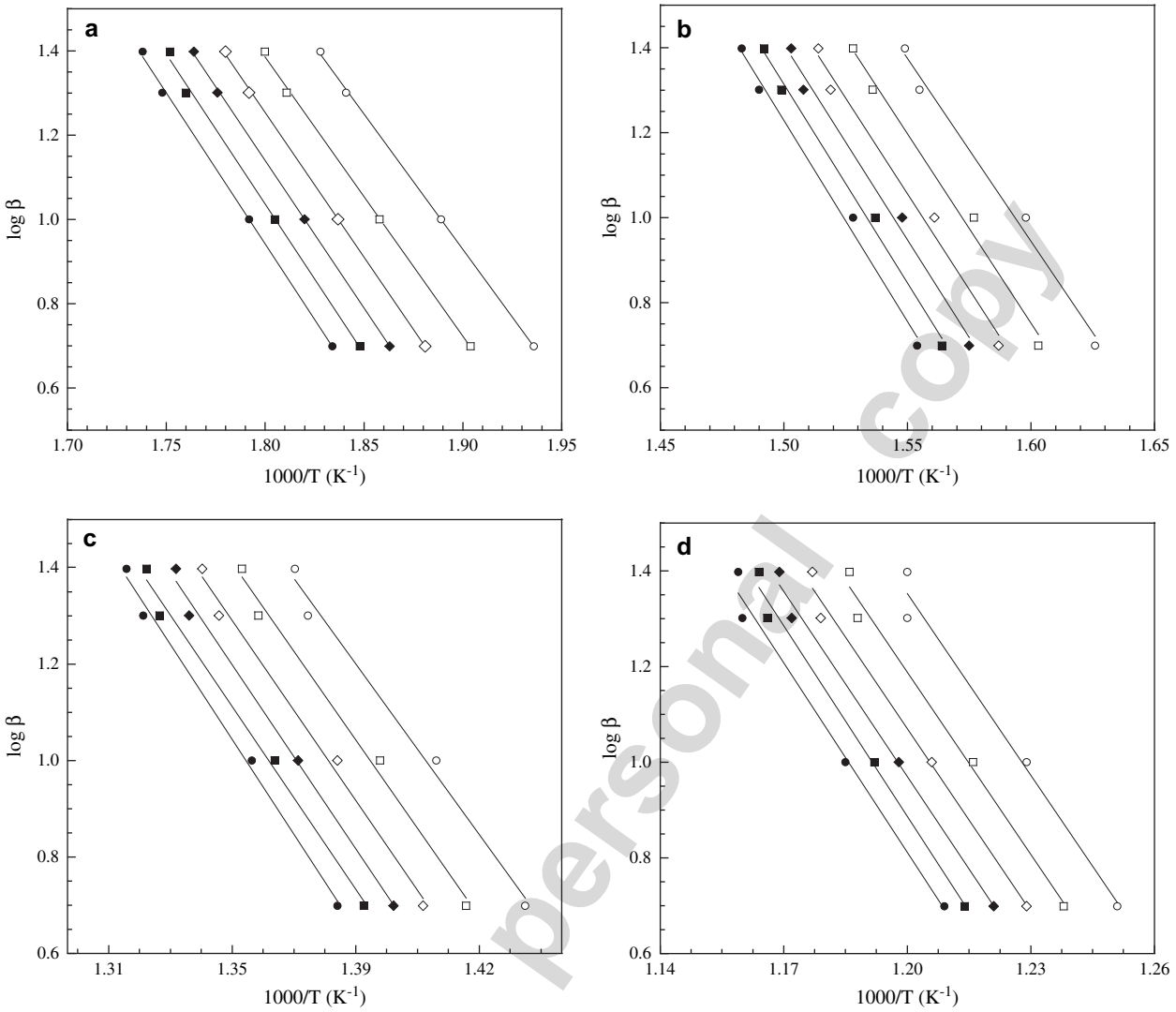

Fig. 9. Plots of log β versus 1000/T according to Flynn–Wall–Ozawa method for the blend (75 wt% of SPI) with weight loss from 5% to 20% conversion for (a) peak 1; (b) peak 2; (c) peak 3; (d) peak 4: (○) 5%, (□) 8%, (◇) 11%, (◆) 14%, (■) 17%, and (●) 20%.

under the resolved curves, the values of all degradation stages of the blends are related to the contents of PBA-a and SPI. It can be seen that the addition of SPI led to the decrease of the % area values in stages 1 and 2 and the increase of the values in stages 3 and 4. These results confirm that that stages 1 and 2 of the degradation in the blends are mainly from the degradation of PBA-a, while stage 4 of the degradation in the blends is from the degradation of SPI. For the stage 3 of degradation, it is proposed to be the degradation of some additional chemical bonding between the PBA-a and the SPI.

After the four overlapped curves were resolved, the conversions were calculated from the areas under the curves by using Simpson's 3/8 rule. Then, the E_a of each one was obtained via three mentioned methods.

5.3. Calculation of the thermal degradation kinetics parameters

The E_a of the thermal degradation process of this blend was determined using three well-known methods for dynamic heating experiment i.e., the Kissinger method, Flynn–Wall–Ozawa method, and Coats–Redfern method.

By using Kissinger method, the E_a can be calculated from the slope of the plot of $\ln(\beta/T_p^2)$ versus $1000/T_p$ (T_p is the temperature at the maximum weight-loss rate) as presented in Fig. 8. The calculated values are shown in Table 3. The obtained E_a values of stages 1, 2, 3, and 4 are 111, 187, 202, 260 kJ/mol, respectively. From the literature [12,31], the Kissinger's method was reported to provide highly reliable values of E_a with an error of less than 5% independent of reaction mechanism, provided that $E/RT > 10$.

The E_a of the blends can also be determined using the method of Flynn–Wall–Ozawa from a linear fitting of ln β versus 1000/T at different conversions (Fig. 9a–d). Owing to the fact that this equation was derived using the Doyle approximation only conversion values in the low range can be used. In this study, the conversion values of 5%, 8%, 11%, 14%, 17%, and 20% were used. Fig. 9a–d shows that the fitting straight lines are nearly parallel. Using Flynn–Wall–Ozawa method, the E_a values corresponding to the different conversions are listed in Table 4. The

Table 4
Activation energies obtained by using Flynn–Wall–Ozawa method for the blend (75 wt% of SPI)

Conversion (%)	E_a (kJ/mol)	R^{2a}	E_a (kJ/mol)	R^{2a}
	Peak 1		Peak 2	
5	117	0.9996	157	0.9895
8	120	0.9992	161	0.9905
11	125	0.9996	164	0.9882
14	127	0.9996	168	0.9917
17	130	0.9970	170	0.9935
20	130	0.9985	173	0.9933
Average	125		166	
	Peak 3		Peak 4	
5	172	0.9900	231	0.9856
8	178	0.9940	231	0.9904
11	181	0.9928	233	0.9912
14	186	0.9954	236	0.9943
17	184	0.9925	239	0.9909
20	190	0.9946	241	0.9898
Average	182		235	

[a] Correlation coefficient.

calculated E_a from this method are 125, 166, 182, and 235 kJ/mol for peaks 1, 2, 3, and 4, respectively.

The method by Coats–Redfern is one of the most widely used procedure for the determination of the reaction processes [10,19,21]. From Eq. (9), proposed by Coats and Redfern, the E_a for all $g(\alpha)$ functions listed in Table 1 can be obtained at constant heating rate. In this study, the same conversion values have been used as those used in the Flynn–Wall–Ozawa methods. Table 5 shows E_a, A, and correlations for conversions in the range 5–20% at constant heating rate of 20 °C/min. It was found that the solid state thermal degradation mechanism of the blends with 75 wt% of SPI is likely to be of F1 type, because this mechanism presents the E_a that is similar to the value obtained by isoconvensional methods. Furthermore in comparison with other mechanisms, this mechanism renders the lowest E_a to start the degradation stage [32]. The type of degradation mechanism is confirmed by Criado method in the next determination.

As presented in Table 6, Coats–Redfern method was applied at the heating rate of 25, 20, 10, and 5 °C/min to determine the average values of the E_a, A, and the degradation mechanism. The E_a calculated by Coats–Redfern method are 116, 174, 223, and 281 kJ/mol. It is clearly shown that the E_a of each degradation stage increases with the increase of the heating rates. In addition, the results suggest F1 type of solid state thermal degradation mechanism for all four stages and all heating rates. The possible reason that the increase of the amount of SPI led to the increase of area under the curve of stage 3 of the blends is that stage 3 correlates with SPI structure. The E_a of this peak was around 218 kJ/mol, which was lower than the bond dissociation energy of Si–C bond (360 kJ/mol), the weakest bond of the base polymers [33]. Hence, the decomposition of the blends could be governed mainly by the molecular structure and kinetic consideration and not by bond energies for stage 3.

By using Coats–Redfern method, the calculated E_a at 20 °C of PBA-a for stages 1, 2, and 3 are 172, 209, and

Table 5
Activation energies obtained by using Coats–Redfern method for several solid state processes at a heating rate of 20 °C/min for the blend (75 wt% of SPI)

Type	E_a (kJ/mol)	ln A (min^{-1})	R^2	Type	E_a (kJ/mol)	ln A (min^{-1})	R^2
Peak 1				Peak 2			
A2	57	10.46	0.9976	A2	82	13.07	0.9976
A3	35	5.55	0.9971	A3	51	7.31	0.9972
A4	24	2.95	0.9965	A4	35	4.30	0.9967
R1	116	22.76	0.9971	R1	164	27.67	0.9971
R2	120	22.93	0.9976	R2	169	27.97	0.9975
R3	121	22.82	0.9977	R3	171	27.90	0.9976
D1	247	48.78	0.9974	D1	339	58.15	0.9973
D2	247	48.78	0.9976	D2	346	58.75	0.9975
D3	252	48.43	0.9979	D3	353	58.58	0.9978
D4	249	47.66	0.9977	D4	348	57.69	0.9976
F1	124	24.50	0.9980	F1	174	29.68	0.9979
F2	6	−1.64	0.8542	F2	10	−0.88	0.9040
F3	21	3.05	0.9470	F3	31	4.23	0.9561
Peak 3				Peak 4			
A2	105	15.23	0.9975	A2	139	34.94	0.9976
A3	66	8.76	0.9972	A3	88	34.48	0.9973
A4	47	5.41	0.9968	A4	63	34.14	0.9969
R1	210	31.70	0.9970	R1	275	35.62	0.9969
R2	217	32.14	0.9975	R2	284	35.65	0.9974
R3	219	32.11	0.9976	R3	287	35.66	0.9975
D1	432	66.21	0.9972	D1	565	36.34	0.9971
D2	441	66.99	0.9975	D2	576	36.36	0.9974
D3	450	66.99	0.9770	D3	588	36.38	0.9977
D4	444	65.99	0.9976	D4	580	36.36	0.9975
F1	223	33.98	0.9978	F1	293	35.68	0.9978
F2	15	−0.20	0.9245	F2	22	33.08	0.9347
F3	42	5.38	0.9603	F3	57	34.05	0.9613

Table 6
Average activation energies obtained by using Coats–Redfern method at 25, 20, 10, 5 °C/min for the blend (75 wt% of SPI)

Heating rate (°C/min)	E_a (kJ/mol)	ln A (min^{-1})	Possible mechanism
Peak 1			
5	113	23.35	F1
10	108	22.21	F1
20	124	24.50	F1
25	119	23.87	F1
Average	116		
Peak 2			
5	161	28.51	F1
10	168	29.10	F1
20	174	29.68	F1
25	175	28.51	F1
Average	170		
Peak 3			
5	206	32.66	F1
10	217	34.14	F1
20	223	33.98	F1
25	252	39.25	F1
Average	225		
Peak 4			
5	287	39.73	F1
10	272	37.24	F1
20	293	35.68	F1
25	270	36.12	F1
Average	281		

263 kJ/mol, respectively (Table 7). The solid state thermal degradation mechanism of PBA-a is proposed to be of F1 type. The PBA-a thermal degradation of this study is in agreement with the results in the literature [34], which reveals the phenolic cleavage at the maximum derivative of peak temperature at around 400 °C.

With the Coats–Redfern method, the calculated E_a at 20 °C of neat SPI for peaks 1 and 2 are 369 and 460 kJ/mol, respectively (Table 8). These calculation results coincide with the bonding energy of Si–C (360 kJ/mol) [33], the weakest bond in PDMS, and that of Si–O (454 kJ/mol) [35]. Hence, the degradation of SPI could possibly be governed mainly by the breaking of Si–C bond and Si–O bond.

Table 8
Activation energies obtained by using Coats–Redfern method for several solid state processes at a heating rate of 20 °C/min of BSF30

Type	Peak 1			Peak 2		
	E_a (kJ/mol)	ln A (min^{-1})	R^2	E_a (kJ/mol)	ln A (min^{-1})	R^2
A2	178	26.64	0.9959	223	30.14	0.9957
A3	115	16.55	0.9956	144	18.89	0.9955
A4	83	11.40	0.9952	104	13.16	0.9951
R1	348	52.80	0.9953	434	59.44	0.9952
R2	358	53.85	0.9958	447	60.66	0.9956
R3	362	54.04	0.9959	452	60.90	0.9958
D1	708	107.96	0.9954	882	121.23	0.9953
D2	722	109.54	0.9958	899	123.04	0.9956
D3	737	110.39	0.9961	917	124.10	0.9959
D4	727	108.82	0.9952	905	122.38	0.9957
F1	369	56.33	0.9962	460	63.30	0.9960
F2	31	3.03	0.9502	40	3.73	0.9569
F3	76	10.99	0.9648	94	12.33	0.9684

From the calculation in the system of SPI, the solid state thermal degradation mechanism is proposed to be of F1 type. In this study, the degradation phenomenon of SPI coincides with that of the literature [35], which reported that the thermal degradation of PDMS in inert atmosphere results in degradation over the range of 400–650 °C.

In comparison of PBA-a, SPI and the blend with 75 wt% of SPI, the E_a of the blend was found to be lower than those of both pure components. This phenomenon corresponds to the research of Nandan et al. [36], who studied the blending system of poly(ether ether ketone)/poly(aryl ether sulphone). They reported that the E_a of the blends were lower than that of the pure components because of different factors that concurrently effect the process of degradation. Firstly, interactions are possible among the different components in the blend during degradation and among the products of degradation. These chemical reactions can lead to an acceleration of the degradation rate with respect to that of pure components. These reactions can be grouped into following processes [37,38].

- Reactions between macromolecules and small molecules,
- reactions between macromolcules and small radicals,

Table 7
Activation energies obtained by using Coats–Redfern method for several solid state processes at a heating rate of 20 °C/min of BA-a

Type	Peak 1			Peak 2			Peak 3		
	E_a (kJ/mol)	ln A (min^{-1})	R^2	E_a (kJ/mol)	ln A (min^{-1})	R^2	E_a (kJ/mol)	ln A (min^{-1})	R^2
A2	81	14.82	0.9969	99	16.67	0.9969	126	19.13	0.9970
A3	51	8.55	0.9964	62	9.80	0.9965	80	11.45	0.9966
A4	36	5.29	0.9959	44	6.24	0.9960	57	7.49	0.9962
R1	162	30.76	0.9964	196	34.27	0.9964	248	38.89	0.9963
R2	167	31.16	0.9969	202	34.76	0.9968	256	39.52	0.9968
R3	169	31.12	0.9970	204	34.75	0.9970	258	39.56	0.9970
D1	333	64.13	0.9966	403	71.15	0.9966	508	80.38	0.9965
D2	340	64.86	0.9969	411	71.99	0.9969	518	81.41	0.9968
D3	347	64.82	0.9972	420	72.07	0.9971	529	81.68	0.9971
D4	342	63.84	0.9970	414	71.01	0.9970	522	80.50	0.9969
F1	172	32.97	0.9972	209	36.66	0.9972	263	41.56	0.9972
F2	11	−0.17	0.9191	14	0.24	0.9283	19	0.91	0.9348
F3	32	5.28	0.9587	39	6.00	0.9606	51	7.22	0.9606

– reactions between macroradicals and small molecules,
– reactions between two small molecules,
– reaction between two macroradicals,
– reaction between macromolecules and macroradicals.

In addition, reactions with small molecules or small radicals can give rise to faster breakage of the macromolecules and to chemical structures that act as stabilizer groups.

These above reasons can explain the phenomenon that the E_a of the blends in many systems [38–40] are not close to the predicted values on the basis of linear additive behaviour, using following equation,

$$E_a = E_{a1}w_1 + E_{a2}w_2 \quad (15)$$

where E_{a1} and E_{a2} are activation energies of the homopolymers, and w_1 and w_2 are the weight fraction of components 1 and 2, respectively [36].

5.4. Determination of the reaction mechanism using Criado method

The $Z(\alpha)-\alpha$ master curves can be plotted using Eq. (13) according to different reaction mechanisms shown in Table 1. The experimental data at 20 °C/min obtained by Flynn–Wall–Ozawa method (Table 4) were substituted into Eq. (14). Fig. 10a–d shows the $Z(\alpha)-\alpha$ master and experimental curve of the blend with 75 wt% of PSI. The results show that the experimental curves of all four steps of degradation belong to F1 reaction mechanism (random nucleation having one nucleus on individual particle) with rate-controlling step of the nucleation process. Figs. 11a–c and 12a,b exhibit the comparison of the experimental curves of pure PBA-a and PSI, respectively. It can be observed that the degradation of pure PBA-a and PSI was proved to obey the F1 mechanism. That means random nucleation with one nucleus on the individual particle. The degradation

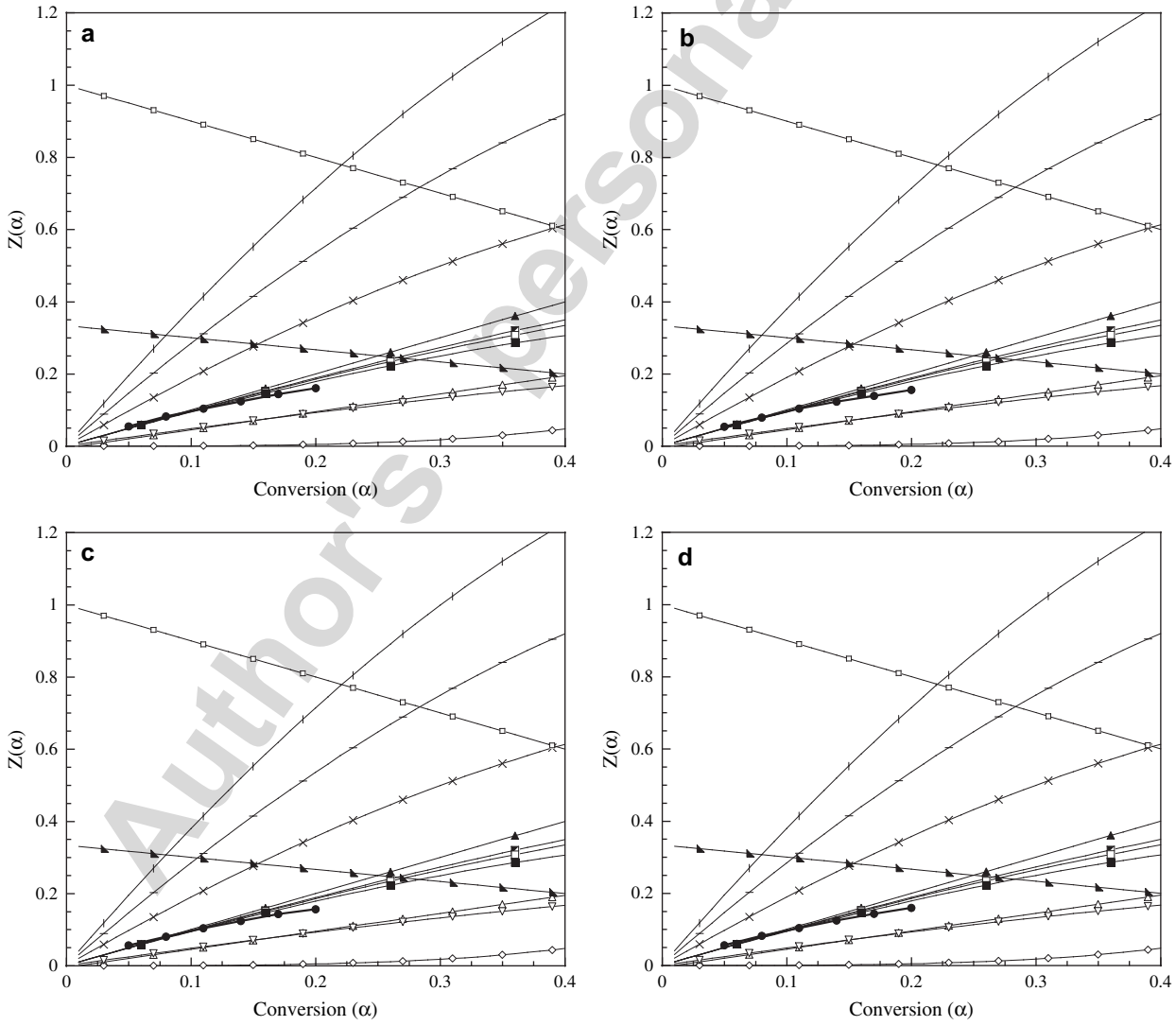

Fig. 10. Plots of $Z(\alpha)$ versus α of the blend (75 wt% of SPI) compared between experimental curve and master curve at different mechanisms for (a) peak 1; (b) peak 2; (c) peak 3; (d) peak 4: (×) A2, (|) A3, (–) A4, (▲) R1, (◩) R2, (□) R3, (△) D1, (◇) D2, (▽) D3, (◆) D4, (■) F1, (▫) F2, (◣) F3, (●) experimental data.

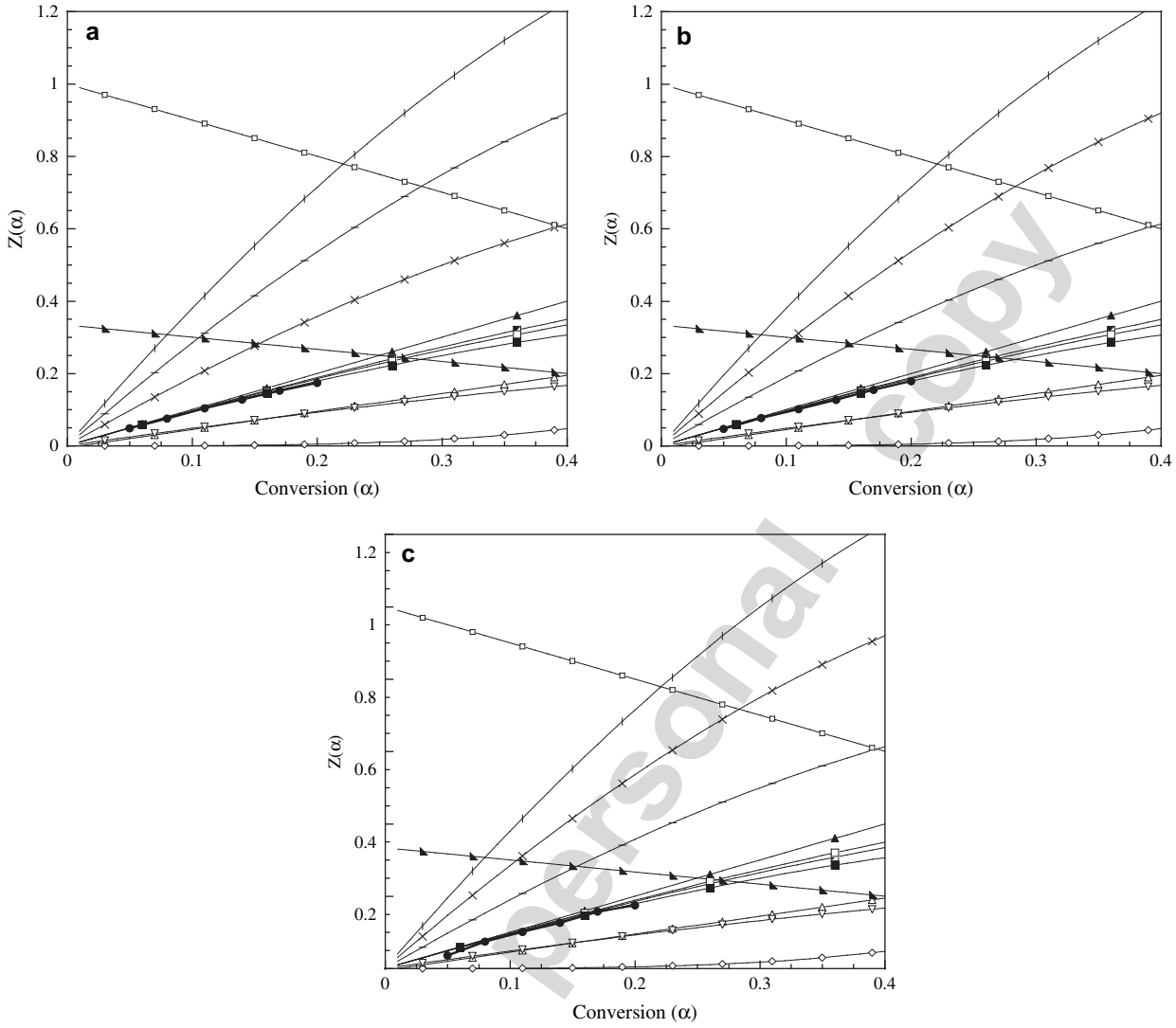

Fig. 11. Plots of $Z(\alpha)$ versus α of PBA-a compared between experimental curve and master curve at different mechanisms for (a) peak 1; (b) peak 2; (c) peak 3; (d) peak 4: (×) A2, (|) A3, (−) A4, (▲) R1, (◩) R2, (□) R3, (△) D1, (◇) D2, (▽) D3, (◆) D4, (■) F1, (▫) F2, (◣) F3, (●) experimental data.

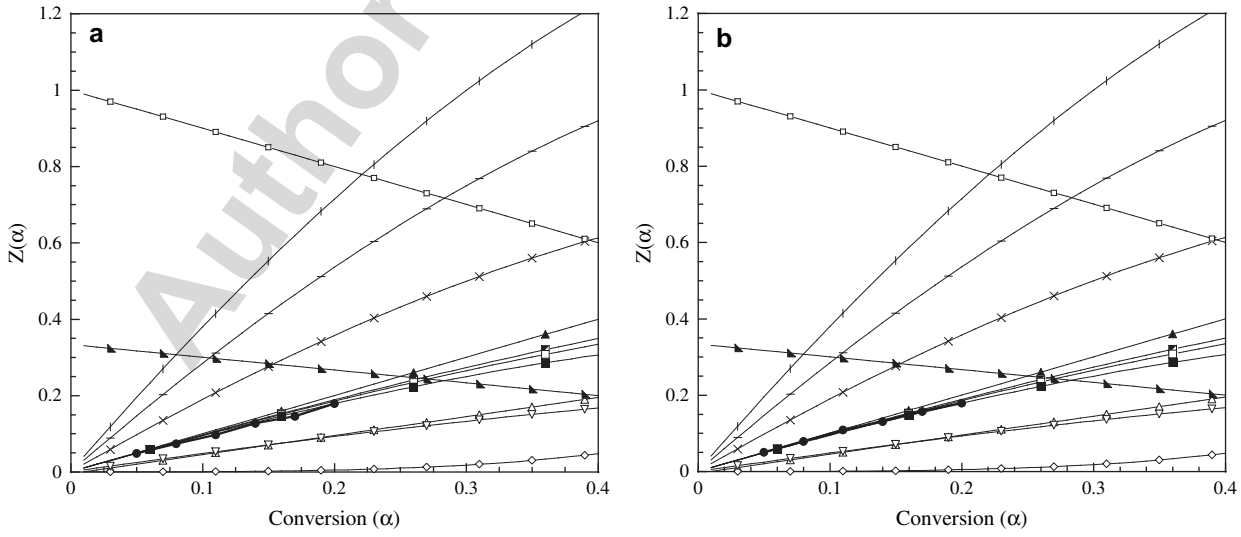

Fig. 12. Plots of $Z(\alpha)$ versus α of BSF30 compared between experimental curve and master curve at different mechanisms for (a) peak 1; (b) peak 2: (×) A2, (|) A3, (−) A4, (▲) R1, (◩) R2, (□) R3, (△) D1, (◇) D2, (▽) D3, (◆) D4, (■) F1, (▫) F2, (◣) F3, (●) experimental data.

was initiated from one random point acting as growth center, which follows unimolecular decay law with first order reaction [41,42].

6. Conclusions

In the blending systems of BA-a monomer and SPI, synergistic behavior of char yield was observed. The possible reason for the increase of char yield is that there was higher cross-link density in the blend than both neat polybenzoxazine and SPI. PBA-a and SPI showed three-stage weight-loss process and two-stage weight-loss process, respectively. The degradation of the blends between benzoxazine monomer and SPI was found to be a complex process composed of at least four overlapping stages, of which the E_a can be calculated. The study of separated curves from Criado method indicates that PBA-a, SPI and their blending systems follow F1 thermal degradation mechanism in the conversion range considered.

Acknowledgements

The authors would like to thank the Thailand Research Fund (TRF) and the Commission on Higher Education for the financial support through the Research Grant for Mid-Career University Faculty of fiscal year 2005–2007. The present research receives partial financial support from the Foundation for the International Exchange of the Faculty of Engineering, Tokyo Institute of Technology. In addition, CU Graduate Thesis Grant of Chulalongkorn University is also acknowledged. Additionally, the authors would like to thank Mettler-Toledo (Thailand) Co., Ltd. for the kind support in the use of thermogravimetric analysis.

References

[1] Ishida H. US Patent 5,543,516; 1996.
[2] Nair CPR. Advances in addition-cure phenolic resins. Prog Polym Sci 2004;29:401−98.
[3] Hemvichian K, Ishida H. Thermal decomposition process in aromatic amine-based polybenzoxazine investigated by TGA and GC−MS. Polymer 2002;43:4391−402.
[4] Takeichi T, Agag T, Zeidam R. Preparation and properties of polybenzoxazine/poly(imide siloxane) alloys: in situ ring-opening polymerization of benzoxazine in the presence of soluble poly(imide-siloxane)s. J Polym Sci Part A Polym Chem 2001;39:2633−41.
[5] Agag T, Takeichi T. Polybenzoxazine−montmorillonite hybrid nanocomposites: synthesis and characterization. Polymer 2000;41:7083−90.
[6] Agag T, Takeichi T. Synthesis and properties of silica-modified polybenzoxazine. Mater Sci Forum 2004;449−452:1157−60.
[7] Furukawa N, Yamada Y, Kimura Y. Preparation and stress relaxation properties of thermoplastic polysiloxane-*block*-polyimides. High Perform Polym 1996;8:617−30.
[8] Yamada Y. Siloxane modified polyimides for microelectronics coating applications. High Perform Polym 1998;10:69−80.
[9] Furukawa N, Yuasa M, Kimura Y. Structure analysis of a soluble polysiloxane-*block*-polyimide and kinetic analysis of the solution imidization of the relavant polyamic acid. J Polym Sci Part A Polym Chem 1998;36:2237−45.
[10] Coats AW, Redfern JP. Kinetic parameters from thermogravimetric data. Nature 1964;201:68−9.
[11] Nam JD, Seferis JC. A composition methodology for multistage degradation of polymers. J Polym Sci Part B Polym Phys 1991;30:601−8.
[12] Barral L, Cano J, Lopez J, Lopez-Bueno I, Nogueira P, Ramirez C, et al. Thermogravimetric study of tetrafunctional/phenol novolac epoxy mixtures cured with a diamine. J Therm Anal Calorim 1998;51:489−501.
[13] Kissinger HE. Reaction kinetics in differential thermal analysis. Anal Chem 1957;29:1702−6.
[14] Ozawa T. A new method of analyzing thermogravimetric data. Bull Chem Soc Jpn 1965;38:1881−6.
[15] Liaw DJ, Shen WC. Curing of acrylated epoxy-resin based on bisphenols. Polym Eng Sci 1994;34:1297−303.
[16] Nam JD, Seferis JC. Generalized composite degradation kinetics for polymeric systems under isothermal and nonisothermal conditions. J Polym Sci Part B Polym Phys 1992;30:455−63.
[17] Flynn JH. The 'temperature integral' − its use and abuse. Thermochim Acta 1997;300:83−92.
[18] Doyle CD. Kinetic analysis of thermogravimetric data. J Appl Polym Sci 1961;5:285−92.
[19] Criado JM, Malek J, Ortega A. Applicability of the master plots in kinetic analysis of a non-isothermal rate. Thermochim Acta 1989;147:377−85.
[20] Criado JM, Perez-Maqueda LA, Gotor FJ, Malek J, Koga N. A unified theory for the kinetic analysis of solid state reactions under any thermal pathway. J Therm Anal Calorim 2003;72:901−6.
[21] Pérez-Maqueda LA, Criado JM, Gotor FJ, Malek J. Advantages of combined kinetic analysis of experimental data obtained under any heating profile. J Phys Chem A 2002;106:2862−8.
[22] Paterson WL. Computation of the exponential trap population integral of glow curve theory. J Comput Phys 1971;7(1):187−90.
[23] Pérez-Maqueda LA, Criado JM. The accuracy of Senum and Yang's approximations to the Arrhenius integral. J Therm Anal Calorim 2000;60:909−15.
[24] Urbanovici E, Popescu C, Seqal E. Improved iterative version of the Coats−Redfern method to evaluate non-isothermal kinetic parameters. J Therm Anal Calorim 1999;58:683−700.
[25] Low HY, Ishida H. Structural effects of phenols on the thermal and thermo-oxidative degradation of polybenzoxazines. Polymer 1999;40:4365−76.
[26] Sperling LH, Hu R. In: Utracki LA, editor. Polymer blends handbook, vol. 1; 2002. p. 426.
[27] Takeichi T, Guo Y, Rimdusit S. Performance improvement of polybenzoxazine by alloying with polyimide: effect of preparation method on the properties. Polymer 2005;46:4909−16.
[28] Chang TC, Wu KH, Liao CL, Lin ST, Wang GP. Thermo-oxidative degradation of siloxane-containing polyimide and unmodified polyimide. Polym Degrad Stab 1998;62:299−305.
[29] Thomas TH, Kendrick TC. Thermal analysis of polydimethylsiloxanes. I. Thermal degradation in controlled atmospheres. J Polym Sci 1969;7:537−49.
[30] Grassie N, MacFarlane IG. The thermal degradation of polysiloxanes [polydimethylsiloxane]. Eur Polym J 1978;14:875−84.
[31] Criado JM, Ortega A. Non-isothermal transformation kinetics: remarks on the Kissinger method. J Non-Cryst Solids 1986;87:302−11.
[32] Albano C, Freitas ED. Thermogravimetric evaluation of the kinetics of decomposition of polyolefin blends. Polym Degrad Stab 1998;61:289−95.
[33] Korshak VV. The chemical structure and thermal characteristics of polymers. Jerusalem: Keter Press; 1971.
[34] Hemvichian K, Kim DH, Ishida H. Identification of volatile products and determination of thermal degradation mechanisms of polybenzoxazine model oligomers by GC−MS. Polym Degrad Stab 2005;87:213−24.
[35] Camino G, Lomakin SM, Lazzari M. Polydimethylsiloxane thermal degradation. Part 1. Kinetic aspects. Polymer 2001;42:2395−402.
[36] Nandan B, Kandpal LD, Mathur GN. Poly(ether ether ketone)/poly(aryl ether sulphone) blends: thermal degradation behaviour. Eur Polym J 2003;39:193−8.
[37] Hamid SH, Amin MB, Maadhah AG. Handbook of polymer degradation. New York: Marcel Dekker; 1992.

[38] Remiro PM, Cortazar MM, Calahorra ME. A study of the degradation of uncured DGEBA/PVP blends by thermogravimetry and their miscibility state. J Mater Sci 1999;34:2627–33.
[39] Erceg M, Kovacic T, Klaric I. Dynamic thermogravimetric degradation of poly(3-hydroxybutyrate)/aliphatic-aromatic copolyester blends. Polym Degrad Stab 2005;90:86–94.
[40] Mohanty S, Mukunda PG, Nando GB. Kinetics of thermal degradation and related changes in the structure of blends of poly(ethylene-*co*-acrylic acid) (PEA) and epoxidized natural rubber (ENR). Polym Degrad Stab 1996;52:235–44.
[41] Moguet F, Bordére S, Tressaud A, Rouquerol F, Llewellyn P. Deintercalation process of fluorinated carbon fibres – II. Kinetic study and reaction mechanisms. Carbon 1998;36:1199–205.
[42] Dinh LN, Cecala CM, Leckey JH, Balooch M. The effects of moisture on LiD single crystals studied by temperature-programmed decomposition. J Nucl Mater 2001;295:193–204.

International Journal of Polymer Anal. Charact., 11: 441–453, 2006

ISSN: 1023-666X print
DOI: 10.1080/10236660600983726

Taylor & Francis
Taylor & Francis Group

Characterization of SiC Whisker-Filled Polybenzoxazine Cured by Microwave Radiation and Heat

S. Rimdusit, V. Jiraprawatthagool, S. Tiptipakorn, and S. Covavisaruch
Polymer Engineering Laboratory, Department of Chemical Engineering, Faculty of Engineering, Chulalongkorn University, Bangkok, Thailand

T. Kitano
Polymer Centre, Tomas Bata University in Zlín, Zlín, Czech Republic

Abstract: The effect of microwave and thermal curing on the properties of SiC_w-filled polybenzoxazine is examined. The benzoxazine resin (BA-a) can be cured thermally above 150°C but was hardly cured by microwave irradiation even using a power up to 1 kW. The presence of only 4% by weight of the SiC_w significantly reduces the processing time of the composites from two hours at 200°C using the traditional thermal cure to less than 20 minutes using a microwave cure power of 270 W. The mechanical and thermal behaviors of the SiC_w-filled polybenzoxazine show no significant difference with either curing methods.

Keywords: Composite; Microwave processing; Polybenzoxazine; Silicon carbide whisker

Received 9 May 2006; accepted 28 August 2006.

This research was supported by the Rajchadapisek Fund of Chulalongkorn University of the year 2005. S.R. also gratefully acknowledges the additional financial support from the Research Grant for Mid-Career University Faculty of the Commission on Higher Education, Ministry of Education, and the Thailand Research Fund 2005–2007.

Address correspondence to S. Rimdusit, Polymer Engineering Laboratory, Department of Chemical Engineering, Faculty of Engineering, Chulalongkorn University, Bangkok 10330, Thailand. E-mail: sarawut.r@chula.ac.th

INTRODUCTION

The application of microwaves was found to be an alternative method for curing thermosets with a significant increase in the rate of reaction.[1] In addition, the microwave-heated thermosetting composite was also shown to possess higher mechanical properties than those cured by conventional thermal process. This was believed to be due to the homogeneity heating that can reduce thermal stress in the composites.[2] In addition, microwave-cured epoxy composites were sometimes found to exhibit stronger interfacial bonding than that of thermal-cured systems.[3] However, microwave heating ability of any material depends significantly on its dielectric constants and dielectric loss factors.[4] Since most polymers possess a low dielectric constant,[5] microwave heating of neat polymers is not favorable. On the other hand, epoxy resins can be used in microwave heating because of the presence of some polar groups in their molecular structure. A significant increase in the rate of reaction was reported and an improvement in some mechanical properties was observed in an earlier study.[6] However, epoxy resins often provide a narrow processing window, have a short storage life, require a curing agent, and must be refrigerated for storage. Moreover, they are rather flammable and possess rather low thermal stability compared to phenolic resin.[7]

Polybenzoxazine is a novel class of phenolic resins that has been developed and studied to overcome the shortcomings of traditional phenolic resins.[8] Polybenzoxazine has the advantages of neither requiring any strong acids as catalysis nor producing any volatile by-product during polymerization. Its cross-linking reaction is achieved by a thermally activated ring-opening reaction.[9] Many attractive properties such as highly tailor-made molecular structure, low melt viscosity, self-polymerization upon heating, near zero shrinkage, high mechanical integrity, excellent electrical properties, high char yield, and ability to be alloyed with various types of existing polymers[10–12] have been reported for polybenzoxazine. However, like most polymeric materials, the low dielectric constant of polybenzoxazine means that it can not be cured conveniently by microwave radiation. Fortunately, the problem of the low dielectric constant of polymers can be improved by adding other suitable high dielectric constant filler.[13]

In order to enhance dielectric constant of material, Kitano et al.[14] reported the use of electro-conductive and inductive fillers such as short carbon fiber and silicon carbide whisker (SiC_w) for the heating or melt processing of polyethylene. The authors suggested that the major advantage of using SiC_w as a microwave-assisted coupling filler is due its effective heating and less sparking during irradiation compared to the use of short carbon fiber.[15] Moreover, SiC_w has been reported to exhibit outstanding toughening ability particularly with a rigid matrix

such as found in many ceramics composite systems.[16] Therefore, it is anticipated that an incorporation of SiC_w into a polybenzoxazine matrix should render at least twofold benefits to the benzoxzine resin. The inherent rigidity of polybenzoxazine may be reduced by the toughening mechanisms occurring in the filled systems, while the high electric constant of the SiC_w should enhance the microwave curability of the filled polybenzoxazine.

EXPERIMENTAL SECTIONS

Materials

The materials in this research were benzoxazine resin and silicon carbide whisker. Benzoxazine resin is based on bisphenol-A, aniline, and formaldehyde. Bisphenol-A (commercial grade) was kindly supplied by Thai Polycarbonate Co., Ltd. (TPCC). Para-formaldehyde (AR grade) was purchased from Merck, and aniline (AR grade) was purchased from APS Finechem. Silicon carbide whisker was supplied by Tokay Carbon Co. All chemicals were used without further purification.

The benzoxazine resin used is based on bisphenol-A, aniline, and formaldehyde in the molar ratio of 1:4:2. This resin was synthesized by using a patented solventless method.[8] The obtained benzoxazine resin is a clear yellowish powder at room temperature and can be melted to yield a low viscosity resin at about 70°–80°C. The resin density is 1.2 g/cm^3 and it has a reported dielectric constant of about 3–3.5.[7] Silicon carbide whisker (SiC_w) used was TWS-200. It is a nearly perfect single crystal with an average diameter of 0.5 μm and density of 3.2 g/cm^3. It has a reported dielectric constant of about 40.[17]

Specimen Preparation

Silicon carbide whisker was thoroughly mixed mechanically with benzoxazine resin in an aluminum container at 85°C for at least 10 min to ensure particle wet-out by the resin. The filler-to-matrix ratios were 0:100, 2:98, 4:96, and 6:94 by weight to yield molding compounds. For the thermal-cured specimen, the compounds were compression-molded to obtain a thickness of about 2 mm. The hot-pressed temperature of 200°C was applied for 2 h at a hydraulic pressure of 35 MPa. In the case of microwave curing, the molding compounds were cured in a microwave digestion oven (MARS5, model 907045) using a Teflon mold at a desired power from 100 to 1 kW and a fixed microwave frequency of 2.45 GHz.

Characterization Methods

The curing characteristics of the benzoxazine-silicon carbide composites were examined by using a differential scanning calorimeter (DSC) (TA, model 2910). For each test, a small amount of the sample ranging from 5 to 10 mg was placed on the aluminum pan and sealed in hermetically with aluminum lids. The experiment was done using a heating rate of 10°C/min to heat the sealed sample from 30° to 300°C under N_2 purging.

A universal testing machine (Instron, model 5567) was used to determine compressive properties under compression mode. The dimension of the specimen was $10 \times 10 \times 3$ mm. The compression test was performed using a 1 kN load cell at a crosshead speed of 1 mm/min according to the procedure outlined in ASTM 695-02.

A dynamic mechanical analyzer (Netzsch, model DMA242) was employed to investigate the specimen's dynamic mechanical properties. The specimen dimension was $40 \times 10 \times 2$ mm. The test was performed under bending mode. The strain was applied sinusoidally at a frequency of 1 Hz. The specimen was heated at the rate of 2°C/min from room temperature to 270°C. The dynamic storage modulus (E′) was determined.

Observation of the interfacial bonding within the composites was investigated using a scanning electron microscope (SEM) (JEOL JSM-6400) at an acceleration voltage of 15 kV. All samples were coated with a thin film of gold using a JEOL ion sputtering device (model JFC-1100E) for 4 min to obtain a thickness of approximately 300 Å before micrographs of the magnified fracture surfaces of the composite were taken.

RESULTS AND DISCUSSION

Figure 1 demonstrates the DSC thermograms with the temperature elevating from 30° to 300°C, showing the influence of benzoxazine resin filled with different SiC_w contents on curing temperature. The step change at about 45°C observed in all thermograms with different SiC_w contents was related to the glass transition temperature of the benzoxazine resin. It is related to the liquefying point of this resin. Polymerization of benzoxazine resin was known to occur by a simple ring-opening addition reaction and does not yield any reaction by-products.[9] The curing exotherm of the benzoxazine molding compound at different SiC_w contents, shows the onset of cure at approximately 150°C. A maximum exotherm peak was observed at 225°C, which is the characteristic of this resin.[18] The silicon carbide whisker has no direct effect on chemical reaction during the curing process of the benzoxazine resins. This is because there is no observable peak shift in the thermograms and the reaction

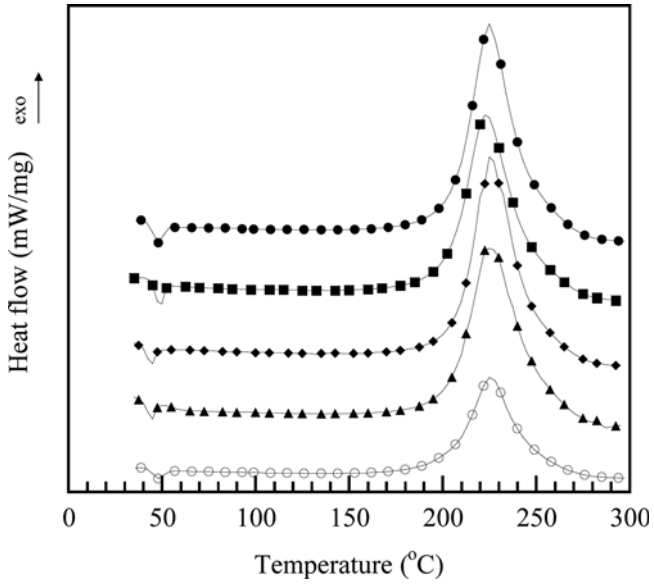

Figure 1. DSC thermograms of benzoxazine molding compound at various SiC_w contents: (●) 0, (■) 2, (◆) 4, (▲) 6, and (○) 20 wt.%.

temperature of SiC ceramics is above 1000°C.[19,20] However, the area under the curing peak was found to decrease with increasing SiC_w content.

Figure 2 demonstrates the effect of microwave heating on benzoxazine resin. The DSC thermogram of benzoxazine resin heated by a microwave at a high power of 1 kW for 30 min shows that under such condition, it was hardly cured; the change of the degree of conversion at this microwave irradiation condition was almost negligible. This is due to the intrinsic nonpolar nature of the benzoxazine resin.[8] However, with the addition of a relatively low content of SiC_w in the range of 4% by weight, the benzoxazine resin was found to be cured relatively well. This is evident in the DSC thermograms shown in Figure 3, when SiC_w of 4% by weight was used. Moreover, the input power needed to heat the SiC_w-filled benzoxazine resin to its full cure can be reduced substantially from over 1 kW to only 270–330 W. Hence it is apparent that the presence of SiC_w has a dramatic effect on curing of the benzoxazine molding compound. It was also found that higher microwave input power or longer irradiating time was needed as the SiC_w content decreased. With SiC_w loading of 4% by weight, the microwave radiation power of 270 W for 20 minutes was found to be the most suitable for processing of the benzoxazine molding compound to yield its fully cured state.

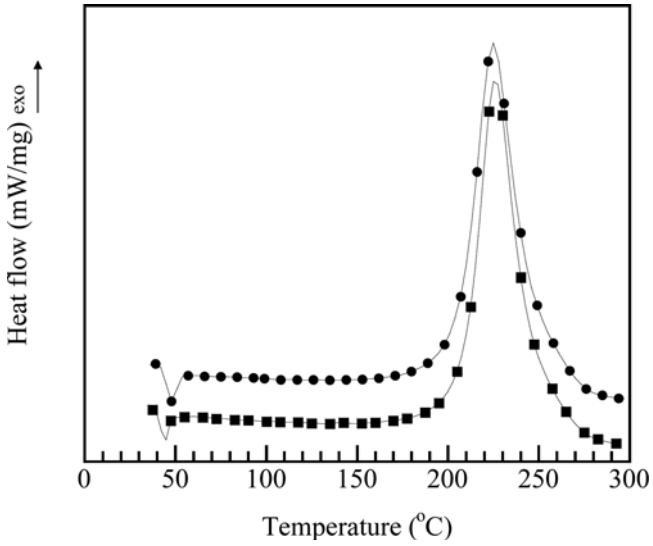

Figure 2. DSC thermograms of benzoxazine resin: (●) BA-a monomer, (■) BA-a monomer after irradiating with microwave power of 1 kW for 15 min.

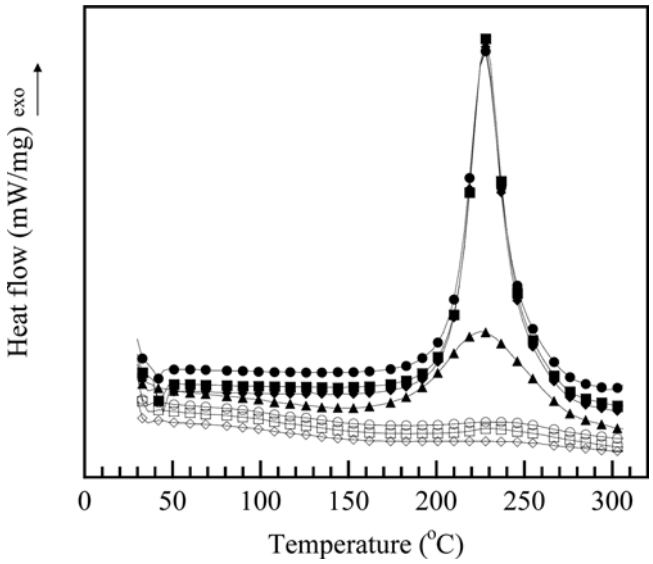

Figure 3. DSC thermograms of microwave-treated 4 wt.% SiC_w-filled polybenzoxazine molding compounds at fixed irradiation time of 15 min: (●) 150, (■) 180, (◆) 210, (▲) 240, (○) 270, (□) 300, and (◇) 330 W.

The conversion-time diagram of the microwave-cured benzoxazine resin filled with 4% by weight of SiC_w at 270 W is compared with that of the regular thermal cure in an oven heating at 200°C in Figure 4. The benefit of using the microwave technique is evidently depicted in the rapid rise of conversion in the microwave-cured compound. As shown in the diagram, curing time of only 20 minutes was required to convert the benzoxazine molding compound to its maximum cure by microwave processing at 2.45 GHz and 270 W, while the traditional oven cure at 200°C required at least 120 minutes.

Figure 5 shows the DSC thermograms depicting the glass-transition temperature (T_g), which was assigned as the midpoint temperature of the heat flow curve[21] of the neat benzoxazine resin and of the SiC_w-filled polybenzoxazine at 2, 4, and 6% by weight of the filler. At a heating rate of 10°C/min, the T_g of the polybenzoxazine was found to be 153°C. The T_g of all the SiC_w-filled polybenzoxazine composites cured thermally show no significant change from that of the neat polybenzoxazine, i.e., ranging from 153° to 160°C. The SiC_w filler was found to elevate the T_g of the composites due to the reinforcing effect of the ceramic filler to the matrix polymer. Boey and Yap[22] reported the maximum T_g of microwave-cured epoxy-amine system to be significantly lower than those achieved by thermal curing, because the sluggish reaction with microwave curing of the epoxy-amine system could entrap the functional group in the cross-link network. The different heating mechanisms, i.e., by

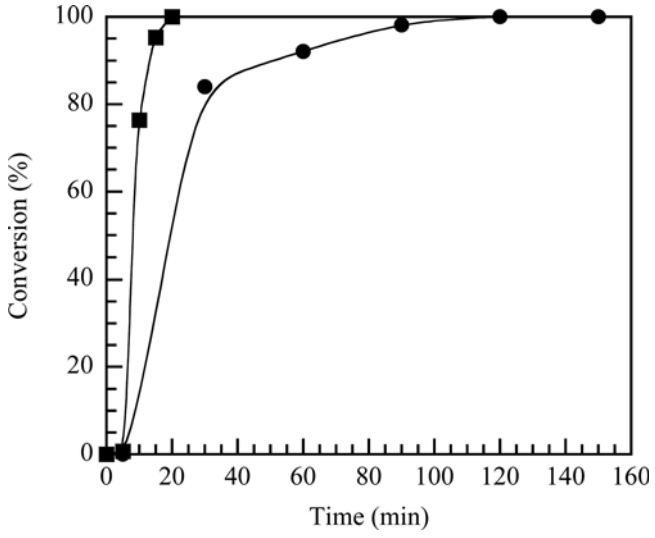

Figure 4. Conversion-time curve of 4 wt.% SiC_w-filled polybenzoxazine composite: (■) microwave-cured at 2.45 GHz, 270 W, (●) thermal-cured at 200°C.

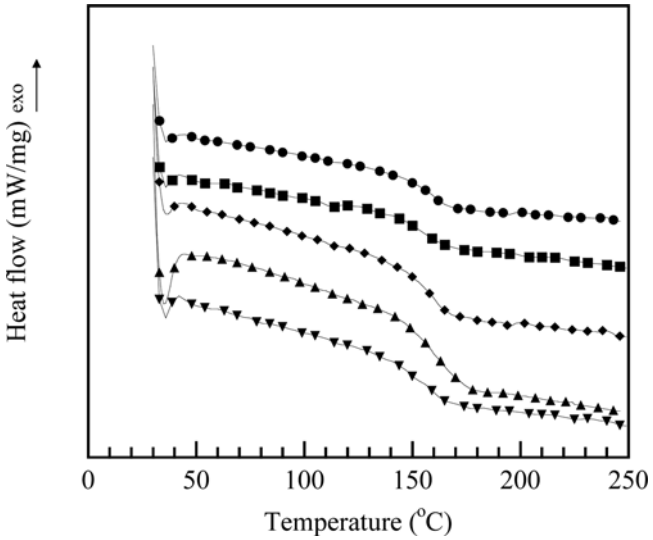

Figure 5. DSC thermograms of fully cured polybenzoxazine composites: (●) heat-cured polybenzoxazine, (□) heat-cured 2 wt% SiC_w, (◆) heat-cured 4 wt.% SiC_w, (▲) heat-cured 6 wt.% SiC_w, (▼) microwave-cured 4 wt.% SiC_w.

conduction of heat throughout the whole compound in the oven-cured technique and sporadic heating from the surface of the tiny silicon carbide whisker as well as the inside-out heating mechanism of the microwave during processing, may be the reasons for the discrepancy in T_g in some epoxy systems as mentioned above. In our case, at 4% by weight of SiC_w content, the microwave-cured SiC_w-filled polybenzoxazine composites possess a T_g of approximately 155°C, which is close to that of the heat-cured composites. The observed similar values of T_g implied no significant change in the curing mechanisms as well as no degradation of our benzoxazine resin upon microwave cure and heat-cure methods. This behavior had also been reported for some resin systems.[3]

Microwave radiation is believed to heat the whole composite simultaneously. In reality, since polymerization took place only within the resin and the reaction is exothermic, the temperature of the surrounding and the mold was always lower than that within the microwave-heated resin. Therefore, a temperature gradient may still exist due to heat conduction from the hot benzoxazine molding compound to the colder surrounding. For this reason, the percent conversion at different locations of the microwave-cured composite was investigated. The results are illustrated in Table I. It is evident that a relatively uniform curing of over 97% conversion was achieved at all locations in our fully cured composite. The maximum cure conversion of nearly 100% was detected at

Table I. Conversion at different positions of 4% by weight SiC_w-filled polybenzoxazine composite cured by microwave irradiation

Distance from center (cm)	Conversion (%)
–2	98.8
–1	98.3
0	100.0
1	98.5
2	97.7

the center of the composite sample. This test verified the uniformity of cure achieved in the microwave-cured polybenzoxazine/SiC_w composites prepared for further property characterization in our study.

Figure 6 exhibits the dynamic flexural moduli of the SiC_w-filled polybenzoxazine composites cured by traditional thermal heating with SiC_w contents ranging from 0 to 6% by weight and microwave heating with constant 4% by weight of SiC_w, the optimal content for microwave processing, with the temperature ranging from 30° to 260°C based on a heating rate of 2°C/min. The storage modulus of SiC_w-filled polybenzoxazine at its glassy state tends to increase with increasing SiC_w fraction in the

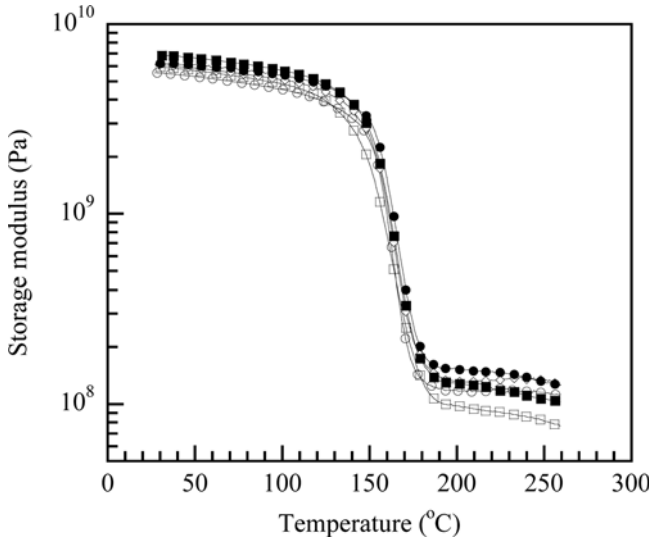

Figure 6. Storage modulus of fully-cured polybenzoxazine composites: (○) heat-cured polybenzoxazine, (□) heat-cured 2 wt.% SiC_w, (◇) heat-cured 4 wt.% SiC_w, (●) heat-cured 6 wt.% SiC_w, (■) microwave-cured 4 wt.% SiC_w.

composites as a result of the reinforcing effect of the more rigid SiC_w filler. At room temperature, the dynamic modulus of SiC_w-filled polybenzoxazine composite increased from 5.5 GPa of a neat polybenzoxazine to 6.2 GPa of the 6% by weight of SiC_w composite. The modulus of the SiC_w-filled polybenzoxazine in the rubbery plateau region was also enhanced by increasing SiC_w content, because the load transfer in the composite occurred mainly through the SiC_w, when the two phases contact. Therefore, the mobility and the deformability of the rubbery matrix could be reduced by the presence of the hard SiC_w. Since there was only a small amount of SiC_w content in the composite, the dynamic mechanical properties showed only marginal increase in values.

The stress-strain relation under axial compression of the polybenzoxazine composites is shown in Figure 7. Apparently, compression load increases with displacement until it reaches the intrinsic yield point of the specimens, and then it drops gradually despite increasing the displacement until composite failure. Strain softening, which was lacking in neat polybenzoxazine, was observed in all SiC_w-filled polybenzoxazine composites. The specific energy absorption (SEA) for the axial compression can be calculated by integrating the area under the load-displacement curves and dividing by the mass of the specimen.[23] From the experiment, the SEAs were found to increase with increasing the SiC_w content from

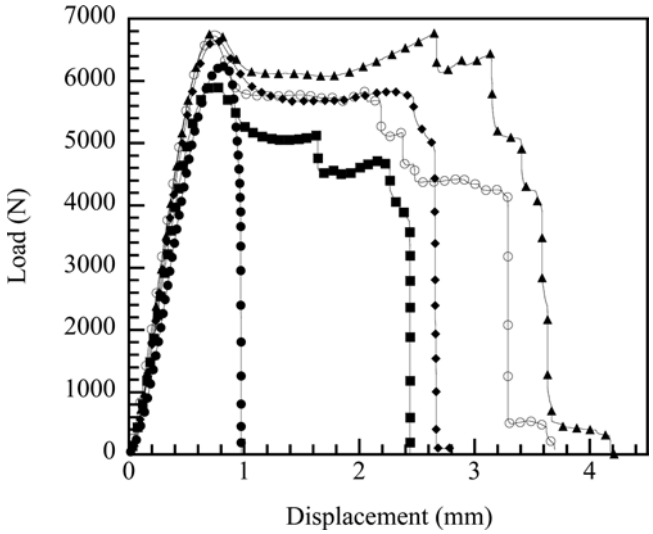

Figure 7. Load-displacement curve under axial compression of polybenzoxazine composites: (●) neat polybenzoxazine, (■) 2 wt.% SiC_w-filled PBZ cured by heat, (◆) 4 wt.% SiC_w-filled PBZ cured by heat, (▲) 6 wt.% SiC_w-filled PBZ cured by heat, (○) 4 wt.% SiC_w-filled PBZ cured by microwave.

the value of 25 kJ/kg of the unfilled polybenzoxazine, 36 kJ/kg for 4% by weight of SiC_w, to 49 kJ/kg of the 6% by weight of SiC_w-filled polybenzoxazine. The result suggested the promotion of energy absorption by the incorporation of SiC_w into the polybenzoxazine matrix. However, at a fixed 4% by weight of SiC_w-filled polybenzoxazine composite, the SEAs of the composites cured by both methods were approximately the same within the range of 31–42 kJ/kg for thermal-cured composites and 32–44 kJ/kg for microwave-cured composites. Both curing methods, therefore, showed negligible effect on changing the mechanical properties of the polybenzoxazine composites.

Figure 8 shows the interfacial characteristics along the fracture surface of the silicon carbide whisker-filled polybenzoxazine (at 2 and 4% by weight of filler) cured by hot-pressing and microwave radiation. The fracture surface of the neat polybenzoxazine is much smoother than that of the SiC_w-filled polybenzoxazine composite. Protruding whiskers and holes, where the whiskers were initially lodged before fracture, were also observed. There were also evidence of whisker pullout and bridging. This fracture characteristic might explain the enhancement of the SEAs of our polybenzoxazine matrix with the addition of the SiC_w, as discussed in the previous section. Moreover, the interfaces between the matrix and the SiC_w filler in the composite cured by microwave radiation revealed the same feature as that observed in the thermally cured composites. The result confirmed

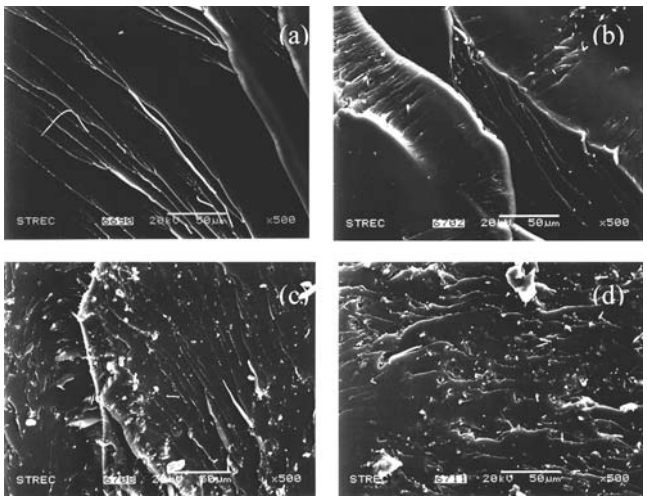

Figure 8. SEM micrographs of fracture surface of SiC_w-filled polybenzoxazine composites: (a) neat PBZ cured by heat, (b) 2 wt.% SiC_w-filled PBZ cured by heat, (c) 4 wt.% SiC_w-filled PBZ cured by heat, (d) 4 wt.% SiC_w-filled PBZ cured by microwave.

the observed similarity in the mechanical properties of our polybenzoxazine composites processed by both microwave and heat.

CONCLUSIONS

The effect of microwave cure and conventional thermal cure on thermal and mechanical properties of SiC_w-filled polybenzoxazine was investigated. The optimal SiC_w content to effectively couple with microwave to yield a fully cured polybenzoxazine was found to be about 4% by weight. The optimum processing condition of SiC_w-filled polybenzoxazine composites for thermal curing was 200°C for two hours, and for microwave curing it was 270 W for 20 minutes. The glass transition temperature and flexural modulus of the composites increased slightly within the evaluated SiC_w content up to 6% by weight and were not significantly affected by the two processing methods. The specific energy absorption upon uniaxial compression was found to increase with the SiC_w content. The SEM micrographs of the composite fracture surfaces revealed substantial adhesion between the SiC_w and the polybenzoxazine matrix.

REFERENCES

[1] Boey, F. Y. C., B. H. Yap, and L. Chia. (1999). Microwave curing of epoxy-amine system – Effect of curing agent on the rate enhancement. *Polym. Test.* **18**, 93–109.
[2] Bai, S. L., V. Djafari, M. Andreani, and D. Francois. (1995). A comparative study of the mechanical behavior of an epoxy resin cured by microwaves with one cured thermally. *Eur. Polym. J.* **31**, 875–884.
[3] Bai, S. L. and V. Djafari. (1995). Interfacial properties of microwave cured composites. *Composites* **26**, 645–651.
[4] Thostenson, E. T. and T. W. Chou. (1999). Microwave processing: Fundamentals and applications. *Compos. Part A Appl. Sci. Manuf.* **30**, 1055–1071.
[5] Wypych, G. (2000). *Handbook of Fillers*, 2nd ed. Toronto: Chem Tech Publishing.
[6] Zhou, J., C. Shi, B. Mei, R. Yuan, and Z. Fu. (2003). Research on the technology and the mechanical properties of the microwave processing of polymer. *J. Mater. Process. Technol.* **137**, 156–158.
[7] Nair, C. P. R. (2004). Advances in addition-cure phenolic resins. *Prog. Polym. Sci.* **29**, 401–498.
[8] Ishida, H. (1996). Process of benzoxazine compounds in solventless systems. U.S. Patent 5,543,516.
[9] Takeichi, T., R. Zeidam, and T. Agag. (2002). Polybenzoxazine/clay hybrid nanocomposites: Influence of preparation method on the curing behavior and properties of polybenzoxazine. *Polymer* **43**, 45–53.

[10] Rimdusit, S., S. Pirstpindvong, W. Tanthapanichakoon, and S. Damrongsakkul. (2005). Toughening of polybenzoxazine by alloying with urethane prepolymer and flexible epoxy: A comparative study. *Polym. Eng. Sci.* **45**, 288–296.

[11] Rimdusit, S. and H. Ishida. (2004). Development of new class of electronic packaging materials based on ternary systems of benzoxazine, epoxy, and phenolic resins. *Polymer* **41**, 7941–7949.

[12] Takeichi, T., Y. Guo, and T. Agag. (2000). Synthesis and characterization of poly(urethanebenzoxazine) films as novel type of polyurethane/phenolic resin composites. *J. Polym. Sci.* **38**, 4165–4176.

[13] Xu, Y., D. D. L. Chung, and C. Mroz. (2001). Thermally conducting aluminum nitride polymer-matrix composites. *Compos. Part A Appl. Sci. Manuf.* **32**, 1749–1757.

[14] Kitano, T., T. Tanegashima, and P. Saha. (1998). Microwave processing of polymer composites. In *The First Asian-Australasian Conference on Composite Materials* (*ACCM-1*), *Osaka, Japan*, 1.1:217-1-4. Asian-Australasian Association for Composite Materials (AACM).

[15] Nightingale, C. and R. J. Day. (2002). Flexural and interlaminar shear strength properties of carbon fiber/epoxy composites cured thermally and with microwave radiation. *Compos. Part A Appl. Sci. Manuf.* **33**, 1021–1030.

[16] Fei, W. D., M. Hu, and C. K. Yao. (2002). Thermal expansion and thermal mismatch stress relaxation behaviors of SiC whisker reinforced aluminum composite. *Mater. Chem. Phys.* **77**, 882–888.

[17] Harper, C. A. (2004). *Electronic Packaging and Interconnection Handbook*, 4th ed. New York: McGraw-Hill.

[18] Rimdusit, S., W. Tanthapanichakoon, and C. Jubsilp. (2006). High performance wood composites from highly filled polybenzoxazine. *J. Appl. Polym. Sci.* **99**, 1240–1253.

[19] Ryu, Z., J. Zheng, M. Wang, and B. Zhang. (2001). Synthesis and characterization of silicon carbide whisker. *Carbon* **39**, 1929–1941.

[20] Satapathy, L. N., P. D. Ramesh, D. Agrawal, and R. Roy. (2005). Microwave synthesis of phase-pure, fine silicon carbide powder. *Mater. Res. Bull.* **40**, 1871–1882.

[21] Cheng, X., Z. Xie, Y. Song, J. Xiao, and Y. Wang. (2006). Analysis and characterization of polycarbosilane. *Int. J. Polym. Anal. Charact.* **11**, 287–298.

[22] Boey, F. Y. C. and B. H. Yap. (2001). Microwave curing of an epoxy-amine system: Effect of curing agent on the glass-transition. *Polym. Test.* **20**, 837–845.

[23] Warrior, N. A., T. A. Turner, F. Robitaille, and C. D. Rudd. (2003). Effect of resin properties and processing parameters on crash energy absorbing composite structure made by RTM. *Compos. Part A Appl. Sci. Manuf.* **34**, 543–550.

Effect of SiC Whisker on Benzoxazine-Epoxy-Phenolic Ternary Systems: Microwave Curing and Thermomechanical Characteristics

Sarawut Rimdusit,[1] Varutrit Jiraprawatthagool,[1] Chanchira Jubsilp,[1] Sunan Tiptipakorn,[1] Takeshi Kitano[2]

[1]*Department of Chemical Engineering, Faculty of Engineering, Chulalongkorn University, Bangkok 10330, Thailand*
[2]*Polymer Centre, Tomas Bata University in Zlín, Zlín 76272, Czech Republic*

Received 12 December 2006; accepted 27 February 2007
DOI 10.1002/app.26383
Published online 1 May 2007 in Wiley InterScience (www.interscience.wiley.com).

ABSTRACT: Microwave radiation at 2.45 GHz with variable power input was investigated as a tool to facilitate the curing reaction of benzoxazine-epoxy-phenolic molding compound i.e., BEP893. Dielectric filler for microwave coupling was silicon carbide whisker (SiC_w). Factors such as whisker loading and input irradiation power were found to have a profound effect on the microwave heating of the BEP893 particularly on the rate of temperature rise and maximum heating temperature. The SiC_w loading of 10% by weight with the microwave irradiation condition of 300 W for 10 min renders the ultimate curing of the molding compound. Significant reduction in processing time of the microwave cured sample compared with the conventional heat cured sample i.e., 150 min at 200°C using conventional heating is the key benefit of this technique. Mechanical properties of the microwave cured and conventional heat cured samples show similar characteristics with slightly lower T_g in the microwave cured samples. © 2007 Wiley Periodicals, Inc. J Appl Polym Sci 105: 1968–1977, 2007

Key words: composites; mechanical properties; thermal properties; crosslinking differential scanning calorimetry (DSC)

INTRODUCTION

Benzoxazine resin (BA) was developed as a high flow, low void resin system with a capability of forming thick samples of either filled or unfilled systems. The resin can be synthesized via a simple and cost-effective solventless technology.[1] In addition, molecular design flexibility of the resin comparable to that of epoxy or polyimide renders wide range of properties of the polymer that can be tailor-made.[2–4] The resin has been shown to possess some useful properties such as ease of processing due to its self-polymerizability upon heating via ring-opening polymerization thus giving no volatile by-products. The polymer shows near-zero shrinkage upon polymerization as well as possesses relatively high T_g and good thermal stability.[5–8] Ishida and Rimdusit have reported the use of BA-m type polybenzoxazine as a matrix for boron nitride filler to obtain a highly filled composite system with high value of thermal conductivity.[9,10] Recently, highly filled wood composites from BA-a type polybenzoxazine with relatively high modulus comparable to natural wood has also been reported.[11]

Those high performance composite properties are attributed to the ability of the low viscosity BA resin to accommodate very high filler loading i.e., up to 75% by volume as well as its good adhesive properties. Moreover, the compatibility of the polybenzoxazine with various resins renders a large number of polymer alloys or copolymers covering wide range of properties.[12–21] The hybrid systems based on BA, epoxy, and phenolic resins are of particular interest in this investigation since the systems show synergistic behaviors in some of their properties in addition to their excellent processbility and high reliability of the cured samples.[17,18] In this investigation, the well-characterized ternary systems namely BEP893 which is the resin mixture of BA resin (B), epoxy resin (E), and phenolic resin (P) at the mass ratio of 8:9:3 is used as a matrix. The processability as well as the cured properties of the resin has already been reported in our previous work.[17]

Microwave energy has been an attractive heating source for material processing due to its capability to interact directly with molecules i.e., by raising their rotational energy level and thus the temperature. The consequence is a more uniform and faster heating of the materials than traditional ways of heat

Correspondence to: S. Rimdusit (sarawut.r@chula.ac.th).
Contract grant sponsor: Research Grant for Mid-Career University Faculty of the Commission on Higher Education, Ministry of Education, Thailand Research Fund 2005-2007, Affair of Commission for Higher Education-CU Graduate Thesis Grant 2005-2006, TJTTP-JBIC Fund of Chulalongkorn University.

conduction or convection.[22–25] The technique has already been utilized in various systems such as to accelerate reaction kinetics in the drug development industry, to cure plywood cement, or to vulcanize rubber in the tire industry.[22] There are a number of investigations on the use of microwave to cure thermosetting resins particularly in epoxy systems and its molding compounds. Some reports e.g., on the epoxy systems, showed promising results in the enhancement of the processing time using microwave radiation comparing with the traditional thermal curing.[26,27]

In this investigation, we utilize microwave energy for the curing process of BEP893 resin filled with inductive or dielectric filler i.e., silicon carbide whisker (SiC_w). The effect of filler loading and input radiation power on microwave coupling of this molding compound as well as the composite properties comparing with those obtained from the conventional heat cure method is to be investigated.

EXPERIMENTAL

Materials

The 4,4′-isopropylidenediphenol and aniline were purchased from Kanto Chemical Co., Inc. (Tokyo, Japan). Paraformaldehyde was from Merck Chemical Ltd. (Notthingham, UK). BA resin based on the above reactants was synthesized using a solventless method as reported elsewhere.[1] The as-synthesized monomer is a clear yellowish solid at room temperature and can be molten to yield a low viscosity resin at about 80°C. The monomer was ground to fine powder and was kept in a refrigerator prior to use. Bisphenol F type epoxy resin (YDF-170) from Tohto Chemical Co., Ltd. (Tokyo, Japan) is a clear liquid at room temperature and was used as-received. Phenolic novolac (PR1501) from Hitachi Chemical Co., Ltd. (Tokyo, Japan) was utilized as an initiator of BA resin's ring opening reaction.[17] In this investigation, the ternary mixture with the mass ratio of BA resin: epoxy resin: phenolic resin of 8:9:3 i.e., BEP893 was chosen as a matrix for SiC_w due to its well characterized properties to yield a relatively high thermal stability matrix.[17]

SiC_w (TWS-200) from Tokai Carbon Co., Ltd. (Tokyo, Japan), having average diameter of 0.5 μm and average length of 30 μm, was used as a filler for this investigation. The filler has a reported density of 3.20 g cm^{-3} and a dielectric constant of about 40.[28,29]

Sample preparation

BEP893 resin was prepared by melt-mixing the three monomers at 80°C for 20 min. The resulting homogeneous and low viscosity mixture can be compounded with SiC_w at this stage. The BEP893 is solid at room temperature and can be ground and kept in a refrigerator for future use.

Molding compound of SiC_w and BEP893 was prepared by dry mixing of the desired amount of the resin and the whisker. The powder mixture was then heated at 80°C and mechanically blended to yield a uniform suspension of the molding compound. About 5 g of the molding compound was used for microwave heating or conventional heating by compression molding. The fully cured composites by compression molding were obtained using temperature of 200°C for 180 min under the hydraulic pressure of 0.1 MPa.

The microwave heating experiment was carried out using a JRC industrial microwave machine model NJA2103A. The operating frequency is 2.45 GHz with variable input power from 0 to 1.2 kW. A microwave generator (synthesizer and amplifier) supplies the radiation energy to a horn antenna which is directed to the surface of the sample. The reflected microwave energy can be measured by a power monitor and was minimized by a turner fitted on a waveguide before a horn antenna. The nonreflected part of the microwave radiation is absorbed by the sample resulting in heating of the material. The evolution of surface temperature of the sample was monitored using infrared thermometer attached on the sidewall of the microwave apparatus. The temperature of the environment inside the microwave applicator was also recorded using an AMOTH8000 fiberoptic thermometer from Anritsu Meter.

Sample characterization

Dielectric property measurement

A LCR meter from Yokogawa-Hewlett–Packard model HP 4284A (20 Hz–1 MHz) equipped with dielectric test adaptor model 16451A (Yokogawa-Hewlett–Packard), having parallel-plate micrometer-typed electrodes was used to determine the capacitance, a corresponding dielectric constant, and a loss tangent of dielectric material. The measurement was performed at room temperature. The test material was in the form of disk shape with a diameter of about 35 mm and a thickness of about 1 mm. A thin layer of high vacuum silicone grease was applied on both specimen surfaces to ensure good contact and to eliminate air gap between the sample and the electrodes.

Differential scanning calorimetry

A differential scanning calorimeter model DSC3100 from MAC Science was utilized to investigate curing behaviors as well as to determine the transition temperature of both filled and unfilled BEP893. The

mass of the sample is ~10 mg. The sample was put in an aluminum pan with lid and was scanned using the heating rate of 10°C min^{-1} from room temperature to 320°C under N_2 purging.

Thermomechanical analysis

Linear thermal expansion coefficient (LCTE) of a specimen was determined using a Seiko Instruments thermomechanical analyzer (model TMA/SS120C) with sample size of 10 × 5 × 1 mm^3. The measurement was performed under tension at 10 g (force control mode). The temperature was scanned twice from 30 to 200°C at a heating rate of 2°C min^{-1}. The value of the LCTE was recorded on the second run and was averaged between 40 and 80°C.

Dynamic mechanical analysis

Dynamic mechanical thermograms of the polymer and its composites were obtained using a dynamic viscoelastic analyzer model DVA-200 from IT Keisoku-Seigyo. The test was performed under tension mode using 1 kgf load cell. The strain amplitude was 0.2% and the frequency used was 10 Hz. The sample was heated at the rate of 2°C min^{-1} from room temperature to 280°C. The samples were in the dimension of 25 × 5 × 1 mm^3.

Scanning electron microscope

The fracture surface morphology of both microwave cured and conventional heat cured samples was obtained by scanning electron microscopy (Akashi Beam Technology model Alpha-30A) at the magnification of 1000× or 2000× with an acceleration voltage of 20–25 kV. Samples were coated with a thin film of gold using a JEOL ion sputtering device (model JFC-1100E) for 4 min to obtain a thickness of ~300 Å before micrographs of the magnified fracture surfaces of the composite were taken.

RESULTS AND DISCUSSION

Characteristics of BEP893 resin and microwave heating

Figure 1 illustrates the DSC thermograms of the uncured and fully cured neat BEP893 matrix. The figure clearly exhibits the thermally curable behavior of this BEP893 resin. The resin's curing exotherm starts at about 140°C with the peak maximum at 243°C. The curing enthalpy of the resin determined from the area under the exothermic peak is 210 J g^{-1}. The fully cured BEP893 exhibits a glass transition temperature (T_g) of about 145°C. This information is essential for microwave heating since the target heating temperature due to microwave irradiation should be well above 140°C to be able to cure this BEP893 resin. In practice, the curing temperature in the range of 180–200°C is preferable to achieve fast curing with minimum thermal degradation of this polymer.[17]

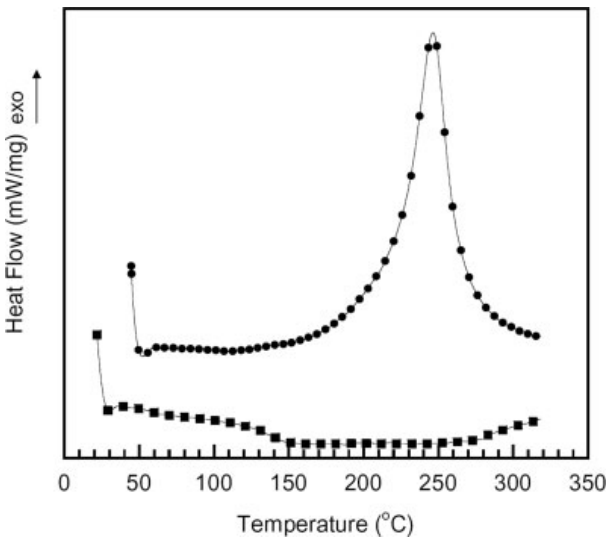

Figure 1 DSC thermograms of the uncured and fully cured BEP893: (●) uncured BEP893, (■) fully cured BEP893.

Figure 2(a,b) exhibit the temperature rise curves due to microwave irradiation of the three starting resins namely BA, epoxy, and phenolic resins, as well as their ternary mixture under this investigation i.e., BEP893 resin. The temperature rise curves as a function of time of the three starting monomers are shown in Figure 2(a). The microwave power used in this investigation was fixed at 1 kW. From the figure, it is evident that only epoxy resin could substantially couple with microwave; thus, rendering the rapid temperature rising beyond 180°C within few minutes. Whereas both BA and phenolic novolac resins show a much slower rate of temperature rising, i.e., the slope of the plot, with the obtained maximum temperature of ~130°C. As a consequence, BA resin solely cannot be cured by microwave irradiation because its maximum attainable temperature, even at a relatively high microwave input of 1 kW, is still rather low for the initiation of its ring-opening polymerization reaction.

The outstanding microwave coupling capability of the epoxy resin is attributed to its relatively polar nature of the resin and makes it one of the most investigated resins for processing by microwave.[24–27] Therefore, the incorporation of substantial amount of epoxy resin into the BA resin should enhance the microwave coupling capability of the resulting mixture. However, in reality, the maximum fraction of

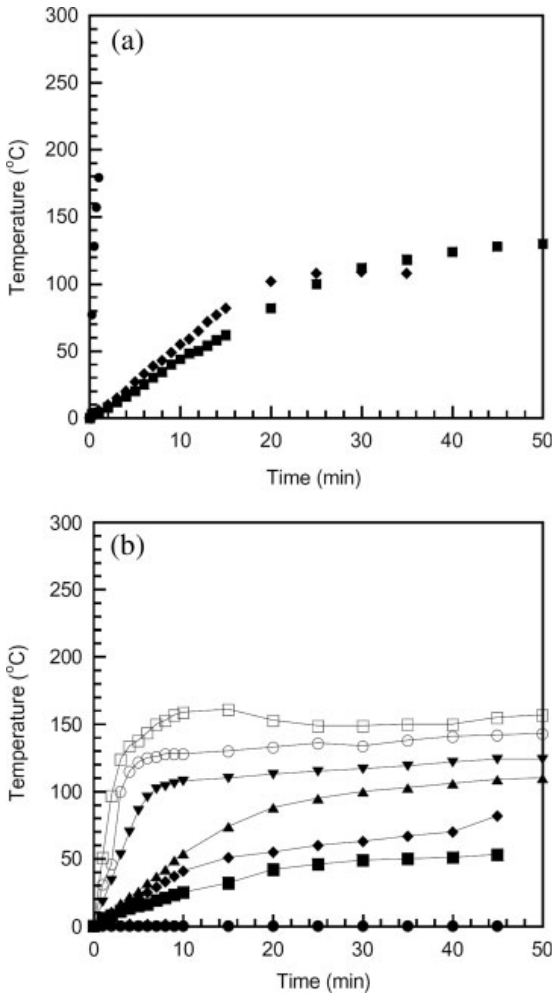

Figure 2 (a) Temperature rise curves at 1 kW of three starting monomers: (●) Bisphenol F epoxy resin, (■) Phenolics resin, and (◆) BA-a benzoxazine resin. (b) Temperature rise curves upon microwave irradiation of BEP893 resin at various microwave input powers: (●) 100 W, (■) 200 W, (◆) 300 W, (▲) 400 W, (▼) 500 W, (○) 600 W, and (□) 1 kW.

the epoxy required is normally limited by the resulting properties of the cured sample. In this work, BEP893 is evaluated for microwave processing due to its relatively good overall cured properties as reported in our previous work.[17]

The temperature rise curves of BEP893 resin at varied microwave input power ranging from 100 W to 1 kW are plotted in Figure 2(b). In this figure, we can see that this BEP893 resin clearly shows improved microwave coupling ability compared with that of the neat BA resin. It was also observed that the initial rate of temperature rise of the resin, which is related to the initial slope of each curve, as well as the maximum achievable temperature rise are increased with increased microwave input power. However, the resin's temperature rise even at the evaluated input power up to 1 kW was found to be only about 160°C, which is still rather low to achieve at fast curing of the BEP893 resin.

Effect of SiC_w on microwave processing of BEP893

Though providing good overall cured properties, the limited microwave coupling ability of the BEP893 resin led to the use of appropriate dielectric fillers to further enhance its microwave heating property. Recently, various types of dielectric fillers have been incorporated in polymeric matrices to further assist in its microwave processing or heating including SiC_w in polypropylene,[30] in EPDM,[31] and in polybenzoxazine[32]; or aluminum powder in epoxy,[33] carbon black in epoxy[34]; as well as polyaniline in polyethylene.[35] Kitano et al.[36] reported the use of electro-conductive and inductive fillers such as short carbon fiber and SiC_w for the heating or melting process of polyethylene. They suggested that the benefit of using SiC_w as microwave-assisted coupling filler was due to its effective heating as well as less sparking event during microwave irradiation comparing with the use of short carbon fiber or carbon black. The other potential benefits of using SiC_w as filler are its excellent reinforcing behavior[30,31] and its reported outstanding toughening ability, particularly in the rigid matrix such as in many ceramics composite systems.[37–40] The filler is, therefore, chosen as the dielectric filler for our BEP893 resin.

Figure 3(a–c) depict the effect of SiC_w contents, i.e., 5, 10, and 15% by weight, on the temperature rise curves of BEP893 at various input microwave irradiation power. From these figures, we can clearly see that the presence of the SiC_w has a dramatic effect on the heating of the BEP893 molding compounds. In Figure 3(a), two significant features were observed from using this inductive filler. First, to reach the target temperature for fast curing of BEP893, i.e., 180–200°C in this case, relatively low SiC_w content of only 5% by weight was found to be sufficient. Moreover, the input power needed to heat the sample above the target temperature was substantially reduced from 1 kW to only about 400 W. From Figure 3(b), the SiC_w loading of 10% by weight with the irradiation power of 100–300 W was found to be sufficient for the microwave processing of the BEP893 resin, while the input power of less than 200 W for the SiC_w loading of 15% by weight was required to effectively cure the resin as seen in Figure 3(c). Finally, Figure 3(d) exhibits the temperature rise curves as a function of SiC_w content compared at a constant microwave input power of 200 W. From the plot, the initial rate of temperature rise of the BEP893 molding compound increases with increasing of SiC_w loading. The phenomenon is attributed to an increase in dielectric constant of a material

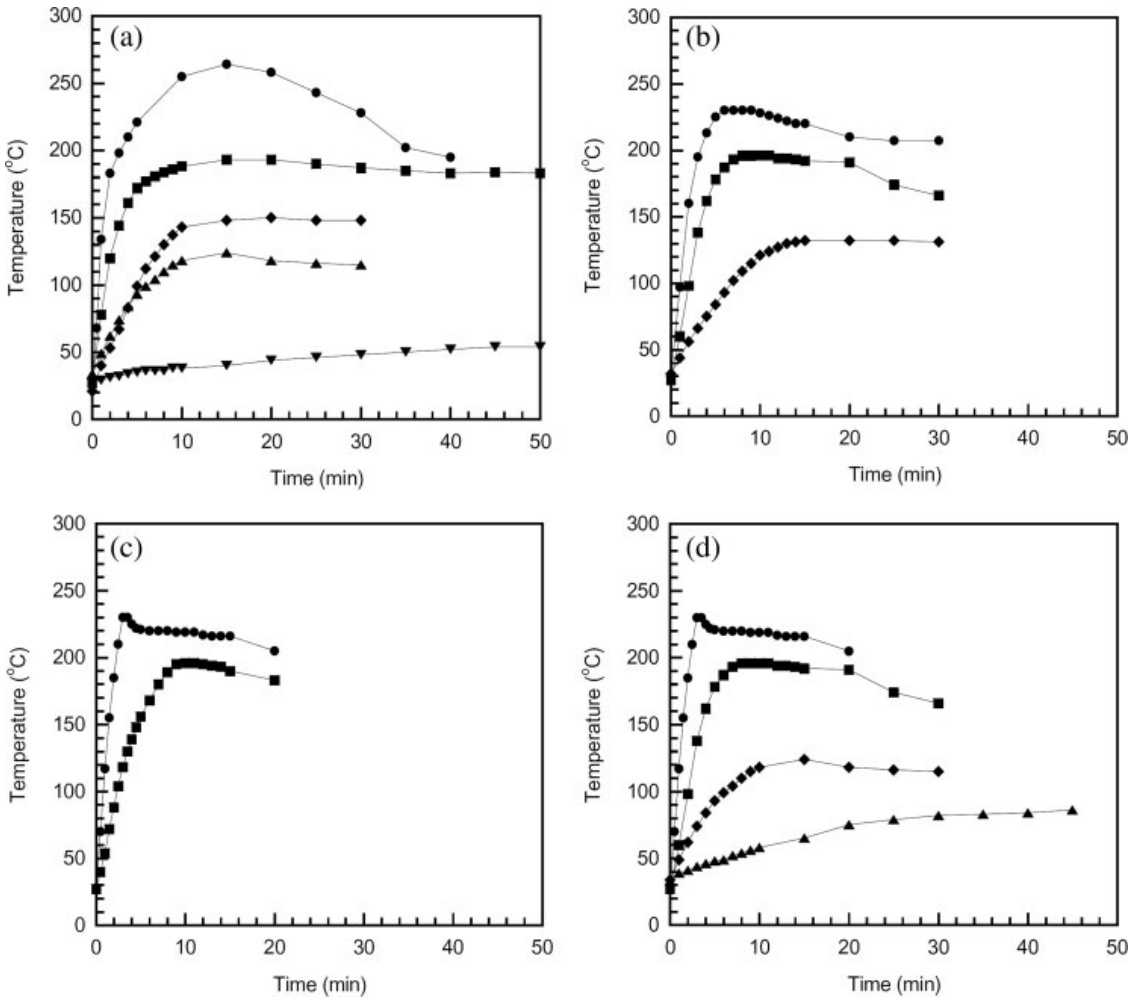

Figure 3 (a) Temperature rise curves of BEP893 molding compound at 5 wt % SiC_w loading: (●) 500 W, (■) 400 W, (◆) 300 W, (▲) 200 W, and (▼) 100 W. (b) Temperature rise curves of BEP893 molding compound at 10 wt % SiC_w loading: (●) 300 W, (■) 200 W, and (◆) 100 W. (c) Temperature rise curves of BEP893 molding compound at 15 wt % SiC_w loading: (●) 200 W, (■) 100 W. (d) Effect of SiC_w loading on temperature rise curves of BEP893 molding compound at a fixed microwave power of 200 W: (●) 15 wt %, (■) 10 wt %, (◆) 5 wt %, and (▲) 0 wt %.

with an incorporation of dielectric filler.[41] SiC_w is a ceramics with reported dielectric constant of up to 40[42] whereas the BEP 893 was measured to be about 4 as illustrated in Figure 4. In theory, the greater the dielectric constant of the material, the higher its microwave coupling ability will be. An addition of the SiC_w was found to systematically raise the dielectric constant of the BEP893 molding compound in a relatively linear manner as depicted in Figure 4, thus resulted in the enhanced microwave coupling of the compound with the filler loading.

Thermomechanical properties of conventional heat cured SiC_w-filled BEP893

The effect of SiC_w loading on dynamic mechanical properties of the fully cured BEP893 composites is shown in Figures 5 and 6. Figure 5 depicts the effect of the whisker loading (in the range of 0–20% by weight) on the storage modulus of the composites. From the plot, the presence of a high modulus SiC_w (400 GPa[28]) was found to significantly enhance both the glassy state modulus and the rubbery plateau modulus of the neat BEP893 matrix due to the reinforcing effect of the filler. Furthermore, the glass transition temperature (T_g) of the sample obtained from the peak position of the loss modulus as shown in Figure 6 was also found to increase with increasing the SiC_w content. The enhancement of the modulus and the T_g implies a relatively good adhesion between this filler and the BEP893 matrix.

There are many factors affecting a LCTE of a composite material including the ratio of filler in a poly-

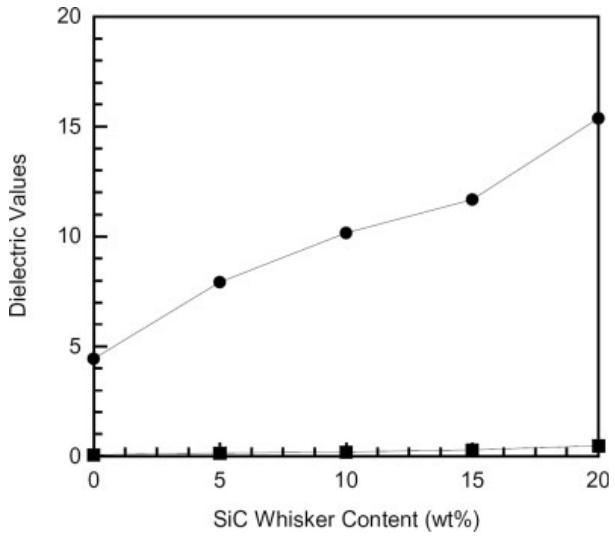

Figure 4 Permittivity and dielectric loss of BEP893 molding compounds as a function of SiC_w loading: (●) permittivity, (■) dielectric loss.

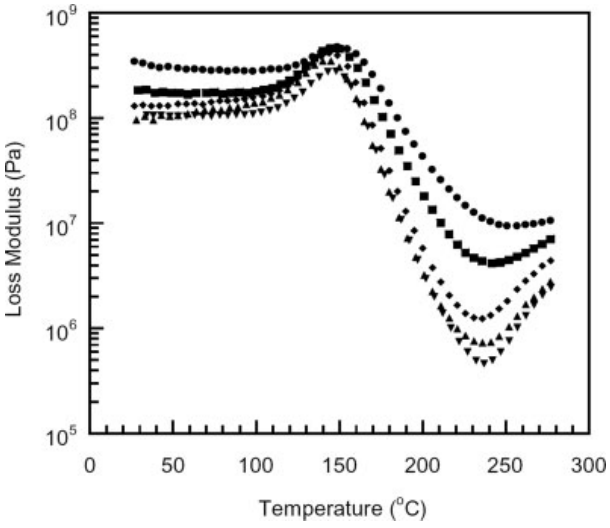

Figure 6 Effect of SiC_w loading on loss modulus of fully cured BEP893 composites: (●) 20 wt %, (■) 15 wt %, (◆) 10 wt %, (▲) 5 wt %, and (▼) 0 wt %.

mer matrix, LCTEs of the filler and the matrix, bond between the filler and the matrix, as well as the degree of polymerization of the resin.[43,44] Figure 7 presents LCTE of SiC_w-filled BEP893 at various contents of the filler. The figure evidently reveals that the LCTE systematically decreases with an increase in the SiC_w content. The reasons for this phenomenon are attributed to the adamantine nature of the whisker with a reported LCTE value as low as 4.7 ppm $^{\circ}C^{-1}$ (ref. 42) and the substantial interfacial interaction between the whisker and the matrix. From this figure, the LCTE value of the unfilled BEP893 was determined to be 64 ppm C^{-1} whereas those of the filled BEP893 are ranging from 51 ppm$^{\circ}$ C^{-1} at 5% by weight of SiC_w to 28 ppm $^{\circ}C^{-1}$ at 20% by weight of SiC_w. The SiC_w is, therefore, useful in lowering the LCTE of the BEP893 matrix. Low LCTE composite is required in some applications such as an electronic encapsulant. In our case, the SiC_w loading of 10% by weight in the BEP893 matrix was chosen for further investigation to compare the composite properties obtained by microwave cure and by

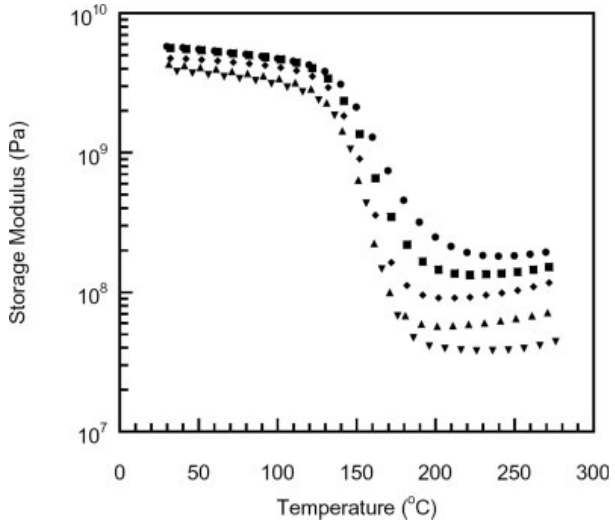

Figure 5 Effect of SiC_w loading on storage modulus of fully cured BEP893 composites: (●) 20 wt %, (■) 15 wt %, (◆) 10 wt %, (▲) 5 wt %, and (▼) 0 wt %.

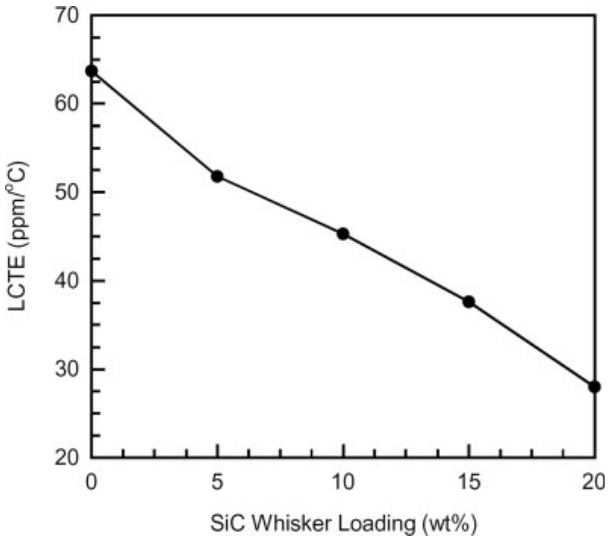

Figure 7 Linear coefficient of thermal expansion (LCTE) of SiC_w-filled BEP893.

conventional heat cure. The loading had been shown to provide sufficient microwave coupling as discussed in the previous section.

Comparison between microwave cured and conventional heat cured BEP893 composites

Figure 8 is the overlay plot of DSC thermograms of BEP893 molding compound at 10% by weight of the SiC_w cured isothermally at 200°C using a conventional oven. The graphs exhibit a systematic decrease in the exothermic curing peak as well as the evolution of T_g of the composite at different curing time. In addition, the peak exotherms were observed to slightly shift to higher temperature and the T_g expectedly increases with the degree of cure.

Figure 9 exhibits the DSC thermograms of the 10% by weight SiC_w-filled BEP893 after curing with microwave at 100, 200, and 300 W using constant cure time of 30 min. It can be clearly seen that the microwave input power significantly affects on the degree of cure of the BEP893 molding compound. Within 30 min, the input microwave power of 300 W was found to completely cure the BEP893 molding compound as signified by the disappearance of the exothermic peak of the DSC thermogram. Only partially cured samples, however, were obtained using 100 and 200 W of the input power. As a consequence, the microwave input power of 300 W was selected to process our molding compound. The optimal microwave irradiation time for curing the BEP893 molding compound using the input power of 300 W was also studied.

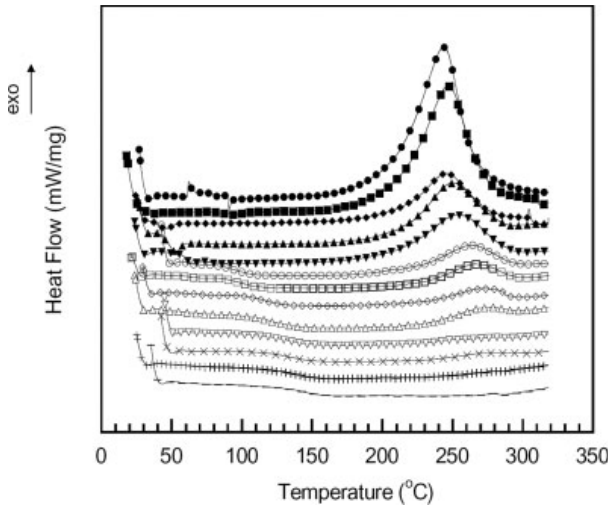

Figure 8 DSC thermograms at different cure time of BEP893 molding compound at 10% by weight of SiC_w: (●) 0 min, (■) 10 min, (◆) 20 min, (▲) 30 min, (▼) 40 min, (○) 50 min, (□) 60 min, (◇) 90 min, (△) 120 min, (▽ 150 min, (×) 180 min, (+) 240 min, and (−) 340 min.

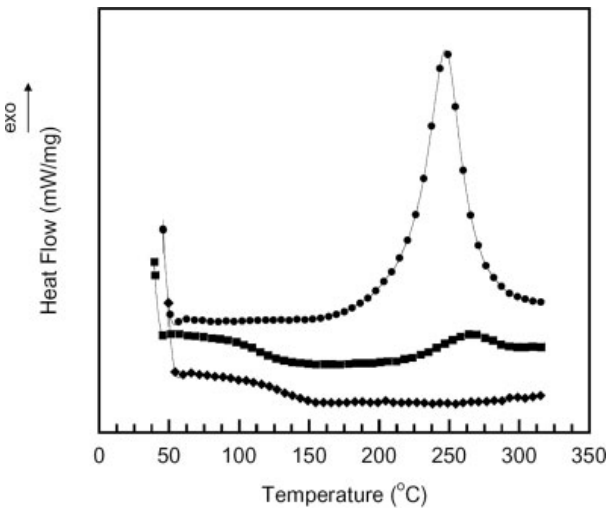

Figure 9 DSC thermograms of 10% by weight of SiC_w-filled BEP893 composites at different microwave powers (irradiation time = 30 min): (●) 100 W, (■) 200 W, and (◆) 300 W.

Figure 10 shows the effect of irradiation time on the conversion of the BEP893 molding compound filled with 10% by weight of SiC_w using a microwave input power of 300 W. The variable cure time of up to 90 min was examined and the cured samples were taken for DSC analysis. From the thermograms, the curing exotherm of the BEP893 molding compound was observed to be drastically reduced even when the cure time of only 5 min was used. The conversion-time diagram of the microwave heated BEP893 molding compound at 300 W and its

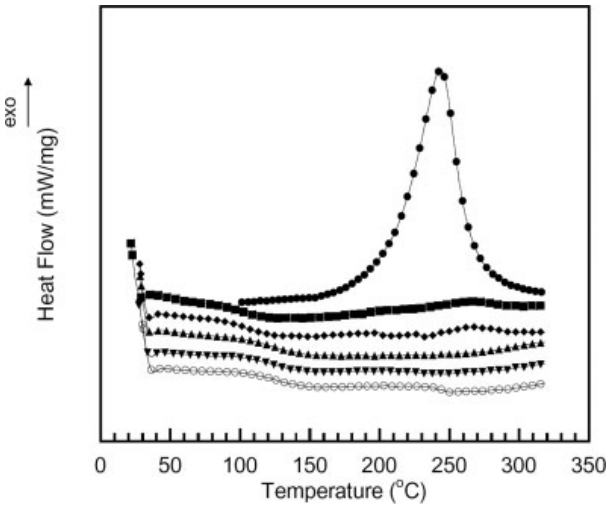

Figure 10 Effect of microwave irradiation time on conversion of 10% by weight of SiC_w-filled BEP893 molding compound at irradiation power = 300 W: (●) 0 min, (■) 5 min, (◆) 10 min, (▲) 20 min, (▼) 30 min, and (○) 90 min.

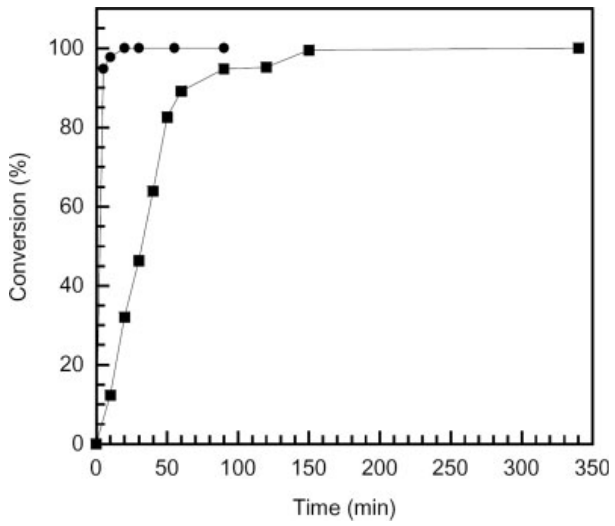

Figure 11 Conversion-time diagram of BEP893 filled with 10% by weight of SiC_w: (●) microwave cured at 300 W, (■) heat cured at 200°C.

conventional heat cured sample at 200°C is shown in Figure 11.

The conversion of each molding compound was calculated from the following equation.

$$\% \text{ conversion } (\alpha) = \frac{(\Delta H_0 - \Delta H)}{\Delta H_0} \quad (1)$$

where ΔH_0 is the curing enthalpy of the starting resin and ΔH is the curing enthalpy of the partially cured sample. Both enthalpies were determined from area under the exotherm in the DSC curve.[20,45]

Figure 11 evidently reveals the main advantage of using microwave technique to accelerate the curing process of the molding compound. From the plot, the curing time of 5 min at the microwave power of 300 W renders the molding compound with about 95% degree of conversion while the curing time of 10 min can provide a degree of conversion of nearly 100%. In the case of a heat cured sample at 200°C, the heating time of at least 150 min was necessary for the same sample to achieve the same degree of conversion. The potential energy saving from a substantial decrease in the processing time utilizing microwave irradiation was, thus, obtained.

The T_g of the BEP893 composites also increases in accordance with the degree of cure. The corresponding T_g-conversion curves of the above microwave cured and conventional heat cured samples, i.e., the systems shown in Figures 8 and 10, are also plotted in Figure 12. The curve shows the development of T_g as a function of percent conversion revealing the trend typically observed in several thermosets.[46–48] In the figure, slightly lower T_g values of the microwave cured samples than those of the conventional heat cured samples were observed. The different heating mechanisms i.e., by conduction throughout the whole sample in a conventionally cured sample and a sporadic heating from the surface of tiny SiC_w as well as the inside-out heating mechanism of the microwave during the processing may be responsible for the observed discrepancy.

Figure 13 depicts the dynamic mechanical characteristics of the fully cured BEP893 composites processed by microwave radiation. It was observed that the storage modulus at room temperature of the composite was about 5.5 GPa which is comparable

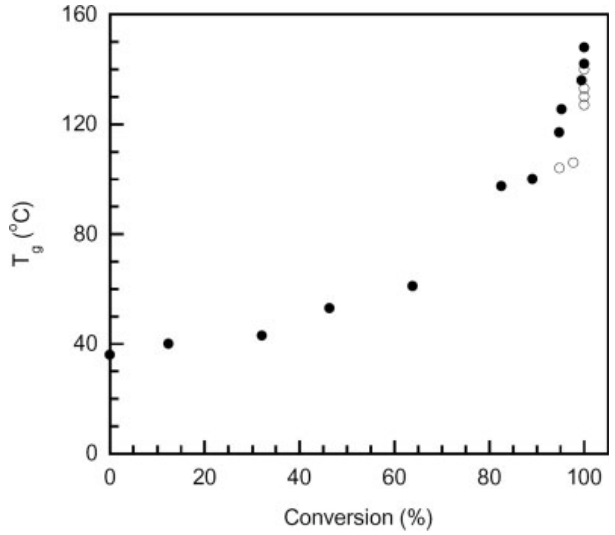

Figure 12 Glass transition as a function of cure conversion of 10 by weight SiC_w-filled BEP893: (○) microwave cured at 300 W, (●) heat cured at 200°C.

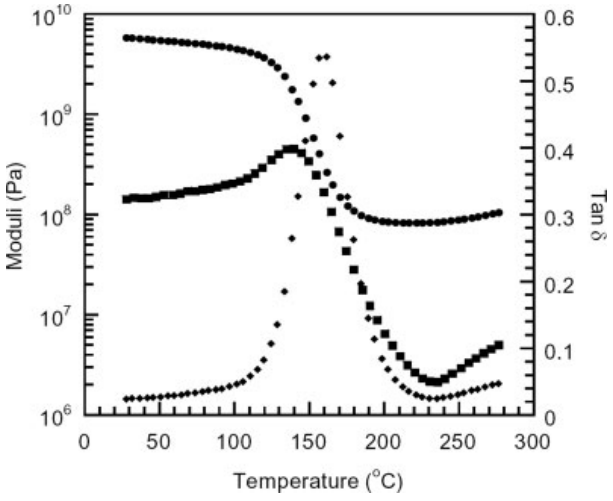

Figure 13 Dynamic mechanical properties of microwave-treated BEP893 composite: (●) storage modulus, (■) loss modulus, and (◆) tan δ.

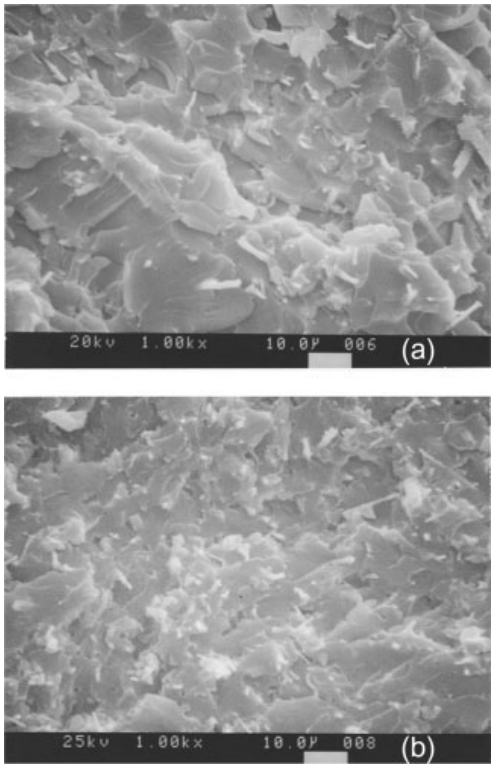

Figure 14 SEM micrographs showing fracture surface of BEP893 composites: (a) microwave cured, (b) heat cured.

to the value of 5.1 GPa of the BEP893 composite conventionally cured shown in Figure 5. The $T_{g,\mathrm{DMA}}$ of the microwave cured sample was determined to be 140°C which is slightly lower than the value of 145°C of the conventional heat cured sample shown in Figure 6. This phenomenon is consistent with the DSC result explained in the previous section.

SEM micrographs of the fracture surface of BEP893 composites cured by microwave irradiation and heat are shown in Figure 14. The micrographs reveal similarity in fracture surface morphology of the microwave cured and the conventional heat cured composite. In both cases, the fracture surfaces show substantial adhesion between the whisker and the matrix as seen from the tight interfaces between the two components with relatively short whisker pull-out length. The good interfacial adhesion of the filler and the matrix also explains the enhancement in dynamic mechanical properties and glass transition temperature of the obtained composites.

CONCLUSIONS

Microwave processing ability and thermomechanical properties of SiC_w-filled BEP893 were investigated. SiC_w was observed to effectively assist the microwave processability of the BEP893 resin. Optimal amount of SiC_w of 10% by weight at relatively low microwave power input of 300 W was found to sufficiently cure the BEP893 resin using a curing time of about 10 min. Microwave cured sample yielded slightly lower T_g than the conventionally cured sample. The different heating mechanisms of the conventional heat-cured and the microwave-cured samples are thought to be responsible for the discrepancies. SEM pictures of the composite fracture surface revealed substantial interfacial adhesion between the BEP893 matrix and the whisker.

References

1. Ishida, H. U.S. Pat. 5,543,516 (1996).
2. Low, H. Y.; Ishida, H. J Polym Sci Part B: Polym Phys 1998, 36, 1935.
3. Ishida, H.; Sanders, D. P. J Polym Sci Part B: Polym Phys 2000, 38, 3289.
4. Wang, Y. X.; Ishida, H. J Appl Polym Sci 2002, 86, 2953.
5. Ning, X.; Ishida, H. J Polym Sci Part A: Polym Chem 1994, 32, 1121.
6. Ning, X.; Ishida, H. J Polym Sci Part B: Polym Phys 1994, 32, 921.
7. Ishida, H.; Allen, D. J. J Polym Sci Part B: Polym Phys 1996, 34, 1019.
8. Ishida, H.; Low, H. Y. Macromolecules 1997, 30, 1099.
9. Ishida, H.; Rimdusit, S. Thermochim Acta 1998, 320, 177.
10. Ishida, H. U.S. Pat. 5,900,447 (1999).
11. Rimdusit, S.; Tanthapanichakoon, W.; Jubsilp, C. J Appl Polym Sci 2006, 99, 1240.
12. Su, Y. C.; Yei, D. R.; Chang, F. C. J Appl Polym Sci 2005, 95, 730.
13. Kimura, H.; Matsumoto, A.; Hasegawa, K.; Ohtsuka, K.; Fukuda, A. J. Appl Polym Sci 1998, 68, 1903.
14. Kimura, H.; Matsumoto, A.; Hasegawa, K. K.; Fukuda, A. J Appl Polym Sci 1999, 72, 1551.
15. Kimura, H.; Murata, Y.; Matsumoto, A.; Hasegawa, K.; Ohtsuka, K.; Fukuda, A. J Appl Polym Sci 1999, 74, 2266.
16. Kimura, H.; Matsumoto, A.; Sugito, H.; Hasegawa, K.; Ohtsuka, K.; Fukuda, A. J Appl Polym Sci 2001, 79, 555.
17. Rimdusit, S.; Ishida, H. Polymer 2000, 41, 7941.
18. Rimdusit, S.; Ishida, H. J Polym Sci Part B: Polym Phys 2000, 38, 1687.
19. Takeichi, T.; Guo, Y.; Rimdusit, S. Polymer 2005, 46, 4909.
20. Rimdusit, S.; Pirstpindvong, S.; Tanthapanichakoon, W.; Damrongsakkul, S. Polym Eng Sci 2005, 45, 288.
21. Takeichi, T.; Guo, Y.; Agag, T. J Polym Sci Part A: Polym Chem 2000, 38, 4165.
22. Wei, J. B.; Shidaker, T.; Hawley, M. C. Trends Polym Sci 1996, 4, 18.
23. Bur, A. J. Polymer 1985, 26, 963.
24. Hill, D. J. T.; George, G. A.; Rogers, D. G. Polym Adv Technol 2001, 12, 169.
25. Rogers, D. G.; Marand, E.; Hill, D. J. T.; George, G. A. High Perform Polym 1999, 11, 27.
26. Boey, F. Y. C.; Yap, B. H.; Chia, L. Polym Test 1999, 18, 93.
27. Wei, Y.; Hawley, M. C.; Delong, J. D.; Demeuse, M. Polym Eng Sci 1993, 33, 1132.
28. Courtney, T. H. Mechanical Behavior of Materials; McGraw-Hill: Singapore, 1990.
29. Wypych, G. Handbook of Fillers, 2nd ed.; Chem Tech Publishing: Toronto, 2000.
30. George, C.; Rechardson, G. C.; Sauer, J. A. Polym Eng Sci 1976, 16, 252.

31. Sohn, M. S.; Kim, K. S.; Hong, S. H.; Kim, J. K. J Appl Polym Sci 2003, 87, 1595.
32. Jubsilp, C.; Takeichi, T.; Covavisaruch, S.; Tanthapanichakoon, W.; Rimdusit, S. In Proceedings of the RP Asia, Bangkok, Thailand, 1–2 September, 2004.
33. Baziard, Y.; Gourdenne, A. Eur Polym Mater 1988, 24, 873.
34. Bouazizi, A.; Gourdenne, A. Eur Polym Mater 1988, 24, 889.
35. Wu, C. Y.; Benatar, A. Polym Eng Sci 1997, 37, 738.
36. Kitano, T.; Tanegashima, T.; Saha, P. In The First Asian-Australasian Conference on Composite Materials (ACCM-1); Asian-Australasian Association for Composite Materials (AACM): Osaka, Japan, 7–9 October, 1998; Vol. 1, p 217.
37. Fei, W. D.; Hu, M.; Yao, C. Mater Chem Phys 2002, 77, 882.
38. Tsutsumi, N.; Takeuchi, N.; Kiyotsukuri, K. J. Polym Sci Part B: Polym Phys 1991, 29, 1085.
39. Taguchi, Y.; Tanaka, M. J Appl Polym Sci 2003, 88, 483.
40. Wang, Q.; Xue, Q.; Liu, W.; Shen, W. J Appl Polym Sci 1999, 74, 2611.
41. Yang, T. C. K.; Tsai, S. H. Y.; Wang, S. F.; Juan, C. C. Compos Sci Technol 2002, 62, 655.
42. Ledoux, M. J.; Huu, C. P. CaTTech 2001, 5, 226.
43. Yamaguchi, R.; Powers, J. M.; Dennison, J. B. Oper Dent 1989, 14, 64.
44. Soderholm, K. J. J Dent Res 1984, 63, 1321.
45. Montserrat, S.; Flagué, C.; Pagès, P.; Málek, J. J Appl Polym Sci 1995, 56, 1413.
46. Barral, L.; Cane, J.; López, A. J.; López, J.; Nagueira, P.; Ramírez, C. J Appl Polym Sci 1996, 61, 1553.
47. Núńez, L.; Taboada, J.; Fraga, F.; Núńez, M. R. J Appl Polym Sci 1997, 66, 1377.
48. Simon, S. L.; Gillham, J. K. J Appl Polym Sci 1993, 47, 461.

Effect of Novel Benzoxazine Reactive Diluent on Processability and Thermomechanical Characteristics of Bi-Functional Polybenzoxazine

Chanchira Jubsilp,[1] Tsutomu Takeichi,[2] Sarawut Rimdusit[1]

[1]*Polymer Engineering Laboratory, Department of Chemical Engineering, Faculty of Engineering, Chulalongkorn University, Bangkok 10330, Thailand*
[2]*School of Materials Science, Toyohashi University of Technology, Tempaku-cho, Toyohashi 441-8580, Japan*

Received 22 September 2006; accepted 22 November 2006
DOI 10.1002/app.25929
Published online 28 February 2007 in Wiley InterScience (www.interscience.wiley.com).

ABSTRACT: Effects of a monofunctional benzoxazine diluent (Ph-a) on properties of a bifunctional benzoxazine resin (BA-a) have been investigated. The BA-a/Ph-a mixtures are miscible in nature rendering the properties highly dependent on their compositions. The viscosity of the BA-a resin can be reduced to one third using only about 10% by weight the Ph-a diluent. The addition of the Ph-a resin into the BA-a resin can also lower the liquefying temperature of the resin mixtures whereas the gel point is marginally decreased. The gel point, which depends on the BA-a/Ph-a mixtures and the cure temperature, was determined by the frequency independence of loss tangent in the vicinity of the sol-gel transition. The relaxation exponent values of the copolymer were found to be 0.24–0.55, which is dependent on the cure temperature. Gel time of the BA-a/Ph-a systems decreases with increasing temperature according to an Arrhenius relation with activation energy of 60.6 ± 1.5 kJ/mol. Flexural moduli of the BA-a/Ph-a polymers also increase with the Ph-a mass fraction, however, with the sacrifice of their flexural strength and glass-transition temperature. J Appl Polym Sci 104: 2928–2938, 2007

Key words: gelation; thermal properties; modification; curing of polymers; thermosets

INTRODUCTION

As polymer applications have been diversified, the improvement of their properties particularly by modification of the existing polymers becomes increasingly important. For instance, a diluent has been used in several polymers or resins to formulate solvent-free compounds for coating, adhesive, or composite applications.[1–6] In the composite fabrication process, the resin viscosity is an important variable, affecting the resin flow-out and wetting characteristics. Furthermore, diluted resins are employed in some formulations to achieve easier handling, increase filler loading, and reduce costs. In the past, organic solvents have been used extensively to lower resin viscosity. However, because of recent stricter environmental regulations on the release of volatile organic compounds (VOC), solvent use has become increasingly restrictive.[4]

Correspondence to: S. Rimdusit (sarawut.r@chula.ac.th).
Contract grant sponsors: Research Grant for Mid-Career University Faculty of the Commission on Higher Education, Ministry of Education, Thailand; Thailand Research Fund 2005–2007; Affair of Commission for Higher Education-CU Graduate Thesis Grant 2005.

Journal of Applied Polymer Science, Vol. 104, 2928–2938 (2007)

Generally, there are two classes of diluents. A reactive diluent is the ingredient that actually undergoes chemical reaction with the resin and becomes part of the polymeric structure. The other type is a nonreactive diluent, which can also lower the viscosity of the base resin but does not take part in the polymer structure formation. The class of resin that most widely used as a reactive diluent is epoxy resin. This type of reactive diluent was reported to provide good properties and enhance processing characteristics of the base resin.[1,4–6] Urethane prepolymer as well as unsaturated polyester had also been investigated as reactive diluents of some major polymer constituents.[7,8] In recent years, a novel class of thermosetting resin based on a benzoxazine structure has gained substantial attraction because of some of its intriguing properties.

Benzoxazine resins were reported to provide self-polymerizable crosslinking system with high thermal and mechanical integrity. The resins are capable of undergoing ring-opening polymerization upon heating without strong acid or base catalysts; therefore, no condensation by-products are released during a fabrication process. Moreover, polybenzoxazines possess several outstanding properties such as good dimensional stability, low moisture absorption, and rela-

tively high glass-transition temperature even though they have relatively low crosslinking density.[6,9–11]

A relatively low a-stage viscosity, one of the most useful properties of benzoxazine resins, results in an ability of the resins to accommodate relatively large quantity of filler while still maintaining their good processability when compared with traditional phenolic resins. Ishida and Rimdusit[10] reported that the use of low melt viscosity benzoxazine resins filled with boron nitride ceramics could improve the composite thermal conductivity with the value as high as 32.5 W/mK at the maximum filler loading of 78.5% by volume. In the system of polybenzoxazine wood, substantial amount of woodflour filler (i.e., up to 70% by volume) was reported to be incorporated in the polybenzoxazine matrix with a significant enhancement in the resulting thermal and mechanical properties of the obtained wood composites.[12]

As some types of bifunctional benzoxazine resins are solid at room temperature, many studies have been done to utilize reactive diluents to lower liquefying temperature as well as to further reduce melt viscosity of the benzoxazine resins. For example, Ishida and Allen[1] reported that an addition of liquid epoxy (EPON825) to a polybenzoxazine greatly increased a crosslink density of the thermosetting matrix and strongly influenced its mechanical properties besides an obvious ability of the epoxy diluent to lower the liquefying temperature of the resin mixtures. Moreover, Rimdusit et al.[5] showed that toughness of polymer alloys of rigid polybenzoxazine and low viscosity flexible epoxy (EPO732) systematically increased with the amount of the epoxy due to an addition of more flexible molecular segments in the polymer hybrids. Although a significant reduction in viscosity and liquefying point was obtained using the epoxy, the resulting benzoxazine-epoxy resin mixtures required higher curing temperature than that of the neat benzoxazine resin. The addition of a small fraction of phenolic novolac resin as an initiator into the benzoxazine-epoxy mixtures was reported to be crucial to help lowering their curing temperature.[6,13]

A liquid monofunctional benzoxazine resin had also been investigated as a reactive diluent of solid benzoxazine resins. The melt viscosity of a bifunctional benzoxazine resin, a bisphenol-A-aniline type (BA-a), was reported to be substantially reduced by the use of a monofunctional benzoxazine resin i.e., 4-cumylphenol-aniline type (C-a).[4] However, the addition of the C-a resin into the solid BA-a resin was reported to lower a crosslink density of the polymer network and led to the decrease in thermal degradation temperature and char yield of the polymer hybrids. Recently, Wang and Ishida[14] investigated a series of monofunctional benzoxazine resins. In their arylamine-based resins, a monofunctional phenol-aniline type benzoxazine (Ph-a) showed superior processability as well as thermal stability to the phenol-toluidine type (Ph-mt) and the phenol-xylidine type (Ph-35x) resins. Degradation temperature and char yield of the Ph-a polymer were also reported to exhibit the values even greater than those of its bifunctional counterpart i.e., BA-a polymer. Its $T_{g,DSC}$ of 142°C is the highest among the three monofunctional resins tested although the value is lower than that of the bifunctional BA-a polymer i.e., 160°C. Finally, curing kinetic analysis of a random copolybenzoxazine of BA-a type and Ph-a type resins has also been reported to exhibit an activation energy of about 50–84 kJ/mol.[15] The obtained activation energy of the copolybenzoxazine is also relatively close to that of the BA-a type resin ($E = 81$ kJ/mol).[15–18]

In this investigation, the Ph-a benzoxazine resin is examined as a novel reactive diluent of a bifunctional benzoxazine resin i.e., BA-a resin. Since the structure of the Ph-a resin resembles the BA-a resin chemically, a miscible mixture of the Ph-a and the BA-a resins should be expected. The processability, thermal, and mechanical properties of the resulting polymer hybrids are also studied.

EXPERIMENTAL

Materials

Monofunctional and bifunctional benzoxazine resins used are phenol-aniline type (Ph-a) and bisphenol-A-aniline type (BA-a). The synthesis procedures are followed those mentioned in Ref. 14. The chemical structures of these resins are shown in Scheme 1. Bisphenol-A was kindly supplied by Thai Polycarbonate Co., Ltd. (TPCC). Formaldehyde was obtained from Merck Co. Phenol and aniline were obtained from Fluka Chemicals Co. The as-synthesized Ph-a resin is a clear yellowish liquid at room temperature while the as-synthesized BA-a benzoxazine resin is a light yellow solid at room temper-

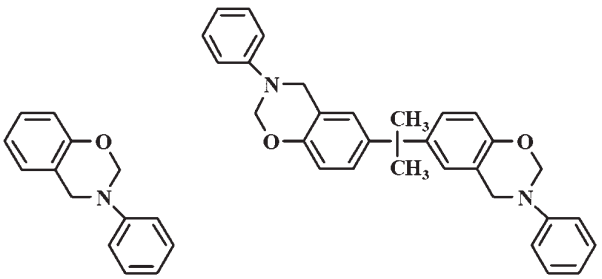

(a) (b)

Scheme 1 (a) The reactive diluent-Ph-a monofunctional benzoxazine monomer structure and (b) the BA-a bifunctional benzoxazine monomer structure.

ature and can be molten to yield a low viscosity resin at about 80°C. The BA-a resin was ground to fine powder and both were kept in a refrigerator prior to use.

Specimen preparation

BA-a/Ph-a polybenzoxazine specimens were prepared by weighing a desired amount of the resin mixture in an aluminum container. The binary systems to be investigated are BP91, BP82, BP73, BP64, BP55, and BP28. In the nomenclature, B stands for the bifunctional BA-a resin whereas P is the monofunctional Ph-a resin. The numbers after the letters are the mass ratio of the two monomers in the respective order. The two resins were mixed mechanically at 80°C for about 15 min to obtain a homogeneous mixture. The mixture was then poured onto a metal mold and cured in an air-circulating oven using a step heating profile as follows to ensure fully cured condition: 100°C for 45 min, 120°C for 45 min, 160°C for 90 min, and 200°C for 120 min. The densities of the poly(BA-a), the poly(Ph-a), and the BA-a/Ph-a polymer hybrids were determined by a water displacement method, ASTM D792-00 (Method A). The dimension of each specimen is $25 \times 60 \times 3$ mm^3.

Rheological property measurement

Dynamic shear viscosity measurements were performed on a parallel plate rheometer using HAAKE RheoStress model RS600. Disposable aluminum plates having 20 mm in diameter were preheated for 30 min with the gap zeroed at the testing temperature. The void-free monomer mixture, which was liquefied at 80°C, was then poured onto the lower plate and the gap was set to 0.5 mm. The temperature was immediately equilibrated at the set point for about 180 s and the test was then started.

Differential scanning calorimetry

The curing behaviors of BA-a/Ph-a resin mixtures were investigated using a differential scanning calorimeter (DSC) model DSC 2910 from TA Instruments. Specimen mass of about 5 mg was sealed in a nonhermetic aluminum pan with lid. The heating rate used was 10°C/min from 30 to 300°C. The experiment was performed under nitrogen purging.

Thermogravimetric analysis

Thermal decomposition characteristic of each specimen was determined using a thermogravimetric analyzer from Perkin–Elmer (Diamond TG/DTA). The experiment was performed under nitrogen purging with a constant flow of 100 mL/min. Sample mass of 15–20 mg was heated using a linear heating rate of 20°C/min from room temperature to 800°C.

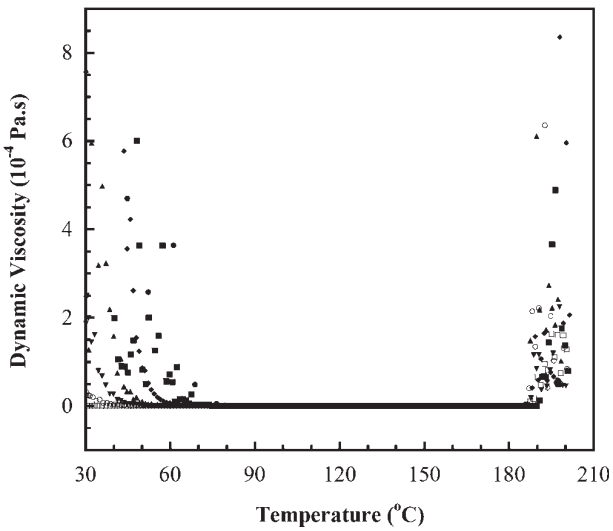

Figure 1 Processing window of the BA-a/Ph-a resin mixtures at various Ph-a resin using a heating rate of 2°C/min: (●) BA-a resin, (■) BP91, (◆) BP82, (▲) BP73, (▼) BP64, (○) BP55, (□) Ph-a resin.

Dynamic mechanical analysis

Dynamic mechanical properties of the specimens were obtained using a dynamic viscoelastic analyzer model DMA 242 C from Netzsch Inc. The test was done under a three point bending mode. The strain amplitude used was 30 μm at the frequency of 1 Hz. The specimen was heated at a rate of 2°C/min from 30 to 250°C. The specimen is $52 \times 10 \times 2.5$ mm^3. Glass-transition temperature was taken from the temperature at the maximum point on the loss modulus curve.

Bending test

The flexural behaviors of the cured copolymers were determined using a universal testing machine (Instron Instrument, model 5567) at room temperature. The specimens were tested according to ASTM D790-00 (Method I). A crosshead speed of 1.2 mm/min was used. Three specimens from each copolymer composition were tested and the average values were reported.

RESULTS AND DISCUSSION

Chemorheological properties of BA-a/Ph-a resin mixtures

All BA-a/Ph-a resin mixtures are miscible giving homogenous and transparent liquid mixtures. The effect of the Ph-a benzoxazine resin on the chemorheology of the BA-a/Ph-a resin mixture is shown in Figure 1. In the rheograms, the temperature of the resin mixture was ramped from about 30°C up to the temperature

beyond the gel point of each sample using a heating rate of 2°C/min and the dynamic viscosity was recorded. On the left hand side of Figure 1, we can see that the liquefying temperature of the binary mixture as indicated by the lowest temperature that the viscosity rapidly approaches its minimum value significantly decreases with increasing the Ph-a mass fraction. For consistency, the temperature at the viscosity value of 1000 Pa s was used as a liquefying temperature of each resin. On the basis of this convention, the liquefying temperatures of BA-a resin, BP82 and BP64 resins are 73, 58, and 42°C, respectively. This is due to the fact that the Ph-a resin used is liquid while the BA-a resin is solid at room temperature. The addition of the liquid Ph-a in the solid BA-a resin yielded a softer solid at room temperature ranging from BP91 to BP64. With increasing the Ph-a mass fraction beyond 40% by weight i.e., BP64, the resin mixture became highly viscous liquid with decreasing viscosity down to the liquid Ph-a having lowest viscosity at room temperature. In practice, lowering the resin liquefying temperature obviously enables the use of lower processing temperature for a compounding process, which is desirable in various composite applications.

On the right hand side of Figure 1, gel temperature of each resin mixture can also be determined. Interestingly, the gel temperature of each resin ranging from BA-a, BP91, to BP55 shows minor influence by an increase in the Ph-a fraction compared to its effect on the liquefying temperature. In this case, the maximum temperature at which the viscosity was rapidly raised above 1000 Pa s was used as gel temperature of each resin. The gel temperatures of BA-a, BP82, BP64, and Ph-a were determined to be 190, 187, 185, and 185°C, respectively. As a result, the addition of the Ph-a diluent seems to marginally affect the gel temperature of the BP resin mixtures with the value of only few degrees lower than that of the BA-a resin. In general, the opposite trend i.e., an increase in the gel temperature with an addition of a reactive diluent has been reported.[19] The addition of the Ph-a diluent to the BA-a resin was, therefore, found to largely maintain the thermal curing or processing condition of the obtained resin mixtures. Furthermore, all the tested BP resin mixtures can maintain their relatively low viscosity within the temperature range of 80–185°C. This behavior provides sufficiently broad processing window for a compounding process in a composite manufacturing.

Dynamic shear viscosity at 90°C of BA-a/Ph-a resin mixture as a function of Ph-a resin content is exhibited in Figure 2. From the experiment, the mixture viscosity was found to be significantly reduced from that of the neat BA-a benzoxazine resin with increasing mole fraction of the Ph-a diluent. For instance, BP91 (mole fraction of BA-a = 0.79 and Ph-a = 0.21) possesses a melt viscosity measured at 90°C to be about 9 Pa s while that of the BA-a resin compared at the same

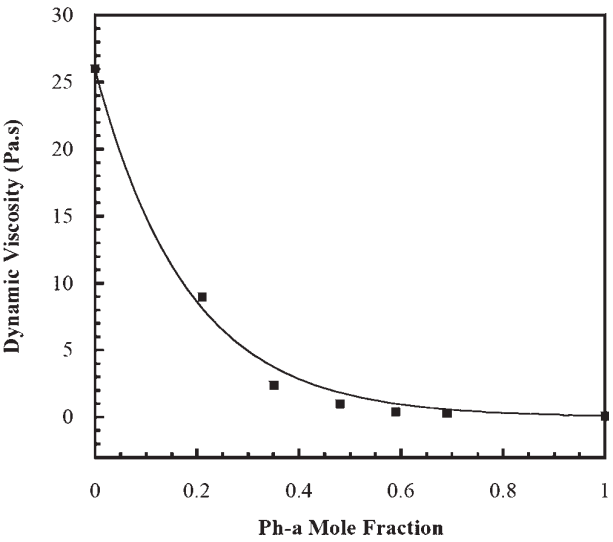

Figure 2 Dynamic viscosity at 90°C of the BA-a/Ph-a resin mixtures at various Ph-a mole fractions: Experimental data (symbol), Predicted data with the Grunberg-Nissan equation (solid line).

temperature is ~ 26 Pa s. The addition of the liquid Ph-a resin of only 10% by weight (0.21 mol fraction) can thus significantly improve processability of the BA-a resin by reducing the a-stage viscosity of the BA-a resin to be about one third. In theory, the lower viscosity of the resin can enhance the ability of the resin to accommodate greater amount of filler and increase filler wetability of the resin during the preparation of the molding compound. Furthermore, we can see that viscosity of the BA-a/Ph-a resin mixture shows a nonlinear relationship with the Ph-a mole fraction. A viscosity model of liquid mixture based on Grunberg-Nissan equation[20] was used to predict the correlation between viscosity and composition fraction. The Grunberg-Nissan equation was the most suitable equation for determining the viscosity of nonassociated liquid mixture as discussed by Monnery et al.[21] However, Irving[22] showed that a good agreement was also obtained for some associated liquid mixture. The calculation of liquid viscosity for a binary mixture using this equation is as follows:

$$\ln \eta_m = \sum_{i=1}^{c} x_i \ln \eta_i + \frac{1}{2} \sum_{i=1}^{c} \sum_{j=1}^{c} x_i x_j G_{i,j} \qquad (1)$$

where $G_{i,i} = 0$. for example, for a binary mixture ($c = 2$)

$$\ln \eta_m = x_1 \ln \eta_1 + x_2 \ln \eta_2 + x_1 x_2 G_{1,2} \qquad (2)$$

In eqs. (1) and (2), η_m is the mean viscosity of liquid mixture (Pa s); η is the viscosity of pure component i and j (Pa s); x_i and x_j are the mole fractions of the component i and j; $G_{i,j}$ is the interaction parameter (Pa s); and c is the number of components.

Since chemical structures of the BA-a benzoxazine resin and the Ph-a resin are similar, the components in a mixture should not interact exclusively with each other and thus should behave in a similar manner as an individual component.[23] Consequently, it was assumed that the interaction parameter ($G_{1,2}$) in eq. (2) would be small and could be neglected. Thus eq. (2) can be written as:

$$\ln \eta_m = x_1 \ln \eta_1 + x_2 \ln \eta_2 \quad (3)$$

In Figure 2, the calculated viscosity curve by the Grunberg-Nissan equation seems to fit well with the experimental viscosity data thus the present assumption is suitable for the prediction of the liquid viscosity of the BA-a/Ph-a resin mixtures in the entire composition range.

Investigation of the gel formation

One important aspect of thermosetting polymers is their gelation behavior, especially, the kinetics of gelation as well as gel time. Sol-gel transition, known as the gel point, is one critical phenomenon that is crucial, especially, for the material processing. The linear viscoelastic properties in a dynamic experiment are sensitive to the three-dimensional network formation and can be used to precisely examine the gel point. Measurements of oscillatory shear moduli have frequently been used to continuously monitor viscoelastic properties in chemically crosslinked networks during the gel evolution. An oscillatory experiment is preferable since minimum deformation is applied to the material, particularly the delicate gel material, at the gel point. The frequency independence principle of the loss tangent in the vicinity of the gel point in accordance with Winter-Chambon criterion has been widely used to define gel point of crosslinked polymers.[19,24–27]

In oscillatory shear mode using a rotational controlled stress rheometer, the range of stress that can be applied to the material is needed to be verified because different types of gels are able to sustain different levels of stress. Therefore, the gel must exhibit a linear relationship between stress and strain, i.e., modulus is constant in the whole stress range used. In the investigation to find the suitable stress range, the gel point is obtained using a frequency of 1 rad/s with 2.5% strain. The gelation temperature used was 140°C for each resin composition i.e., BP91, BP73, and BP55. After reaching the gel point, which was defined by the crossover of the storage and loss modulus during an isothermal cure (ASTM D4473), the temperature of each BA-a/Ph-a resin mixture was immediately lowered and equilibrated at 120°C to suppress further gelation process while still maintaining the fluidity of the sol fraction. The stress sweep experiment at the gel point of the three different compositions of the BA-a/Ph-a resin mixtures was then performed using a frequency of 1 rad/s within the stress range of 60–250 Pa. The results are shown in Figure 3. From the plots, we can observe that all of the BA-a/Ph-a systems show a fairly constant modulus in this stress range. This means that a linear viscoelastic relationship can be obtained in this chemically crosslinked systems in the vicinity of their gel points.

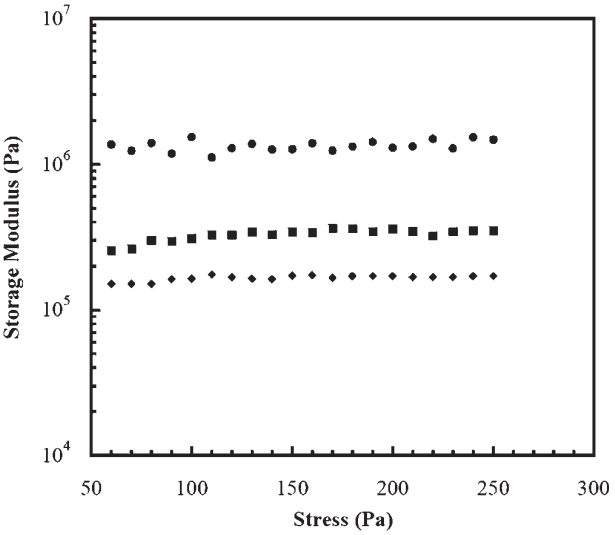

Figure 3 Stress sweep experiment at the gel points of BP systems: (●) BP91, (■) BP73, (◆) BP55.

In the rest of our experiments, the minimum constant stress value of 60 Pa will be used for gel point determination to ensure both linear viscoelastic relationship as well as minimum gel network rupturing. The dynamic moduli of a curing system under oscillatory shear, generally, follow the power law at the gel point.[19,28–30] The power law equation at the gel point may be used to examine the gel time and the corresponding value of the relaxation exponent is obtained from eq. (4)

$$\tan \delta = G''/G' = \tan(n\pi/2) \quad (4)$$

when n is the relaxation exponent.

Figure 4 is a plot of tan δ at different frequencies as a function of heating time of BP91 using the gelation temperature of 140°C. The gel time is obtained from the point where the loss tangent is frequency independent. Experimentally, it is the point where the loss tangents of different frequencies intersect each other. From the plot, the values of tan δ intersect at a time = 198 min corresponding to the gel time, t_{gel}, of this resin. The gel times for the BA-a/Ph-a systems at different temperatures were also obtained from the tan δ plots similar to that in Figure 4. The relationship of gel time as a function of temperature of the BA-a/Ph-a

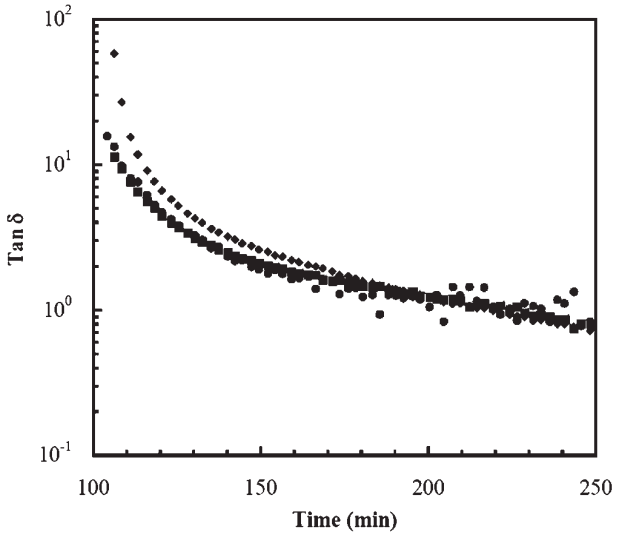

Figure 4 Loss tangent at various frequencies as a function of time for BP91at 140°C: (●) 10 rad/s, (■) 31 rad/s, (◆) 100 rad/s.

systems was presented in Table I. We can see that the gel time of all resin mixture compositions tends to decay exponentially with increasing temperature. This is due to the fact that increasing the processing temperature increases the rate of crosslinking of BA-a/Ph-a systems. Consequently, at higher temperature, the systems reach their gel points more quickly and the gel times are shorter. From the table, the gel time of BP91 ranges from 198 min at 140°C to about 63 min at 170°C. Moreover, at the same temperature, we can observe that the gel time decreases with increasing the Ph-a content, which is likely due to the faster crosslinking rates of the mixtures. For instance, at 140°C, the gel time of BP91 = 198 min, BP73 = 185 min, and BP55 = 182 min. This also implies that the curing conversion of the BP resin can also increase with the Ph-a content compared at the same processing condition.

As mentioned in eq. (4), at the gel point, a power law may be used to examine the corresponding value of the relaxation exponent, n, for each gelling systems. The relaxation exponent is a specific parameter that is related to the growing clusters in a material near the gelation threshold. For the BA-a/Ph-a systems, the relaxation exponent at the gel point was determined from the tan δ plots and by using eq. (4). Figure 5 exhibits the relaxation exponent values of BP91, BP73, and BP55 at different cure temperature. The values were almost unchanged with the resin composition. Moreover, the relaxation exponent tends to decrease with increasing the cure temperature. Recently, the relaxation exponent values of the chemical gel systems have been reported to show a nonuniversal value and vary with the gelling system. The values of the relaxation exponents of the chemical gels were reported to be 0.2–0.7 in PDMS system,[31] 0.5–0.7 in polyurethane system,[32] and 0.68–0.72 in BA-m benzoxazine system[29] etc. In this work, the relaxation exponent values of BA-a/Ph-a systems were found to be 0.24–0.55 depending on the cure temperature. This indicates that the cure temperature shows some effect on the structure of the network clusters formed at the gel point for these BA-a/Ph-a resins.

Furthermore, from the gel times calculated at different temperatures, we can determine apparent activation energies for the BA-a/Ph-a systems. The curing reaction can be represented by a generalized kinetic equation:

$$\frac{dx}{dt} = k(T)\, f(x) \tag{5}$$

where $k(T)$ is the rate constant, t is the reaction time, $f(x)$ represents an arbitrary functional form for the curing conversion, T corresponds to the temperature of the reaction. The rate constant, $k(T)$, is temperature dependent according to Arrhenius law shown in eq. (6)

$$k(T) = A \exp(-E/RT) \tag{6}$$

TABLE I
Gelation Times of BA-a/Ph-a Systems at Different Temperature

	Gelation time, T_{gel} (min)		
Temperature (°C)	BP91	BP73	BP55
140	198	185	182
150	152	147	142
160	94	89	82
170	63	62	58

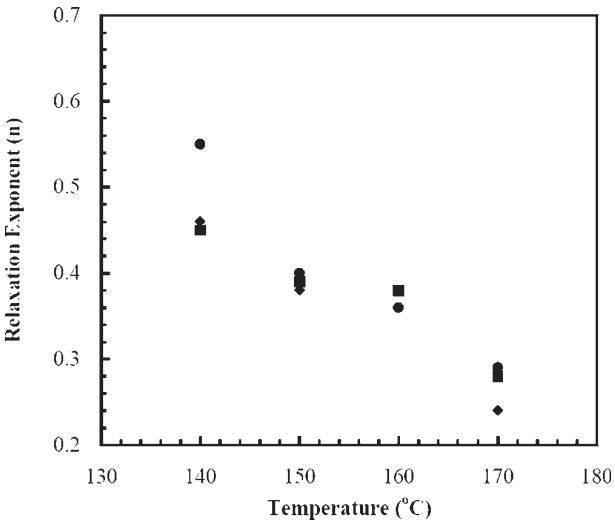

Figure 5 The relaxation exponent (n) from gel point as a function of cure temperature: (●) BP91, (■) BP73, (◆) BP55.

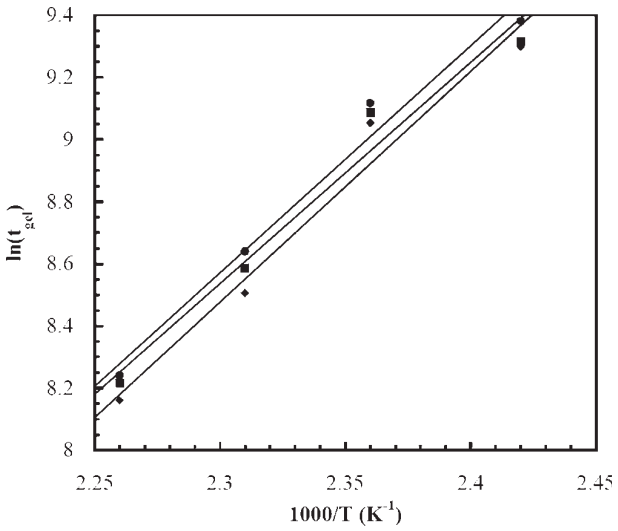

Figure 6 Plots of gel times as a function of 1/T based on rheological data at various Ph-a mass fractions: (●) BP91, (■) BP73, (◆) BP55.

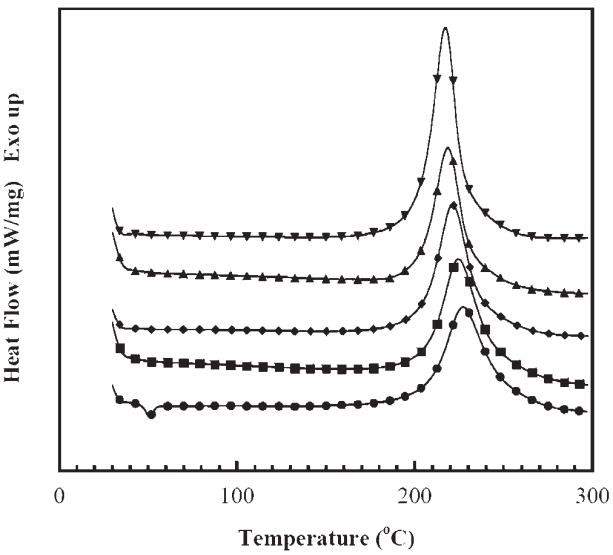

Figure 7 DSC thermograms of the BA-a/Ph-a resin mixtures at different Ph-a resin contents: (●) BA-a resin, (■) BP82, (◆) BP55, (▲) BP28, (▼) Ph-a resin.

An integration of eq. (5) from the onset of the cross-linking reaction ($t = 0$, and $x = 0$) to the gel point ($t = t_{gel}$, and $x = x_c$) yields

$$\ln(t_{gel}) = \ln\left(\int_0^{x_c} dx/f(x)\right) - \ln(A) + E/RT \quad (7)$$

where t_{gel} is the gel time, A is the pre-exponential factor, E is the activation energy, and T is temperature in Kelvin.

Thus, the activation energies for gelation can be determined from the slope of the plots between $\ln(t_{gel})$ against $1/T$ as depicted in Figure 6 and the corresponding activation energies are summarized in Table II. We can notice that the activation energy values of BP91, BP73, and BP55 are approximately the same. This means that the Ph-a reactive diluent does not significantly affect the kinetics of the gelation process of the resin mixtures. The apparent activation energy value averaged from the slopes of the plots was determined to be 60.6 ± 1.5 kJ/mol. The value is in the same range as that of epoxy molding compound, using the same technique to determine the gel point, i.e., E = 61–73 kJ/mol.[30,33]

TABLE II
Apparent Activation Energy Values Obtained from Rheological Tests for BA-a/Ph-a Systems at Various Ph-a Resin Contents

BP contents	Activation energy (kJ/mol)
BA-a	88[a]
BP91	61
BP73	59
BP55	62

[a] E-value of benzoxazine resin (BA-a) from Ref. 29.

Curing reaction investigation by calorimetry

The DSC thermograms for the curing reaction of the BA-a resin, the Ph-a diluent, and the BA-a/Ph-a mixtures at various compositions are shown in Figure 7. From the thermograms, we observed only single dominant exothermic peak of the curing reaction in each resin composition. The phenomenon suggests that the reaction to form a network structure of these binary mixtures takes place simultaneously at about the same temperature. In our previous work, the split of the curing exotherms with an addition of a reactive diluent, i.e., in benzoxazine-epoxy resin mixture, has been observed. In these resin systems, the newly formed exothermic peak at higher temperature was attributed to the interaction between the benzoxazine monomer and the epoxy diluent whereas the peak at lower temperature was due to the reaction among the benzoxazine monomers.[13]

On the contrary, the curing peak temperature observed in our BA-a/Ph-a mixtures in Figure 7 is systematically shifted to a slightly lower temperature with increasing the Ph-a diluent. This is due to the fact that the curing peak exotherm of the BA-a resin was determined to be 228°C while that of the Ph-a diluent was found to be 217°C. Our Ph-a diluent thus possesses a slightly low curing temperature comparing with the base BA-a resin. The addition of Ph-a diluent into the BA-a resin, therefore, renders a positive effect on curing reaction of the obtained resin mixture by

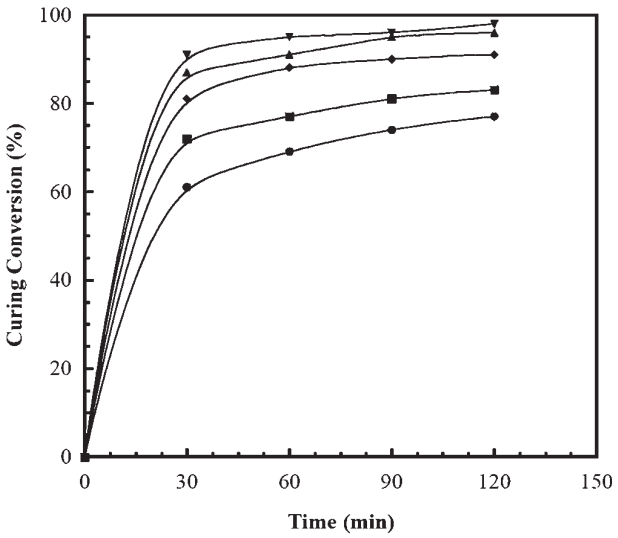

Figure 8 Conversion-time curve of thermally cured the BA-a/Ph-a mixtures at 180°C: (●) BA-a resin, (■) BP82, (◆) BP55, (▲) BP28, (▼) Ph-a resin.

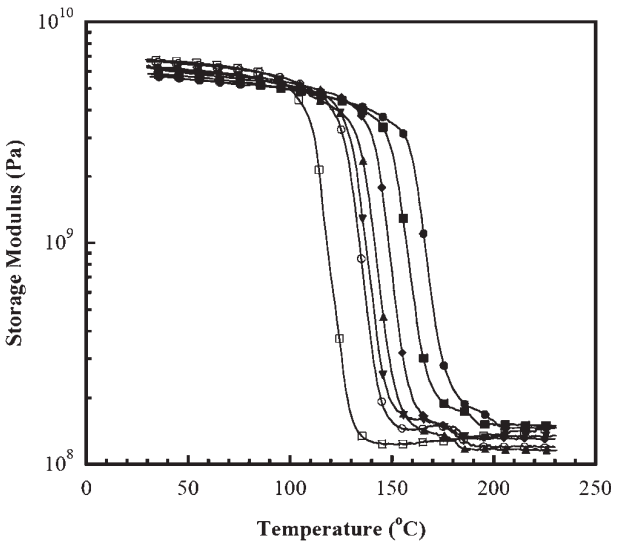

Figure 9 Storage modulus of the BA-a/Ph-a polymer as a function of temperature at different Ph-a contents: (●) poly(BA-a), (■) BP91, (◆) BP82, (▲) BP73,(▼) BP64, (○) BP55, (□) poly(Ph-a).

lowering its curing temperature even though of only marginally. A relationship between curing conversion with curing time of the BA-a/Ph-a resin mixtures at 180°C is illustrated in Figure 8. The trend of each curve is similar to the observed dramatic increase in the degree of conversion at the first 30 min of the curing program. The longer curing time beyond 30 min can increase the degree of conversion of each resin marginally with the maximum achievable conversion depending on the resin composition. From the plot, the curing conversions at 180°C and 120 min of the Ph-a, BP28, BP55, BP82 and BA-a polymers are 98, 96, 91, 83, and 76%, respectively. This result also suggests that our Ph-a reactive diluent renders a faster curing than the BA-a. Its presence in the BA-a can help lowering the curing temperature of the resulting resin mixtures.

Mechanical property of the polymer hybrids

The effect of the Ph-a composition on the dynamic mechanical properties of the BA-a/Ph-a polymers is depicted in Figures 9–11. The storage modulus in the glassy state region reflecting molecular rigidity of the BA-a/Ph-a polymer networks is shown in Figure 9. From this figure, we can clearly see that the storage modulus of the poly(Ph-a) is higher than that of the poly(BA-a). The storage modulus at the room temperature of the poly(Ph-a) exhibits a value of about 6.7 GPa whereas that of the poly(BA-a) is $\sim$ 5.7 GPa. The Ph-a network is thus stiffer molecularly than the BA-a network. Moreover, the storage modulus of the BA-a/Ph-a polymers was found to systematically increase when the Ph-a resin composition increased as a result of the addition of the more rigid molecular segments of the poly(Ph-a) into the network as discussed above. However, the presence of the Ph-a fraction in the poly(BA-a) network trends to lower the rubbery plateau modulus of the polymer hybrids as seen in Figure 9. This behavior implies that the crosslinked density of the polymer hybrids decreases with an increase of the Ph-a fraction.

The glass transition temperatures (T_g's) of the BA-a and Ph-a polymers as well as their copolymers were determined from the loss modulus peak in the dynam-

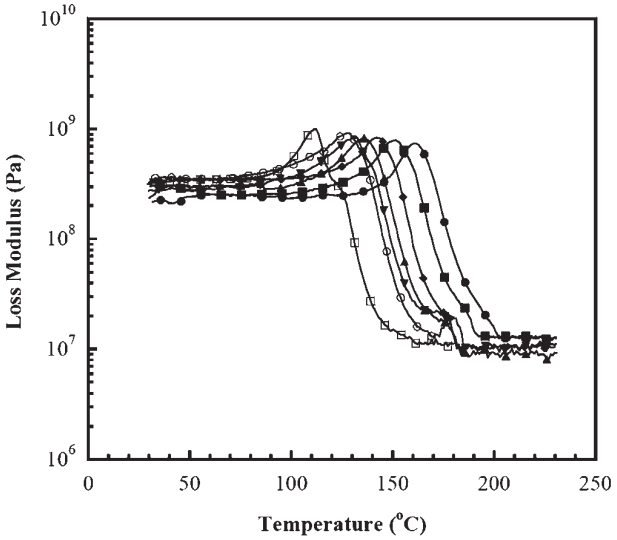

Figure 10 Loss modulus of the BA-a/Ph-a polymer as a function of temperature at different Ph-a contents: (●) poly (BA-a), (■) BP91, (◆) BP82, (▲) BP73,(▼) BP64, (○) BP55, (□) poly(Ph-a).

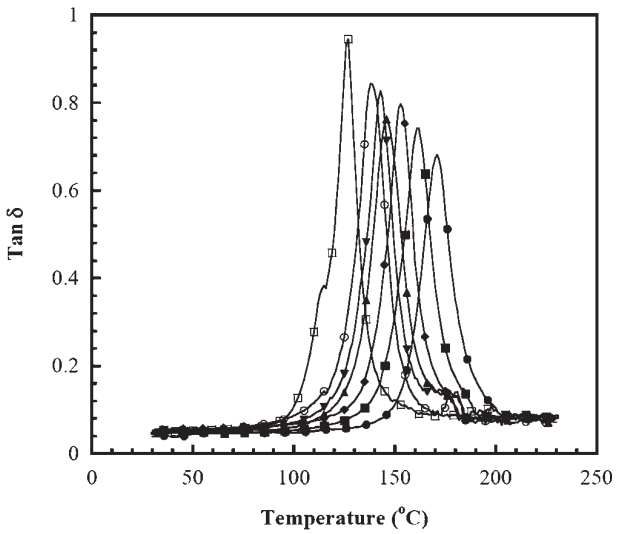

Figure 11 Tan δ of the BA-a/Ph-a polymers as a function of temperature at different Ph-a contents: (●) poly(BA-a), (■) BP91, (◆) BP82, (▲) BP73, (▼) BP64, (○) BP55, (□) poly(Ph-a).

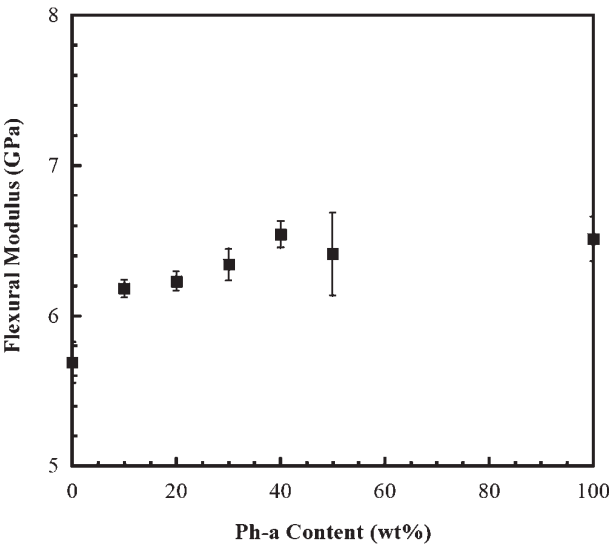

Figure 12 Flexural modulus of the BA-a/Ph-a polymers as a function of Ph-a compositions.

ical mechanical thermograms as seen in Figure 10. The average T_g, DMA of the poly(Ph-a) and poly(BA-a) were reported to be about 115 and 160°C, respectively.[5,9,12,14] In Figure 10, the T_gs of the BP polymer hybrids were expectedly found to increase with the mass fraction of BA-a polymer. In our study, the T_gs of poly(BA-a), BP82, BP64, and poly (Ph-a) were determined to be 160, 142, 128, and 111°C, respectively. The T_g values of both parent polymers are consistent with those reported elsewhere[5,9,12,14] with the T_gs of their polymer hybrids varied systematically depending on the composition of the BP polymers. The loss modulus curve for each BP composition also reveals only one α-relaxation peak suggesting the presence of a single phase material in these polymer hybrids. In theory, if the two starting materials have undergone phase separation upon copolymerization, two glass transition peaks sould be expected, one for each of the starting homopolymer.

The tan δ curve of the BA-a/Ph-a polymers at various Ph-a compositions is also illustrated in Figure 11. Again, only a single tan δ peak was observed in each BP polymer which is in good agreement with the loss modulus result in Figure 10. The magnitude of the α-relaxation from the tan δ peak reflects trend in large scale segmental mobility in the polymer network. In the network, a greater separation between crosslinks permits greater mobility of chain segments while the width of the α-relaxation peak of the tan δ curve relates to network homogeneity. From our experiment, the maximum amplitude of the α-relaxation peak was found to increase with increasing the Ph-a resin composition. This behavior suggests the lower crosslinking density of the BP polymers when the Ph-a mass fraction increases thus allowing greater segmental mobility in the polymers. The lower degree of crosslinking of the BP polymers with the amount of the Ph-a content was also confirmed by the lower rubbery plateau modulus of the polymer hybrids with increasing the amount of the Ph-a diluent as appeared in Figure 9. Moreover, the widths at half height of the α-relaxation peaks are about the same for all Ba-a/Ph-a polymers. This implies that the degree of network homogeneity of the two polymers as well as their hybrids is likely to be similar.

Figure 12 shows the flexural moduli of the specimens at different Ph-a contents. From this plot, the

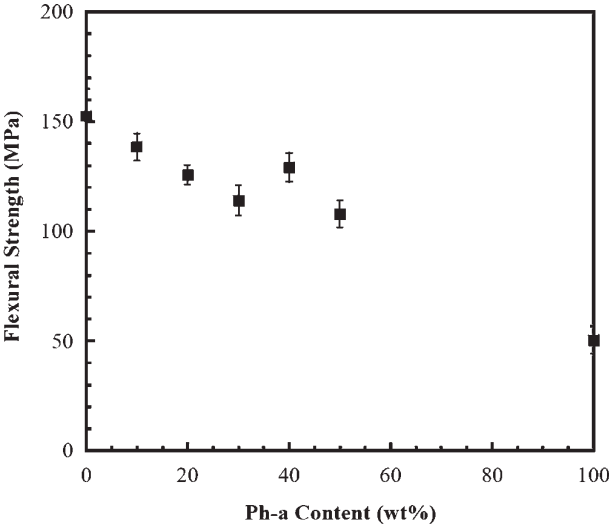

Figure 13 Flexural strength of the BA-a/Ph-a polymers as a function of Ph-a compositions.

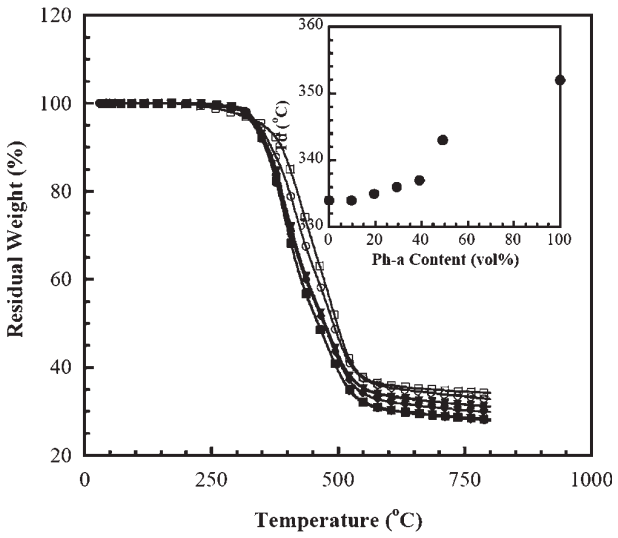

Figure 14 TGA thermograms of the BA-a/Ph-a polymers at different Ph-a mass fractions: (●) poly(BA-a), (■) BP91, (◆) BP82, (▲) BP73, (▼) BP64, (○) BP55, (□) Poly(Ph-a).

flexural moduli of the samples were found to increase with increasing the Ph-a resin. This correlation is in good agreement with the modulus values obtained from our dynamic mechanical analysis in the previous section. The flexural modulus of the poly(BA-a) was calculated to be 5.69 ± 0.14 GPa, while that of the poly(Ph-a) was 6.51 ± 0.15 GPa. Furthermore, the flexural modulus values of the BA-a/Ph-a polymers at various Ph-a contents ranging from 0 to 50% by weight tends to increase with the poly(Ph-a) mass fraction. For instance, BP55 possesses a flexural modulus value of about 6.41 ± 0.28 GPa, which is also close to that of poly(Ph-a). The phenomenon is attributed to the ability of the Ph-a diluent to easily react to form a crucial part of the BA-a polymer networks as a result of their similarity in chemical nature. In Figure 13, the flexural strength of the poly(Ph-a) was found to be significantly lower than that of the poly(BA-a) i.e., 50 MPa versus 152 MPa of poly(BA-a). Additionally, the flexural strength of the BA-a/Ph-a polymers was observed to decrease with increasing the Ph-a content in the polymer hybrids from 0 to 50% by weight. The lower degree of crosslinking of the poly(Ph-a) comparing with that of poly(BA-a) might be responsible for the observed characteristics. The phenomenon is also understandable as the Ph-a resin has functional groups only half of those of the BA-a resin. Its ability to crosslink is thus inferior to that of the BA-a resin.

Thermal degradation behaviors of BA-a/Ph-a polymers

The TGA thermograms of the poly(BA-a), the poly (Ph-a), and the BA-a/Ph-a polymers are shown in Figure 14. Intriguingly, all specimens exhibit an improvement in their degradation temperature at 5% weight loss and char yield over the poly(BA-a) with an addition of the Ph-a diluent. The degradation temperature at 5% weight loss of the poly(BA-a) was determined to be 334°C comparing with the value of 352°C of the poly(Ph-a). In addition, the decomposition temperature of the BA-a/Ph-a polymers was found to gradually increase with increasing the mass fraction of the poly(Ph-a) as shown in the inset of Figure 14. This behavior can be explained by the fact that there is no isopropyl moiety in the poly(Ph-a) structure. Therefore, the less stable, weaker moieties in the poly(Ph-a) structure are eliminated whereas in poly(BA-a), the isopropyl linkages from its bisphenol-A structure has been reported to undergo thermal decomposition at relatively lower temperature.[14,34,35]

The study on a bisphenol-A-based polybenzoxazine exposed to ultraviolet radiation has revealed that the isopropyl linkage is the reactive site of cleavage and oxidation.[36] Moreover, the substituents of poly(Ph-a) are also different from that of poly(BA-a). Poly(BA-a) has only one unblocked ortho position to form the hydroxyl group that is subjected to electrophilic aromatic substitution upon its ring-opening polymerization while the poly(Ph-a) has two unblocked positions, one at the ortho and another at the para position. The study on polybenzoxazine model dimers has also demonstrated that the absence or presence of the substituents has profound effects on thermal decomposition patterns and the char formation of the dimers. Therefore, the absence of isopropyl moiety along with the absence of substituents at both ortho and para positions is likely responsible for the greater thermal stability of the poly(Ph-a).[36,37] Other possibilities, such as fewer short-chain branches in the poly(Ph-a) structure, which can serve as the initiation sites of the degradation process, can also attribute to the improvement of its thermal stability. As a result, the char yield of the BA-a/Ph-a polymers systematically increases from that of the poly(BA-a) with an increase in the Ph-a content.

CONCLUSIONS

The monofunctional Ph-a resin can effectively serve as a reactive diluent of the bifunctional BA-a resin to further improve the latter processability. The viscosity and liquefying temperature of the BA-a/Ph-a mixtures were found to significantly decrease with the Ph-a mass fraction. The resin mixture renders miscible, homogeneous, and void-free cured specimen with the properties highly dependent on the composition of the resin mixture. The gelation exponent, n, of the BA-a/Ph-a mixtures is dependent on the cure temperature while the activation energy for the gelation pro-

cess of the BA-a/Ph-a mixtures was found to be constant and independent on the Ph-a mass fraction. The incorporation of the poly(Ph-a) into the poly(BA-a) can improve the stiffness as well as the thermal stability (in terms of degradation temperature at 5% weight loss and char yield) of the specimens whereas the T_g and flexural strength of the BA-a/Ph-a polymers were found to decrease with the Ph-a mass fraction.

The authors greatly acknowledge the Center of Excellence in Catalyst and Catalytic Reaction Engineering (Prof. Piyasan Praserthdam), Chulalongkorn University for TGA measurement. Bisphenol A is kindly supported by Thai Polycarbonate Co., Ltd. (TPCC).

References

1. Ishida, H.; Allen, D.J. Polymer 1996, 37, 4487.
2. Park, L. J.; Lee, H. Y.; Han, M.; Hong, S. K. J Colloid Interface Sci 2004, 270, 288.
3. Takeichi, T.; Guo, Y.; Rimdusit, S. Polymer 2005, 46, 4909.
4. Huang, M. T.; Ishida, H. Polym Polym Compos 1999, 7, 233.
5. Rimdusit, S.; Pirstpindvong, S.; Tanthapanichakoon, W.; Damrongsakkul, S. Polym Eng Sci 2005, 45, 228.
6. Rimdusit, S.; Ishida, H. Polymer 2000, 41, 7941.
7. Brzozowski, Z. K.; Bratychak, M. M. React Funct Polym 1997, 33, 217.
8. Takeichi, T.; Guo, Y.; Agag, T. J Polym Sci Part A: Polym Chem 2000, 38, 4165.
9. Ishida, H.; Allen, D. J. J Polym Sci Part B: Polym Phys 1996, 34, 1019.
10. Ishida, H.; Rimdusit, S. Thermochim Acta 1998, 320, 177.
11. Ishida, H. U.S. Pat. 5,543,516 (1996).
12. Rimdusit, S.; Tanthapanichakoon, W.; Jubsilp, C. J Appl Polym Sci 2006, 99, 1240.
13. Rimdusit, S.; Ishida, H. J Polym Sci Part B: Polym Phys 2000, 38, 1687.
14. Wang, Y. X.; Ishida, H. J Appl Polym Sci 2002, 86, 2953.
15. Su, Y. C.; Yei, D. R.; Chang, F. C. J Appl Polym Sci 2005, 95, 730.
16. Ishida, H.; Rodriquez, Y. Polymer 1995, 36, 3151.
17. Ishida, H.; Rodriquez, Y. J Appl Polym Sci 1995, 58, 1751.
18. Jubsilp, C.; Damrongsakkul, S.; Takeichi, T.; Rimdusit, S.; Thermochim Acta 2006, 447, 131.
19. Rimdusit, S.; Ishida, H. Rheol Acta 2002, 41, 1.
20. Grunberg, L.; Nissan, A. H. Nature 1949, 164, 799.
21. Monnery, W. D.; Svrcek, W. Y.; Mehrotra, A. K. Can J Chem Eng 1995, 73, 3.
22. Irving, J. B. Viscosity of binaryliquid mixtures: A survey of mixture equations, 1977. NEL Report 630.
23. Allen, C. A. W.; Watts, K. C.; Ackman, R. G.; Pegg, M. J. Fuel 1999, 78, 1319.
24. Kjøniksen, A. L.; Nyström, B. Macromolecules 1996, 29, 5215.
25. Chiou, B. S.; English, R. J.; Khan, S. A. Macromolecules 1996, 29, 5368.
26. Commereuc, S.; Bonhomme, S.; Verney, V.; Lacoste, J. Polymer 2000, 41, 217.
27. Meng, J.; Hu, X. C.; Boey, F. Y.; Li, L. Polymer 2005, 46, 2766.
28. Winter, H. H.; Mours, M. Adv Polym Sci 1997, 134, 167.
29. Ishida, H.; Allen, D. J. J Appl Polym Sci 2001, 79, 406.
30. Kwak, G. H.; Park, S. J.; Lee, J. R. J Appl Polym Sci 2001, 81, 646.
31. Scanlan, J. C.; Winter, H. H. Macromolecules 1991, 24, 47.
32. Winter, H. H.; Morganelli, P.; Chambon, F. Macromolecules 1988, 21, 532.
33. Halley, P. J. J Appl Polym Sci 1997, 64, 95.
34. Ishida, H.; Sanders, D. P. J Polym Sci Part B: Polym Phys 2000, 38, 3289.
35. Hemvichian, K.; Ishida, H. Polymer 2002, 43, 4391.
36. Macko, J. A.; Ishida, H. J Polym Sci Part B: Polym Phys 2000, 38, 2687.
37. Hemvichian, K.; Laobuthee, A.; Chirachanchai, S.; Ishida, H.; Polym Degrad Stab 2000, 76, 1.

Available online at www.sciencedirect.com
SCIENCE DIRECT
Thermochimica Acta 447 (2006) 131–140
thermochimica acta
www.elsevier.com/locate/tca

Curing kinetics of arylamine-based polyfunctional benzoxazine resins by dynamic differential scanning calorimetry

Chanchira Jubsilp [a], Siriporn Damrongsakkul [a], Tsutomu Takeichi [b], Sarawut Rimdusit [a,*]

[a] *Polymer Engineering Laboratory, Department of Chemical Engineering, Faculty of Engineering, Chulalongkorn University, Pathumwon, Bangkok 10330, Thailand*

[b] *School of Materials Science, Toyohashi University of Technology, Tempaku-cho, Toyohashi 441-8580, Japan*

Received 2 February 2006; received in revised form 28 April 2006; accepted 15 May 2006
Available online 22 May 2006

Abstract

In this study, the curing kinetics of polyfunctional benzoxazine resins based on arylamine, i.e. aniline and 3,5-xylidine, designated as BA-a and BA-35x, respectively, were investigated. Non-isothermal differential scanning calorimetry (DSC) at different heating rates is used to determine the kinetic parameters and the kinetic models of the curing processes of the arylamine-based polyfunctional benzoxazine resins were proposed. Kissinger, Ozawa, Friedman, and Flynn–Wall–Ozawa methods were utilized to determine the kinetic parameters of the curing reaction. BA-a resin shows only one dominant autocatalytic curing process with the average activation energy of 81–85 kJ mol^{-1}, whereas BA-35x exhibits two dominant curing processes signified by the clear split of the curing exotherms. The average activation energies of low-temperature curing (reaction (1)) and high-temperature curing (reaction (2)) were found to be 81–87 and 111–113 kJ mol^{-1}, respectively. The reaction (1) is found to be autocatalytic in nature, while the reaction (2) exhibits *n*th-order curing kinetics. In addition, the predicted curves from our kinetic models fit well with the non-isothermal DSC thermogram.

Keywords: Benzoxazine resin; Cure kinetics; Activation energy; Autocatalytic curing

1. Introduction

Polyfunctional benzoxazine resins which can be modified by changing the amine group on the ring structure were reported to provide self-polymerizable crosslink-system with high thermal and mechanical integrity [1–3]. The polymers undergo ring-polymerization upon heating without the aid of a curing agent (strong acid and alkaline); therefore, no condensation by-products are released during a fabrication process as well as no corrosion of processing equipments. Moreover, polybenzoxazines possess several outstanding properties such as near-zero shrinkage after curing, low water absorption, and relatively high glass transition temperature even though it has relatively low cross-linking density [1,4]. In recent years, Ishida and Sanders [5–7] disclosed improving thermal and mechanical properties of polybenzoxazines based on alkyl-substituted aromatic amines (e.g. BA-35x type benzoxazine). A series of benzoxazine resins have been synthesized that, upon polymerization, produced a varying amount of phenolic Mannich bridges, arylamine Mannich bridges, and methylene linkages. For the 3,5-xylidine-based benzoxazine, its thermal degradation temperature at 5% weight loss was reported to be 350 °C which is higher than that of BA-a type benzoxazine, i.e. about 315 °C. In theory, polybenzoxazines with additional amounts of arylamine Mannich bridges, and methylene linkages showed improved mechanical and thermal properties as a result of greater crosslink densities. Correlations between the observed mechanical properties and network structures of polybenzoxazines were reported [8]. Consequently, the polybenzoxazine and its alloys were investigated as a high performance matrix of composite materials such as in electronic packaging applications [9–14]. In order to make on optimum use of the benzoxazine resins, it is important to understand the nature of their curing process, the structure of the cured material, and how its kinetic parameters can be influenced by temperature, etc. The curing reaction is a very complex process because many reactive processes sometimes occur simultaneously. The final properties of the crosslinked benzoxazine resins depend significantly on the kinetics of the curing reaction concerned

* Corresponding author. Tel.: +662 2186862; fax: +662 2186877.
E-mail address: sarawut.r@chula.ac.th (S. Rimdusit).

0040-6031/$ – see front matter © 2006 Elsevier B.V. All rights reserved.
doi:10.1016/j.tca.2006.05.008

with extent of curing, the curing conditions, etc. [2,15]. Therefore, the study of the curing kinetics contributes to both a better knowledge of process development and an improvement of the quality of final products related to the structures of the polymer network [16,17]. In addition, the availability of reliable methods for cure monitoring also plays a crucial role in process control and optimization of the polymer network processing [18].

There are several techniques previously used to examine the kinetics of the polybenzoxazine curing, for instance, differential scanning calorimetry (DSC) [2,16,19,20–28], Fourier Transform Infrared Spectroscopy (FTIR) [29], and rheokinetic measurements [20]. Among these, differential scanning calorimetry has been the most utilized technique for the determination of kinetic parameters and the corresponding rate equation of the polybenzoxazine curing [2,15,19,21–27]. In general, the kinetic parameters estimated from DSC dynamic experiments were reported to agree relatively well with those estimated by other methods [30]. The basic assumption for the application of DSC is that the measured of heat flow, dH/dt, is proportional to the reaction rate, $d\alpha/dt$. Without knowing the exact reaction mechanism, it is reasonable to assume that the reaction rate at a given time is only a function of the conversion fraction particularly in the isothermal method [18].

1.1. Kinetic analysis

Kinetic analysis of non-isothermal resin-cured system is based on the rate equation [22]

$$\frac{d\alpha}{dt} \equiv \beta \frac{d\alpha}{dT} = k(T) f(\alpha) \tag{1}$$

where $k(T)$ is a temperature-dependent reaction rate constant, $f(\alpha)$ the differential conversion function depending on the reaction mechanism, and $\beta = dT/dt$ is a constant heating rate. The rate constant, $k(T)$, is temperature dependent according to Arrhenius law shown in Eq. (2)

$$k(T) = A \exp\left(-\frac{E_a}{RT}\right) \tag{2}$$

where A is the pre-exponential factor, E_a is the activation energy, and T is the absolute temperature.

Non-isothermal method, a more precise measure to evaluate the curing kinetic parameters, is carried out at different heating rates. This method is very attractive because the kinetic data can be obtained in a relatively short period of time. Nevertheless, there are some complications in the mathematical analysis of the temperature integral which are inherent to the non-isothermal approach. In addition, the isothermal method renders the destabilization of the DSC heat flow at the beginning of the measurement which leads to experimental errors. The two methods also cover different temperature domains as discussed by Sbirrazzuoli et al. [23]. Moreover, considering the shape of curing peak, the number of peaks and/or shoulders in the isothermal and non-isothermal DSC thermograms may be different. Although there is only a single peak in the isothermal DSC thermogram, a peak and a shoulder may appear in the non-isothermal DSC thermogram. Consequently, the kinetic parameters obtained from an isothermal cure study may not be good in predicting the non-isothermal curing behaviors [31]. The non-isothermal method which involves single or multiple dynamic temperature scans has been applied extensively in the study of the curing reactions of thermosetting polymers [16,17,32]. Four kinetic methods widely used to study dynamic kinetics of thermosetting polymers are Kissinger, Ozawa, Friedman, and Flynn–Wall–Ozawa methods.

1.1.1. The Kissinger method

Kissinger method is based on a linear relationship between the logarithm of β/T_p^2 with the inverse of the peak temperature of the exothermic curing reaction, through the following expression [25,33]:

$$\ln\left(\frac{\beta}{T_p^2}\right) = \ln\left(\frac{Q_p A R}{E_a}\right) - \frac{E_a}{RT_p} \tag{3}$$

where $Q_p = -[df(\alpha)/d\alpha]_{\alpha=\alpha_p}$.

The graphic representation of Eq. (3) allows us to examine both the activation energy and the pre-exponential factor of curing kinetics.

1.1.2. The Ozawa method

A similar method to Kissinger method is Ozawa method, which relates the logarithm of the heating rate and the inverse of the exothermic peak temperature. Therefore, the curing activation energy can be determined from the resultant slope [34].

$$\ln \beta = \ln\left(\frac{AE_a}{R}\right) - \ln F(\alpha) - 5.331 - 1.052\left(\frac{E_a}{RT}\right) \tag{4}$$

$$F(\alpha) = \int_0^\alpha \frac{d\alpha}{f(\alpha)} \tag{5}$$

where $F(\alpha)$ is a constant function.

1.2. Isoconversional method

The isoconversional method assumes that both of the activation energy and pre-exponential factor are the functions of the degree of curing. In addition, the isoconversional approach can be used to evaluate both simple and complex chemical reactions. The significance of this technique is that no kinetic rate expression is assumed for the data evaluation [35]. Two different isoconversional methods are as follows.

1.2.1. Friedman method

The Friedman method, differential isoconversional method, is used to determine a kinetic model of the curing process. The method is based on Eqs. (1) and (2) that leads to:

$$\ln \frac{d\alpha}{dt} = \ln \beta \frac{d\alpha}{dT} = \ln[A f(\alpha)] - \frac{E_a}{RT} \tag{6}$$

In case of the nth-order reaction:

$$f(\alpha) = (1-\alpha)^n \tag{7}$$

From (1), (2), and (7)

$$\ln[Af(\alpha)] = \ln\left[\frac{d\alpha}{dt}\right] + \frac{E_a}{RT} = \ln A + n\ \ln(1-\alpha) \quad (8)$$

The value of $\ln[Af(\alpha)]$ can be obtained from the known values of $\ln[d\alpha/dt]$ and E_a/RT. Therefore, the plot of $\ln[Af(\alpha)]$ and $\ln(1-\alpha)$ yields a straight line which the slope providing the reaction order. The intercept is the natural logarithm of the frequency factor if the reaction mechanism is of the nth-order kinetics. The rate, $d\alpha/dt$, at each temperature can be determined from

$$\frac{d\alpha}{dt} = \frac{\varphi}{\Delta H} \quad (9)$$

where ΔH is the enthalpy of the curing reaction and φ is the measured heat flow normalized with the sample mass.

1.2.2. Flynn–Wall–Ozawa method

The isoconversional integral method was also proposed independently by Flynn, Wall, and Ozawa [25] using Doyle's approximation of the temperature integral. This method is based on Eqs. (10) and (11).

$$\ln\beta = \ln\left(\frac{AE_a}{R}\right) - \ln g(\alpha) - 5.331 - 1.052\left(\frac{E_a}{RT}\right) \quad (10)$$

$$g(\alpha) = \int_0^\alpha \frac{d\alpha}{f(\alpha)} \quad (11)$$

where $g(\alpha)$ is the integral conversion function.

Thus, for a constant α, the plot of $(\ln\beta)$ versus $(1/T)$ obtained from DSC thermograms using various heating rates should render a straight line where the slope allows the determination of the apparent activation energy. The apparent activation energy received from the Flynn–Wall–Ozawa analysis is reported to be more reliable than that from the Friedman analysis. Moreover, the Flynn–Wall–Ozawa method, owing to its integrating character, exhibits less sensitivity to noise than the Friedman method. The latter, however, provides a better visual separation of more reaction steps as well as information concerning the existence of an autocatalytically activated process [36].

The advantage of these four kinetics methods over other non-isothermal methods is that they do not require prior knowledge of the reaction mechanism in order to quantify kinetic parameters [18]. Some of these methods had been used to determine the kinetic parameters of benzoxazine resins. Recent work by Ishida and Rodriguez [2,15] examined the curing kinetic of benzoxazine resin (BA-a) with and without catalysts by using both isothermal and non-isothermal differential scanning calorimetry. They reported that the curing of benzoxazine precursors was an autocatalysed reaction prior to diffusion control stage. The apparent activation energy by Kissinger and Ozawa method of the curing process was found to be about 102–116 kJ mol^{-1} in an uncatalysed system and 99–107 kJ mol^{-1} in a catalysed system, with an overall order of reaction of about 2. The phenol moiety of the ring-opened benzoxazine monomers was reported to have a catalytic effect on the curing reaction, i.e. reducing a reaction induction time and increasing reaction rate. Weak acids such as adipic acid and sebacic acid can also be effectively used as catalysts for benzoxazine resin. The kinetic analysis of other systems of benzoxazine resins such as random co-polybenzoxazine of BA-a type and P-a type benzoxazines has also been reported [19]. The isothermal curing process of the co-polybenzoxazine precursor involves an autocatalytic-type curing mechanism. In the dynamic DSC experiments, the activation energy was found to be 72 kJ mol^{-1} based on the Kissinger method and 84 kJ mol^{-1} using the Flynn–Wall–Ozawa method. Furthermore, in the isothermal experiments, the activation energy was reported to be 50 kJ mol^{-1} based on the Kamal method, whereas the total order of reaction is between 2.66 and 3.03, depending on the isothermal curing temperature. Moreover, comparison of the activation energy of polybenzoxazine to that of an epoxy resin-based underfill material used in electronic packaging as reported by He [18] indicates nearly the activation energy values of the epoxy system to be 87 kJ mol^{-1} based on the Kissinger method. Sbirrazzuoli et al. [22–26] and Vyazovkin et al. [21,27] also investigated the curing kinetics of various epoxy resin systems utilizing the isoconversional analysis. The authors observed a dependence of the effective activation energy on the extent of cure with the value approaching 70 kJ mol^{-1} when the extent of cure reached 0.8, i.e. the system of DGEBA + HHMPA + DMBA [22].

To our best knowledge, the effect of alkyl-substituted arylamines in the curing kinetics of the polyfunctional benzoxazine resins has not been explored. It is, therefore, of interest to investigate that of the polyfunctional benzoxazine resins based on arylamine, i.e. aniline and 3,5-xylidine. The curing kinetics of the systems were examined by non-isothermal differential scanning calorimetry at different heating rates in order to understand the reaction kinetics of both systems and be the way of achieving successful processing.

2. Experimental

2.1. Materials

The BA-a type benzoxazine based on bisphenol-A, formaldehyde, and aniline, and the BA-35x type based on bisphenol-A, formaldehyde, and 3,5-xylydine were synthesized by patented solventless technology [37]. Bisphenol-A and paraformaldehyde were received from Thai Polycarbonate Co. Ltd. and Merck Company, respectively. A series of aromatic amines, i.e. aniline (99%) and 3,5-xylidine (98%), purchased from Fluka Chemika were used as received. A series of benzoxazine resin based upon alkyl-substituted arylamines were investigated [5,6] as shown in Scheme 1.

2.2. GPC measurements

Gel permeation chromatography (GPC) analysis was performed at 40 °C on a Waters 600 using three Waters Styragel® HT columns (Styragel® HT 0.5, Styragel® HT 1, and Styragel® HT 4). Molecular weights are relative to monodisperse polystyrene standards. Samples were prepared by dissolving the benzoxazine resins in tetrahydrofuran (THF) mobile phase at

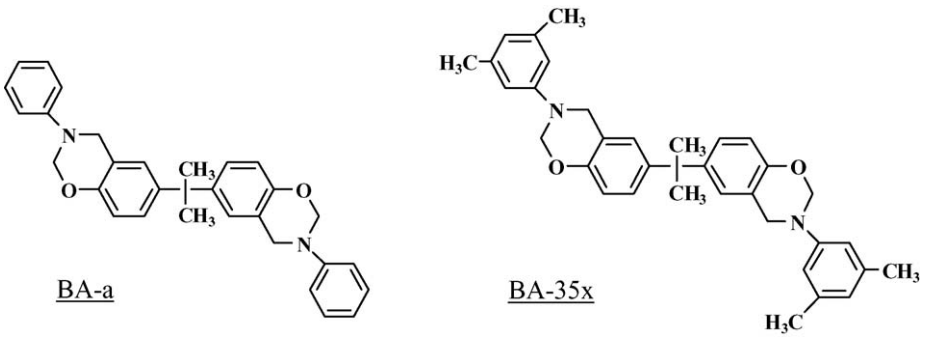

Scheme 1. Arylamine-based benzoxazine monomers.

30 °C in order to reach the final concentration of 0.25% (w/v). The detector was Waters 2414 refractive index (RID).

2.3. DSC measurements

A differential scanning calorimeter model 2910 from TA Instruments was employed to study the exothermic curing reactions. The samples were scanned by non-isothermal method from 30 to 290 °C at five different heating rates of 1, 2, 5, 10, and 20 °C/min under a constant flow of nitrogen at 50 ml/min.

3. Results and discussion

3.1. Curing reaction

The heat flows of BA-a and BA-35x from the conventional DSC mode are shown in Figs. 1 and 2, respectively. From these figures, information about the nature of the curing reaction such as initial curing temperature, peak temperature, and the curing range of the both resins at different scan rates could be derived. It can be observed that the exothermic peak shifts to a higher temperature with higher heating rate. In our systems, the heating rates show no effect on the total exothermic reaction heat estimated from the area under the exothermic peak of BA-a and BA-35x. The average total exothermic reaction heat of BA-a and BA-35x is 341 and 299 J g^{-1}, respectively. It is noticed that the curing reaction of BA-a has more amount of heat released than that of BA-35x. This suggests that BA-a would be more sensitive to accelerate the curing than BA-35x. Moreover, the step changes of the thermograms of both resins at the temperature range of 45–60 °C are the glass transition temperature of the benzoxazine monomers or $T_{g,o}$. From Fig. 3, one can observe that BA-a benzoxazine shows only one exothermic peak of the non-isothermal DSC traces while BA-35x type benzoxazine shows overlapped exothermic peaks or a small shoulder beside the main peak. Thus, it is suggested that the curing reaction of BA-35x type benzoxazine has at least two cure stages; the curing reaction at lower temperature was caused by reaction (1) and the one occurring at higher temperature was caused by reaction (2). The individual reaction may be calculated by a combination of programmed and isothermal techniques. To verify the two curing reactions of BA-35x, further experiments on isothermal curing of partially cured samples (5–120 min) at 160 °C are depicted in Fig. 4. It can be noticed that the thermogram of partially cured BA-35x resin at 5 min shows no significant change of the exothermal peak temperature (200 °C) and still indicates the

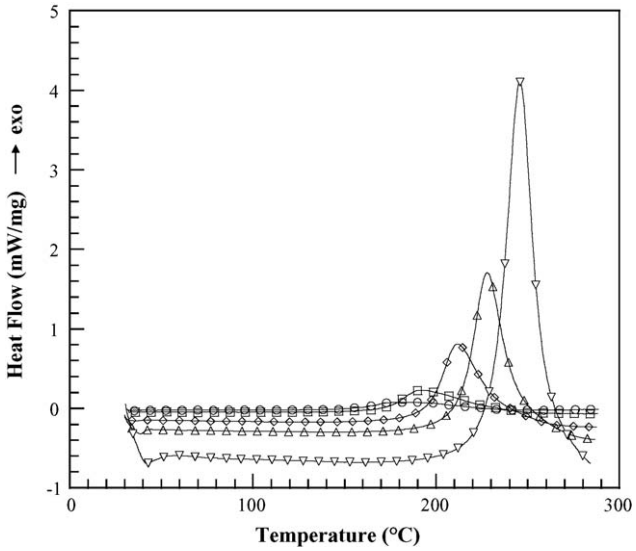

Fig. 1. DSC thermograms of BA-a resin at different heating rates: (◯) 1 °C/min, (□) 2 °C/min, (◇) 5 °C/min, (△) 10 °C/min, and (▽) 20 °C/min.

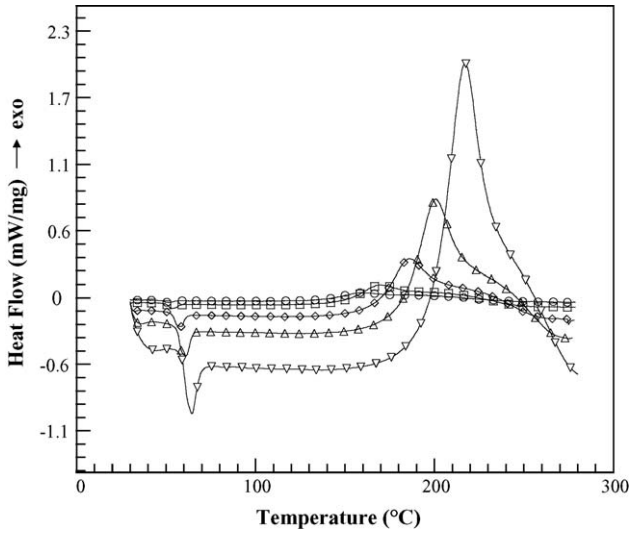

Fig. 2. DSC thermograms of BA-35x resin at different heating rates: (◯) 1 °C/min, (□) 2 °C/min, (◇) 5 °C/min, (△) 10 °C/min, and (▽) 20 °C/min.

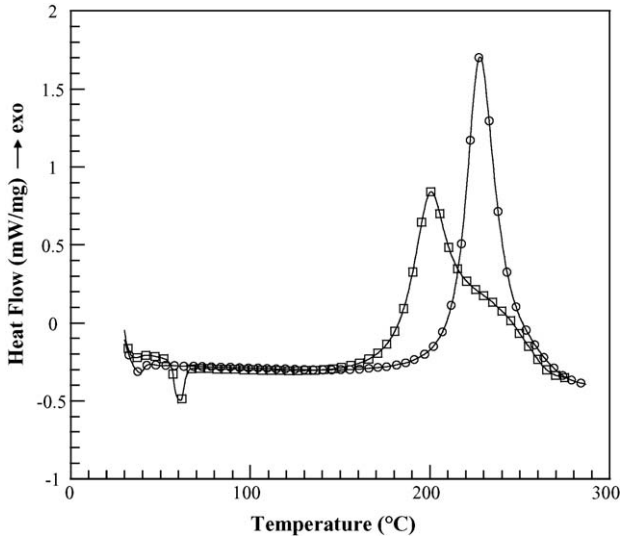

Fig. 3. DSC thermograms of two types of benzoxazine resins at 10 °C/min: (◯) BA-a resin and (□) BA-35x resin.

overlapped exothermic peaks, i.e. the effect of the second reaction to the first peak is small. However, when the sample is cured to 10 min, the peak temperature is shifted to 210 °C, revealing stronger effect of the second reaction on the first peak. When the sample is cured to 15 min, the first peak almost disappears as the second peak is obviously observed. The partially cured BA-35x resin to 120 min clearly shows only one exothermic peak at higher temperature, implying that the effect of the first reaction to the second peak temperature could be neglected. The results in Fig. 4 ensure that there are two reaction phases in the hypothetical product.

The kinetics of the DSC curves for BA-35x at the heating rates of 1–20 °C/min were analysed using PeakFit v4.12. In order to separate two exothermic peaks, and to analyse the distinct characterization of each, Pearson VII distribution was used as

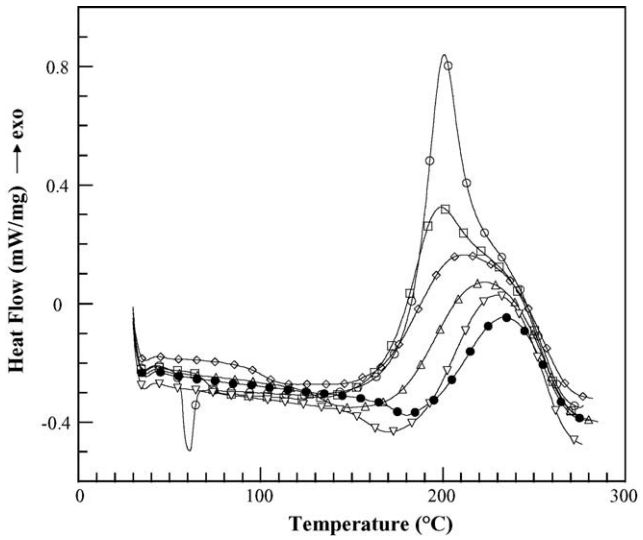

Fig. 4. DSC thermograms of BA-35x resin by using 10 °C/min heating rate after isothermal curing of 160 °C at different curing times in oven: (◯) uncured BA-35x monomer, (□) 5 min, (◊) 10 min, (△) 15 min, (▽) 60 min, and (●) 120 min.

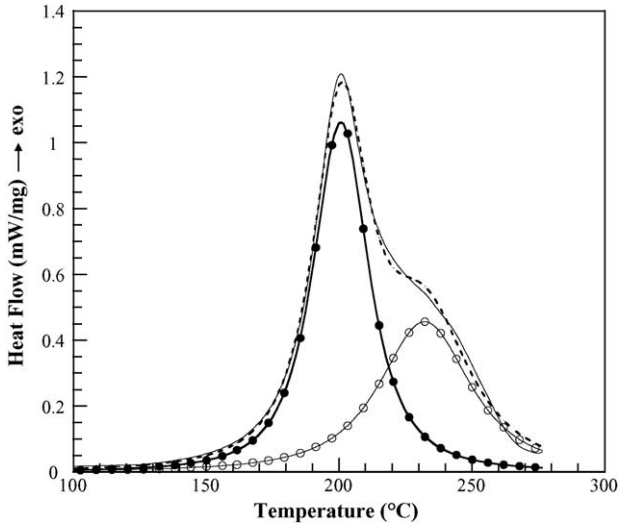

Fig. 5. DSC thermograms of BA-35x resin recorded at 10 °C/min: the DSC thermogram (solid line), the calculated DSC thermogram (dash line), (●) reaction (1), and (◯) reaction (2).

shown in Fig. 5. The DSC thermograms were recorded for the curing reaction of the BA-35x sample at 10 °C/min (solid line) and calculated data from PeakFit v4.12 (dash line) with two distinct peaks (peak I—black circles and peak II—white circles).

3.2. Kinetic model

As the multiple heating rate methods for non-isothermal analysis proposed by Kissinger and Ozawa can be used as an alternative way of calculating the activation energy without assuming any model of kinetic parameters and without integrating the exothermic peak, the logarithm plots of heating rate versus the reciprocal of the absolute peak temperature of BA-a resin are given in Fig. 6. They are shown that a good linear relationship between the heating rate and the reversal of the exothermic peak temperature can be obtained. The average acti-

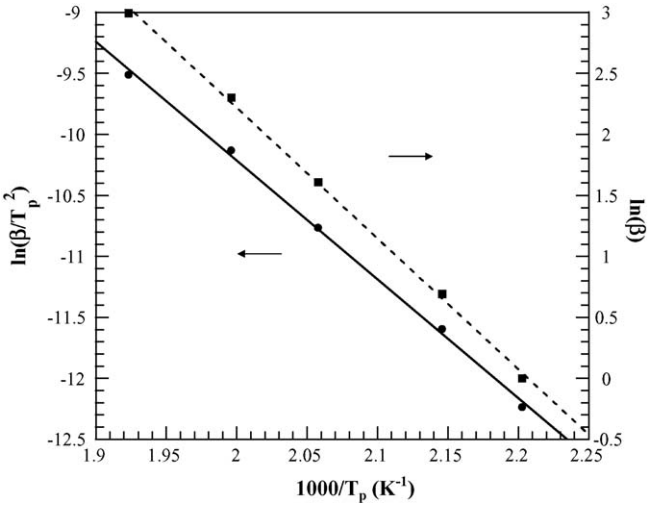

Fig. 6. (●) Kissinger method and (■) Ozawa method plots for averaged activation energy determination of the BA-a resin.

Table 1
Average activation energy of BA-a and BA-35x obtained by Kissinger and Ozawa methods

Method	Average activation energy (E_a, kJ mol^{-1})		
	BA-a resin	BA-35x resin	
		Reaction (1) (E_{a1})	Reaction (2) (E_{a2})
Kissinger	81	81	111
Ozawa	85	87	113

vation energy values of BA-a and BA-35x resins calculated from the slopes of the plots are listed in Table 1. BA-a resin shows only one dominant cueing kinetic process with the average activation energy of 81–85 kJ mol^{-1}, whereas BA-35x exhibits two major curing processes. The average activation energies of BA-35x for reactions (1) and (2) were 81–87 and 111–113 kJ mol^{-1}, respectively. In addition, the average activation energy values obtained from Kissinger and Ozawa methods are not significantly different. From the results, the calculated values of the activation energy values of BA-a and BA-35x are different from other reported works [2,15] because the molecular weight distribution of the benzoxazine precursor is different as indicated by GPC results. The precursor obtained is a mixture of monomers, dimers, and other oligomers formed in subsequent reactions during the synthesis, for instance, in case of BA-a, the molecular weight is 431, 498, and 807 g mol^{-1}, respectively, while those of BA-35x are 462, 562, and 964 g mol^{-1}, respectively. Typically, the molecular weight of purified BA-a and BA-35x type benzoxazine monomers is 463 and 527 g mol^{-1}, respectively [38]. Furthermore, considering the system of BA-35x, one can see that the activation energy of reaction (2) is much higher than that of reaction (1). As a result, reaction (1) is more sensitive to the temperature than reaction (2).

From the results, we can observe that the average activation energy value of reaction (1) for BA-35x resin is almost the same as the average activation energy of BA-a resin. This implies that the curing mechanism in the first stage of BA-35x resin is the same as that of BA-a resin. This mechanism is the heterocyclic ring opening polymerization of benzoxazine precursors since the oxazine ring is the reactive site for curing of the benzoxazine. The conformation of an oxazine ring containing benzoxazine is a distorted semichair structure, with the nitrogen and the carbon between the oxygen and nitrogen on the oxazine sitting, respectively, above and below the benzene ring plane. This resulting oxazine ring strain leads to the ring-opening polymerization to occur under certain conditions [39], whereas the second exothermic peak of the reaction (2), indicated by the high-temperature shoulder, corresponds to the side reactions which generate the bisphenolic methylene linkages and possible reaction to the *para* position of the arylamine ring called arylamine Mannich bridge and methylene linked structures. In addition, Ishida and Sanders [7] have reported different network structures of polybenzoxazine (BA-a and BA-35x types) investigated by FTIR. They found that the FTIR absorbed peak position of BA-35x after polymerization shows a large band centered at 847 cm^{-1} corresponding to the out-of-plane, in-phase hydrogen wagging mode

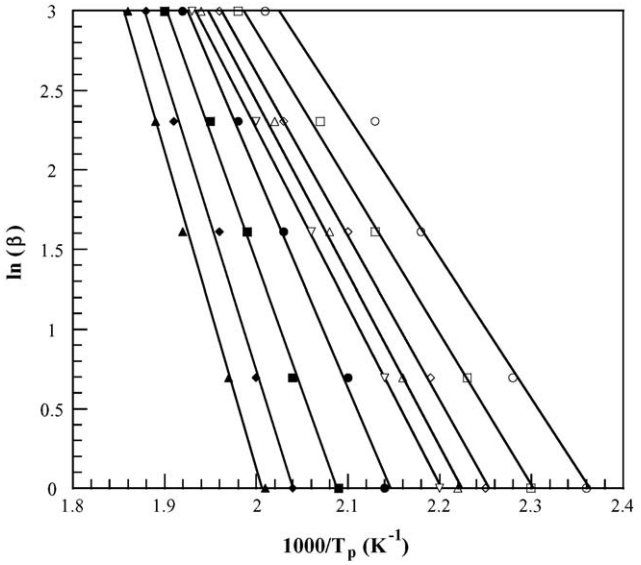

Fig. 7. Flynn–Wall–Ozawa plots at various degrees of curing of the BA-a resin: (◯) $\alpha = 0.05$, (□) $\alpha = 0.10$, (◊) $\alpha = 0.20$, (△) $\alpha = 0.30$, (▽) $\alpha = 0.40$, (●) $\alpha = 0.60$, (■) $\alpha = 0.80$, (♦) $\alpha = 0.90$, and (▲) $\alpha = 0.95$.

of the 1,2,3,5-tetrasubstituted arylamine ring, but this peak cannot be observed for BA-a resin. However, the spectrum of both polybenzoxazine types centered at 878 cm^{-1}. This band agrees with the frequency predicted for the out-of-plane, out-of-phase hydrogen wagging node for the 1,2,3,5-tetrasubstituted aromatic ring.

Moreover, a more complete assessment of the apparent activation energy of benzoxazine resins throughout the entire conversion range may be obtained using the isoconversional methods that are the Flynn–Wall–Ozawa and Friedman methods. If the data fall into a straight line, the slope should then correspond to E_a/R at the particular conversion. For instance, Figs. 7 and 8 are Flynn–Wall–Ozawa and Friedman plots of

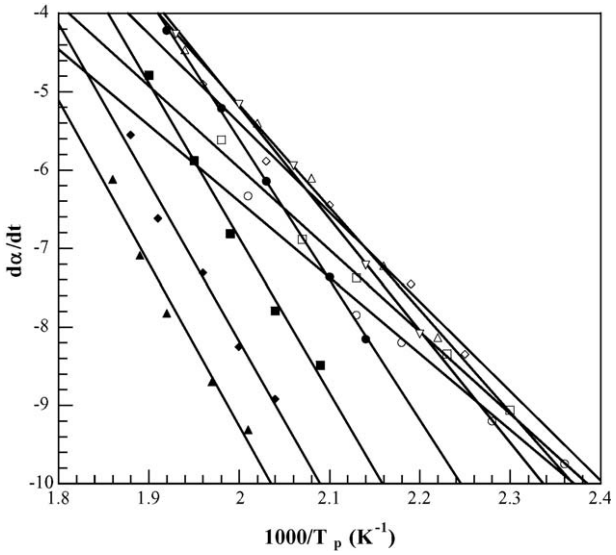

Fig. 8. Friedman plots at various degrees of curing of the BA-a resin: (◯) $\alpha = 0.05$, (□) $\alpha = 0.10$, (◊) $\alpha = 0.20$, (△) $\alpha = 0.30$, (▽) $\alpha = 0.40$, (●) $\alpha = 0.60$, (■) $\alpha = 0.80$, (♦) $\alpha = 0.90$, and (▲) $\alpha = 0.95$.

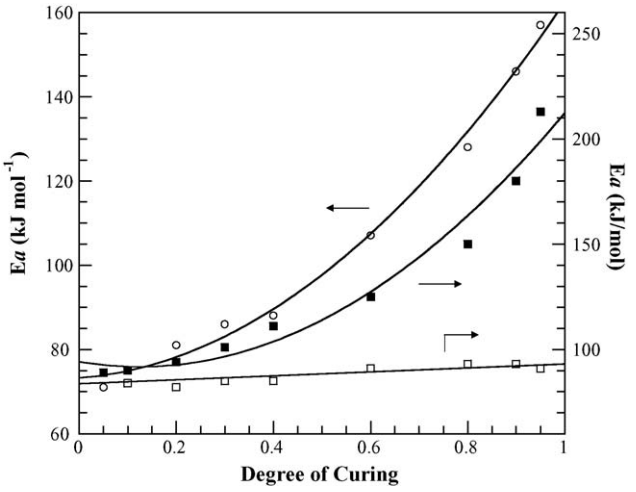

Fig. 9. Values of the apparent activation energy obtained from Flynn–Wall–Ozawa plots at different degrees of curing: (◯) BA-a resin, (□) BA-35x (reaction (1)), and (■) BA-35x (reaction (2)).

BA-a resin system for $\alpha = 0.05$–0.95, respectively. A good linear relationship was observed from both Flynn–Wall–Ozawa and Friedman plots. Values of E_a of BA-a and BA-35x resins obtained in this manner at different degrees of curing are shown in Figs. 9 and 10. From the plots, the dependence of the apparent activation energies of both benzoxazine resins as a function of degree of curing was observed. The effect has been known in literatures as a kinetic compensation effect [40]. As there was no significant difference in the calculated activation energy values either using differential or integral kinetic methods, the activation energy obtained from Kissinger method was then selected for further determining the reaction order of our systems as recommended by Sbirrazzuoli et al. [25].

As previously mentioned, the mechanisms of the curing reaction of thermoset resins usually have two general kinetic reactions, an *n*th-order and an autocatalytic reaction [41]. In this work, the method used to find kinetic model is Friedman method. For *n*th-order reaction, the average activation energy from Kissinger method is taken as a constant, Eq. (8) may be written as:

$$\ln[Af(\alpha)] = \ln A + n\ \ln(1-\alpha) \tag{12}$$

Friedman suggested that the relationship between $\ln[Af(\alpha)]$ against $\ln(1-\alpha)$ should yield a straight line of which the slope corresponds to the order of n of the reaction. Otherwise, for autocatalytic process, the Friedman plot would show a maximum of $\ln(1-\alpha)$ approximately around -0.51 to -0.22 which is equivalent to α of about 0.2–0.4. This is due to the autocatalytic nature that shows the maximum reaction rate at 20–40% conversion. The results are in good agreement with several works reported [42–44].

Fig. 11 shows Friedman plots of reactions (1) and (2) of BA-35x resin, respectively. In case of reaction (1), since $\ln[Af(\alpha)]$ and $\ln(1-\alpha)$ are not linearly related, this implies that the curing reaction is autocatalytic in nature. In contrast, the plot for reaction (2) shows linear relationship indicating *n*th-order kinetic behavior. Using the same analysis for BA-a (not shown here), only single peak reaction is obtained suggesting the behavior of autocatalytic reaction. According to other works reported, the autocatalytic nature of the reaction kinetics of this resin can be explained by the generation of free phenol groups while the benzoxazine ring starts to open. These groups can actually accelerate further ring opening [2,15].

For the *n*th-order model, it is assumed that the reaction obeys Eq. (13)

$$\frac{d\alpha}{dt} = A\ \exp\left(-\frac{E_a}{RT}\right)(1-\alpha)^n \tag{13}$$

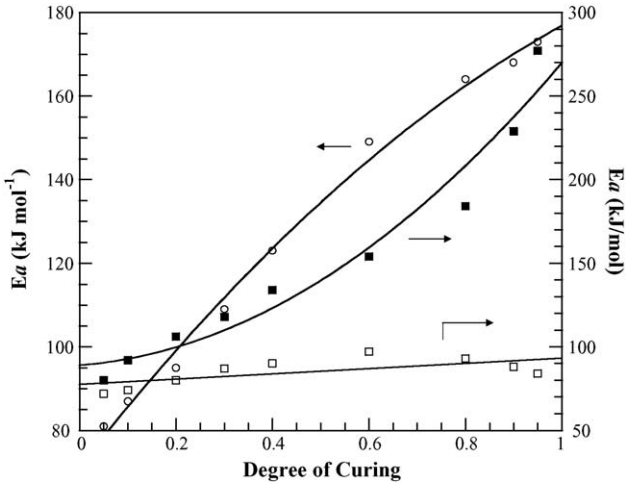

Fig. 10. Values of the apparent activation energy obtained from Friedman plots at different degrees of curing: (◯) BA-a resin, (□) BA-35x (reaction (1)), and (■) BA-35x (reaction (2)).

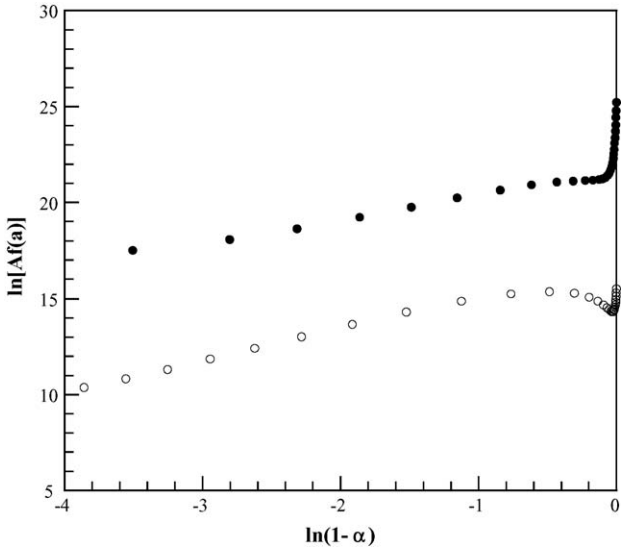

Fig. 11. Plots of $\ln[Af(\alpha)]$ vs. $\ln(1-\alpha)$ of BA-35x resin using the heating rate of 10 °C/min and using the average activation energy from Kissinger method: (◯) reaction (1) and (●) reaction (2).

Table 2
The kinetic parameters evaluated for the curing of the BA-a system

Heating rate (°C/min)	E (kJ mol^{-1})	ln A (s^{-1})	Mean	n	Mean	m	Mean
1	81	14.57	15.60	1.7	1.7	0.4	0.8
2		14.99		1.9		0.4	
5		16.12		2.1		1.0	
10		16.28		1.6		1.2	
20		16.05		1.2		1.0	

Table 3
The kinetic parameters evaluated for the curing of the BA-35x system (reaction (1))

Heating rate (°C/min)	E (kJ mol^{-1})	ln A (s^{-1})	Mean	n	Mean	m	Mean
1	81	16.37	16.83	1.6	1.7	0.6	0.8
2		16.26		1.3		0.5	
5		17.00		1.8		0.9	
10		17.42		2.0		1.1	
20		17.08		1.7		1.1	

Conversely, the autocatalytic model considers independent reaction orders: m and n, as shown in Eq. (14)

$$\frac{d\alpha}{dt} = A \exp\left(-\frac{E_a}{RT}\right)(1-\alpha)^n \alpha^m \quad (14)$$

Theoretically, Eqs. (13) and (14) could be solved by multiple nonlinear regressions because the curing rate is an exponential function of the reciprocal of the absolute temperature. By taking the logarithm of Eqs. (13) and (14), a linear expression for the logarithm of curing rate can be obtained.

$$\ln\left(\beta\frac{d\alpha}{dt}\right) = \ln A - \left(\frac{E_a}{RT}\right) + n\ \ln(1-\alpha) \quad (15)$$

$$\ln\left(\beta\frac{d\alpha}{dt}\right) = \ln A - \left(\frac{E_a}{RT}\right) + n\ \ln(1-\alpha) + m\ \ln(\alpha) \quad (16)$$

Eqs. (15) and (16) can be solved by multiple linear regression, in which the dependent variable is ln(dα/dt), and the independent variables are ln α, ln$(1-\alpha)$, and $1/T$. Therefore, the values of A, m, and n can be obtained using the average activation energy from Kissinger method. The degree of curing is chosen between the beginning of the reaction and the maximum peak of degree of curing ($\alpha = 0.1$–0.5). The results of the multiple linear regressions analysis for all heating rates used of BA-a and BA-35x

Table 4
The kinetic parameters evaluated for the curing of the BA-35x system (reaction (2))

Heating rate (°C/min)	E (kJ mol^{-1})	ln A (s^{-1})	Mean	n	Mean
1	111	21.52	21.46	1.8	1.4
2		21.47		1.4	
5		21.39		1.3	
10		21.45		1.0	
20		–		–	

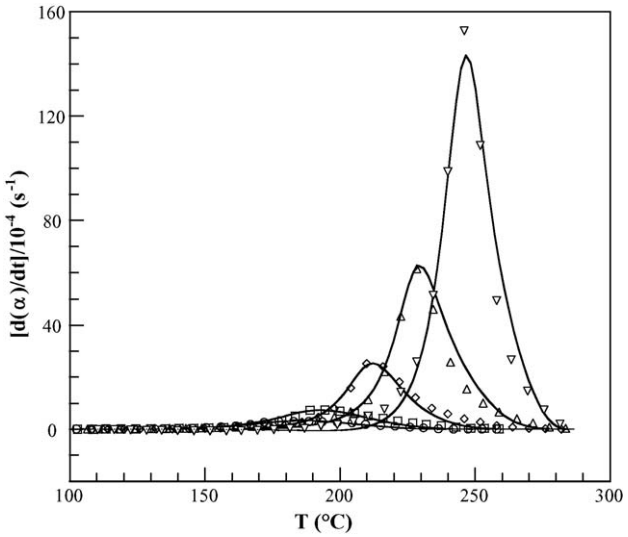

Fig. 12. Experimental (symbols) and calculated (solid lines) DSC peaks corresponding to the curing process of BA-a resin: (◯) 1 °C/min, (□) 2 °C/min, (◊) 5 °C/min, (△) 10 °C/min, and (▽) 20 °C/min.

(reactions (1) and (2)) are listed in Tables 2–4, respectively. It can be seen that the variation of A, m, and n with the heating rate for both BA-a and BA-35x systems is in the same range as those reported by Ishida and Rodriquez [2,15]. Consequently, we obtain a mathematical model for autocatalytic kinetics of BA-a system as,

$$\frac{d\alpha}{dt} = (5.96 \times 10^6) \exp\left(\frac{-9743}{T}\right)(1-\alpha)^{1.7}\alpha^{0.8} \quad (17)$$

Similarly mathematical models for autocatalytic kinetics of BA-35x (reaction (1)) and for nth-order kinetics of BA-35x (reaction (2)) are presented in Eqs. (18) and (19), respectively.

$$\frac{d\alpha}{dt} = (2.04 \times 10^7) \exp\left(\frac{-9743}{T}\right)(1-\alpha)^{1.7}\alpha^{0.8} \quad (18)$$

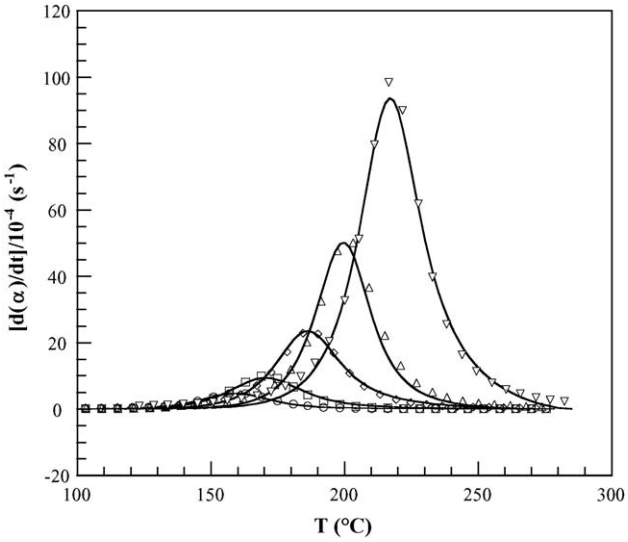

Fig. 13. Experimental (symbols) and calculated (solid lines) DSC peaks corresponding to the first curing process (reaction (1)) of BA-35x resin: (◯) 1 °C/min, (□) 2 °C/min, (◊) 5 °C/min, (△) 10 °C/min, and (▽) 20 °C/min.

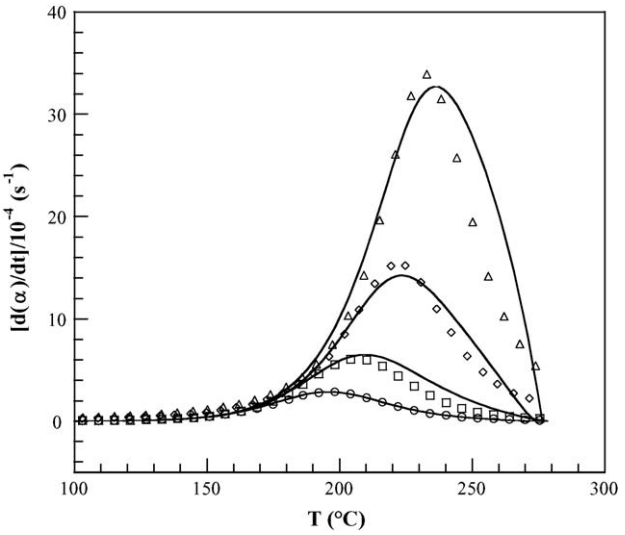

Fig. 14. Experimental (symbols) and calculated (solid lines) DSC peaks corresponding to the second curing process (reaction (2)) of BA-35x resin: (◯) 1 °C/min, (□) 2 °C/min, (◇) 5 °C/min, and (△) 10 °C/min.

$$\frac{d\alpha}{dt} = (2.09 \times 10^9) \exp\left(\frac{-13,351}{T}\right) \alpha^{1.4} \quad (19)$$

The experimental results are compared with those predicted from the models for both systems, as shown in Figs. 12–14. It is clearly seen that the calculated data from the model are in good agreement with the experimental results.

4. Conclusions

The curing reaction of polyfunctional benzoxazine resins based on two types of arylamine, aniline and 3,5-xylidine, was studied. It was found that the curing process of BA-a was a single curing reaction, while the curing reaction of BA-35x was composed of two processes (reactions (1) and (2)), as evidenced by the presence of a double peak on the DSC thermograms.

By using Kissinger, Ozawa, Flynn–Wall–Ozawa, and Friedman methods approach, the obtained activation energy values of both resins are almost invariable. In addition, the activation energy value of BA-a is close to that of BA-35x (reaction (1)). This indicates the same mechanism of the curing reaction of both exothermic peaks. In the case of BA-35x, the activation energy value at the reaction (1) is much smaller than that of the reaction (2). Therefore, reaction (1) is more sensitive to the temperature than reaction (2). The reaction orders of reactions (1) and (2) are also different. This leads to the fact that there are two different mechanisms involved in the curing reactions. The autocatalytic models are proposed to adequately describe the curing kinetics of the BA-a and BA-35x (reaction (1)) systems while the *n*th-order model is found to present the curing process of the BA-35x (reaction (2)). Evidently, the kinetic models of the curing reactions of the both resins are in good agreement with non-isothermal DSC results.

Acknowledgments

The present research receives partial financial support from the Thailand Research Fund (TRF-RTA of Prof. Dr. Wiwut Tanthapanichaloon) 2002–2005 and the Industry-University Joint Research Fund of Center of Excellence in Particle Technology, Chulalongkorn University. One of the authors, S.R., also receives additional financial supports from the Research Grant for Mid-Career University Faculty of the Commission on Higher Education and Thailand Research Fund 2005–2007. The Ratchadapisek Fund of Chulalongkorn University is also acknowledged. Bisphenol-A is kindly donated by Thai Polycarbonate Co. Ltd. (TPCC).

References

[1] H. Ishida, D.J. Allen, J. Polym. Sci. Polym. Phys. 34 (1996) 1019.
[2] H. Ishida, Y. Rodriguez, Polymer 36 (1995) 3151.
[3] H.D. Kim, H. Ishida, J. Phys. Chem. A 106 (2002) 3271.
[4] S. Rimdusit, H. Ishida, Polymer 41 (2000) 7941.
[5] H. Ishida, D.P. Sanders, US Patent 6,160,079 (2000).
[6] H. Ishida, D.P. Sanders, J. Polym. Sci. Polym. Phys. 34 (2002) 3289.
[7] H. Ishida, D.P. Sanders, Macromolecules 33 (2000) 8149.
[8] M.T. Huang, H. Ishida, Polym. Polym. Compos. 7 (1999) 233.
[9] S. Shen, H. Ishida, Polym. Compos. 17 (1996) 710.
[10] H. Ishida, T. Chaisuwan, Polym. Compos. 24 (2003) 597.
[11] H. Ishida, S. Rimdusit, Thermochim. Acta 320 (2001) 177.
[12] S. Rimdusit, H. Ishida, Polymer 41 (2000) 7941.
[13] L.W. Helen, US Patent pending 20,040,261,660 A1 (2004).
[14] T. Takeichi, R. Zeidam, T. Agag, Polymer 43 (2002) 45.
[15] H. Ishida, Y. Rodriguez, J. Appl. Polym. Sci. 58 (1995) 1751.
[16] D. Rosu, C.N. Cascaval, F. Mustata, C. Ciobanu, Thermochim. Acta 383 (2002) 119.
[17] D. Rosu, A. Mititelu, C.N. Cascaval, Polym. Test. 23 (2004) 209.
[18] Y. He, Thermochim. Acta 367–368 (2001) 101.
[19] Y.C. Su, D.R. Yei, F.C. Chang, J. Appl. Polym. Sci. 95 (2005) 730.
[20] S. Rimdusit, Ph.D. Thesis, Case Western Reserve University, Cleveland, OH, 2000, p. 183.
[21] S. Vyazovkin, N. Sbirrazzuoli, Macromolecules 29 (1996) 1867.
[22] N. Sbirrazzuoli, S. Vyazovkin, Thermochim. Acta 388 (2002) 289.
[23] N. Sbirrazzuoli, L. Vincent, J. Bouillard, L. Elegant, J. Therm. Anal. 56 (1999) 783.
[24] N. Sbirrazzuoli, D. Brunel, L. Elegant, J. Therm. Anal. 38 (1992) 1509.
[25] N. Sbirrazzuoli, Y. Girault, L. Elegant, Thermochim. Acta 293 (1997) 25.
[26] N. Sbirrazzuoli, S. Vyazovkin, A. Mititelu, C. Sladic, L. Vincent, Macromol. Chem. Phys. 204 (2003) 1815.
[27] S. Vyazovkin, A. Mittitelu, N. Sbirrazzuoli, Macromol. Rapid Commun. 24 (2003) 1060.
[28] R.B. Prime, in: E.A. Turi (Ed.), Thermal Characterization of Polymeric Materials, Academic Press, San Diego, 1997, p. 435 (Chapter 5).
[29] P. Kornpraditsin, M.S. Thesis, Chulalongkorn University, Bangkok, Thailand, 2002.
[30] D.J. Liaw, W.C. Shen, Polym. Eng. Sci. 34 (1994) 1279.
[31] L. Sun, S.S. Pang, A.M. Sterling, I.I. Negulescu, M.A. Stubblefield, J. Appl. Polym. Sci. 86 (2002) 1911.
[32] S. Montserrat, J. Malek, Thermochim. Acta 228 (1993) 47.
[33] J. Malek, Themochim. Acta 138 (1989) 337.
[34] T. Ozawa, J. Chem. Anal. 2 (1970) 301.
[35] M.R. Kessler, S.R. White, J. Polym. Sci. Polym. Chem. 40 (2002) 2373.
[36] J. Opfermann, E. Kaisersberger, Thermochim. Acta 203 (1992) 167.
[37] H. Ishida, US Patent 5,543,546 (1996).
[38] H. Ishida, D.J. Allen, Polymer 37 (1996) 4487.

[39] Y.X. Wang, H. Ishida, Macromolecules 33 (2000) 2839.
[40] V.L. Zvetkov, Polymer 42 (2001) 6687.
[41] H. Zhao, J. Gao, Y. Li, S. Shen, J. Therm. Anal. Calorim. 74 (2003) 227.
[42] T.H. Hsieh, A.C. Su, J. Appl. Polym. Sci. 41 (1990) 1271.
[43] W.G. Kim, J.Y. Lee, K.Y. Park, J. Polym. Sci. Polym. Chem. 31 (1993) 633.
[44] L.W. Chen, S.C. Fu, C.S. Cho, Polym. Int. 46 (1998) 325.

รายละเอียดของการประดิษฐ์

ชื่อที่แสดงถึงการประดิษฐ์

เกราะกันกระสุนพอลิเมอร์คอมพอสิทจากเบนซอกซาซีน-ยูรีเทนอัลลอย (Benzoxazine - Urethane Alloy) และเส้นใยทนแรงขีปนะ (Ballistic Impact)

สาขาวิทยาการที่เกี่ยวข้องกับการประดิษฐ์

วิศวกรรมวัสดุในส่วนที่เกี่ยวข้องกับพอลิเมอร์คอมพอสิทสำหรับต้านแรงปะทะทนแรงขีปนะ

ลักษณะและความมุ่งหมายของการประดิษฐ์

เกราะกันกระสุนพอลิเมอร์คอมพอสิทโดยใช้เมตริกชนิดเบนซอกซาซีนอัลลอยได้ถูกพัฒนาให้มีน้ำหนักเบา และมีระดับการป้องกันสูง ทั้งนี้เป็นที่ทราบกันดีว่าการใช้วัสดุสองชนิดขึ้นไปโดยอย่างน้อยหนึ่งชนิดทำหน้าที่เป็นเมตริกและวัสดุที่เหลือทำหน้าที่เป็นสารเสริมแรงหรือสารเติมเพื่อผลิตเป็นวัสดุคอมพอสิท แม้วัสดุเริ่มต้นทั้งคู่อาจไม่สามารถกันกระสุนได้ หรือกันได้แต่อาจไม่ดีนัก หากทำเป็นคอมพอสิทก็จะสามารถเพิ่มระดับการป้องกันให้สูงขึ้นได้ เนื่องจากการทำเป็นวัสดุคอมพอสิทสามารถออกแบบให้มีกลไกการรับแรงและสลายพลังงานที่เพิ่มขึ้นได้มาก ทั้งนี้จากงานวิจัยที่ผ่านมาพบว่าเรซินชนิดใหม่ประเภทเบนซอกซาซีนเรซิน (Benzoxazine resin) นอกจากจะสามารถสังเคราะห์ได้ง่าย รวดเร็วและปลอดภัย มีสมบัติด้านการขึ้นรูป สมบัติทางกล และทางความร้อนที่โดดเด่นเมื่อเทียบกับเรซินส่วนใหญ่ที่ใช้ในทางการค้าในปัจจุบันแล้ว ยังพบว่ามีคุณสมบัติที่สำคัญคือสามารถดัดแปรร่วมกับเรซินหรือพอลิเมอร์อื่นๆได้อย่างหลากหลายและให้สมบัติการใช้งานที่กว้างขวาง รวมทั้งยังสามารถปรับสมบัติได้ค่อนข้างละเอียด (fine tuning) ให้เหมาะสมกับสารเติมหรือสารเสริมแรงต่างๆได้ดีและมีความเป็นไปได้สูงในการพัฒนาเพื่อเป็นเมตริกที่เหมาะสมกับเส้นใยเสริมแรงต่างๆ เพื่อพัฒนาเกราะคอมพอสิทกันกระสุนน้ำหนักเบาสมรรถนะสูงเพื่อทดแทนเกราะกันกระสุนที่นำเข้าจากต่างประเทศ

การใช้เบนซอกซาซีน-ยูรีเทนอัลลอยในสัดส่วนองค์ประกอบที่เหมาะสมเป็นเมตริกและเสริมแรงด้วยเส้นใยทนแรงขีปนะเช่นเคฟลาร์ ฯลฯ จึงทำให้ได้เกราะพอลิเมอร์คอมพอสิทสมรรถนะสูง และนอกจากวัสดุคอมพอสิทที่มีองค์ประกอบของเมตริกที่เหมาะสมจะมีกลไกการสลายแรงจากการวิ่งกระทบของกระสุนที่สำคัญหลายชนิดดังกล่าวแล้ว การจัดเรียงตัวของแผ่นคอมพอสิทที่เหมาะสมในชิ้นงานเกราะ ก็เป็นปัจจัยหนึ่งที่พบว่าทำให้เกราะคอมพอสิทกันกระสุนมีประสิทธิภาพการป้องกันที่มากยิ่งขึ้นได้

วัตถุประสงค์หลัก คือ การพัฒนาเกราะกันกระสุนน้ำหนักเบาประเภทพอลิเมอร์คอมพอสิทจากเมตริกอัลลอยระหว่างเบนซอกซาซีนเรซินและยูรีเทนเรซิน ร่วมกับเส้นใยอะรามิดหรือเส้นใยทนแรงขีปนะอื่นๆ ที่สามารถใช้ต้านการเจาะทะลุของกระสุนที่ระดับมาตรฐาน NIJ (National Institute of Justice) ระดับ I-IIIA โดยยังรักษาโครงสร้างโดยรวมของเกราะพอลิเมอร์คอมพอสิทไว้ได้

วัตถุประสงค์ต่อมาคือการหาการจัดเรียงตัวของแผ่นพอลิเมอร์คอมพอสิทที่ทำให้ได้เกราะที่มีประสิทธิภาพการต้านการเจาะทะลุของกระสุนที่ระดับการยิงตามมาตรฐาน NIJ

ภูมิหลังของศิลปะหรือวิทยาการที่เกี่ยวข้อง

การพัฒนาเกราะกันกระสุนสามารถแบ่งออกเป็น 2 กลุ่มด้วยกัน คือ กลุ่มเกราะอ่อน และกลุ่มเกราะคอมพอสิทแข็ง ซึ่งพอลิเมอร์มีความสำคัญอย่างมากในการพัฒนางานทางด้านเกราะทั้ง 2 กลุ่ม เนื่องจากวัสดุพอลิเมอร์สามารถช่วยให้เกราะมีน้ำหนักเบาลงได้มากทำให้ใช้งานได้สะดวกมากยิ่งขึ้นและยังเป็นองค์ประกอบสำคัญในการดูดกลืนพลังงานจลน์จากการปะทะแบบขีปนะ ในสงครามเวียดนามก็ได้เคยมีการนำเส้นใยไนลอนร่วมกับเส้นใยแก้วมาทำเป็นเกราะกันกระสุน เนื่องจากขีดความสามารถดังกล่าว เกราะอ่อนที่ทำจากเส้นใยพอลิเมอร์ความแข็งแรงสูงได้มีรายงานการพัฒนามาตั้งแต่ ค.ศ. 1963 โดยประสิทธิภาพของเกราะกันกระสุนจะขึ้นอยู่กับคุณสมบัติของส้นใยที่ใช้ และจากรายงานที่ผ่านมาแสดงให้เห็นว่าเส้นใยที่มีความเหมาะสมในงานทางด้านเกราะนั้น จะต้องมีความแข็งแรงสูง และควรจะมีค่าความเร็วเสียงรวมถึงค่าการดูดกลืนพลังงานจำเพาะที่สูงด้วย สำหรับเส้นใยที่สามารถนำมาใช้งานดังกล่าวมีหลายประเภท เช่น เส้นใยอะรามิด (เช่น เคฟลา, ทาวารอน, โนเมกซ์ ฯลฯ), เส้นใยพอลิเอทิลีน (สเปคตา หรือ ไดนีมา) หรือเส้นใยเบนซอกซาโซน (ไซลอน)

อย่างไรก็ดีการออกแบบเกราะน้ำหนักเบาเพื่อให้มีระดับของการป้องกันที่สูงขึ้น จำเป็นต้องออกแบบให้อยู่ในรูปวัสดุประกอบแต่งหรือคอมพอสิท ทั้งนี้เป็นที่ทราบกันดีว่าการใช้วัสดุสองชนิดเพื่อผลิตเป็นวัสดุคอมพอสิทแม้วัสดุเริ่มต้นทั้งคู่อาจไม่สามารถกันกระสุนได้หรือได้แต่อาจไม่ดีนัก หากทำเป็นคอมพอสิทก็จะสามารถเพิ่มระดับการป้องกันให้สูงขึ้นได้ เนื่องจากการทำเป็นวัสดุคอมพอสิทสามารถออกแบบให้วัสดุมีกลไกการสลายพลังงานที่เพิ่มขึ้นได้มาก ด้วยเหตุนี้จึงเป็นที่มาของการใช้เส้นใยแก้วซึ่งในทางปฏิบัติไม่สามารถทนการทะลุทะลวงของกระสุนได้ดีนัก แต่เมื่อนำมาประกอบเป็นคอมพอสิทโดยเลือกใช้เมตริกที่เหมาะสมก็จะสามารถทำหน้าที่เป็นเกราะที่ดีได้ เช่นที่ได้มีการเปิดเผยในสิทธิบัตร US 5,215,813 เส้นใยเคฟลาร์เป็นเส้นใยพอลิเมอร์ประเภทหนึ่งที่ประสบความสำเร็จค่อนข้างสูงเมื่อนำมาใช้งานด้านเกราะกันกระสุน เนื่องจากเป็นเส้นใยที่มีสมบัติทางกลที่สูง และมีน้ำหนักเบา

สามารถต้านการเจาะทะลุของกระสุนได้ดี เพื่อให้เกราะจากเส้นใยเคฟลาร์สามารถคงรูปได้ดีเมื่อถูกแรงขีปนะ ได้มีการรายงานในการใช้เส้นใยเคฟลาร์ร่วมกับพอลิเมอร์เมตริกหลายประเภทเพื่อใช้งานเป็นเกราะคอมพอสิทกันกระสุนเช่นในการประดิษฐ์ที่เปิดเผยในสิทธิบัตร US 3,956,447 ซึ่งได้ใช้เส้นใยเคฟลาร์ร่วมกับเมตริกอีพอกซีแบบยืดหยุ่น, สิทธิบัตร US 4,181,768 การพัฒนาเกราะกันกระสุนจากเส้นใยเคฟลาร์ในเมตริกของไนลอน, สิทธิบัตร US 4,550,044 และ สิทธิบัตร US 4,639,387 เป็นการออกแบบเกราะกันกระสุนพอลิเมอร์คอมพอสิทน้ำหนักเบาจากเส้นใยเคฟลาร์และเส้นใยแก้วกับพอลิเอสเทอร์และยูรีเทนอิลาสเตอเมอร์ตามลำดับ ทั้งนี้เรซินกลุ่มฟีโนลิกเป็นตัวอย่างระบบเรซินสำคัญระบบหนึ่งทีใช้เป็นเมตริกเสริมแรงด้วยเส้นใยเคฟลาร์ซึ่งได้มีการเปิดเผยเช่นในสิทธิบัตร US 4,639,387, สิทธิบัตร US 5,190,802 เป็นต้น เนื่องจากฟีโนลิกเป็นเรซินที่มีราคาถูก ขึ้นรูปโดยใช้เทคนิคที่ไม่ซับซ้อน อย่างไรก็ตามในปฏิกิริยาการบ่มตัวของฟีโนลิกเรซินจะต้องมีขั้นตอนการกำจัดน้ำซึ่งเป็นผลพลอยได้จากการบ่มออกไปด้วย มิฉะนั้นจะทำให้เกิดฟองอากาศในชิ้นงานและจะส่งผลกระทบต่อสมบัติทางกลของชิ้นงานได้ นอกจากนี้ฟีนอลิกเรซินบางชนิดต้องใช้สารช่วยบ่มในการเกิดปฏิกิริยาเป็นพอลิเมอร์

ปัญหาที่พบในปัจจุบันจากการออกแบบเกราะพอลิเมอร์คอมพอสิทคือ การพัฒนาเมตริกเพื่อให้มีคุณลักษณะที่เหมาะสมกับเส้นใยยังมีอยู่น้อยมาก อันอาจเนื่องมาจากข้อจำกัดด้านสมบัติของเมตริกที่ใช้ส่วนใหญ่ในปัจจุบันที่ไม่สามารถดัดแปรให้มีสมบัติที่เหมาะสมกับเส้นใยที่ใช้ได้ ทำให้เกราะกันกระสุนที่ได้อาจไม่ใช่คอมพอสิทที่มีสมรรถนะที่สูงสุดเท่าที่ควรจะเป็น ส่งผลให้เกราะคอมพอสิทกันกระสุนที่ได้มีความหนา น้ำหนัก รวมถึงต้นทุนการผลิตที่อาจสูงกว่าความเป็นจริง ในการประดิษฐ์นี้ได้พัฒนาเมตริกที่เหมาะสมสำหรับเส้นใยเคฟลาร์หรือเส้นใยที่มีสมบัติเทียบเท่าเคฟลาร์ โดยใช้เรซินชนิดใหม่ประเภทเบนซอกซาซีนเรซิน เนื่องจากมีสมบัติเด่นด้านการขึ้นรูป สมบัติทางกล และสามารถทำเป็นอัลลอยด์ร่วมกับเรซินอื่นๆ ได้หลากหลายชนิด

เบนซอกซาซีนเรซินเป็นเรซินชนิดใหม่ในตระกูลฟีโนลิก ที่ได้ถูกพัฒนาขึ้นเพื่อแก้ไขข้อบกพร่องของ ฟีโนลิกเรซินดั้งเดิม เพื่อให้มีคุณสมบัติเหมาะสมกับการใช้งานเป็นเมตริกของวัสดุประกอบแต่งสมรรถนะสูง เนื่องจากเบนซอกซาซีนเรซิน สามารถสังเคราะห์ได้ง่าย มีต้นทุนการผลิตที่ต่ำ มีโครงสร้างโมเลกุลที่สามารถดัดแปลงให้มีสมบัติตามต้องการได้หลากหลาย สมบัติเด่นหลายประการ เช่นการมีค่าความหนืดก่อนการขึ้นรูปที่ต่ำทำให้อาบเส้นใยได้ง่ายและทั่วถึง มีการหดตัวจากการขึ้นรูปใกล้ศูนย์ ทำให้ลดปัญหาการเกิดความเค้นในชิ้นงาน มีสมบัติทางกล และทางความร้อนที่สูง นอกเหนือจากการไม่เกิดผลพลอยได้จากปฏิกิริยาพอลิเมอไรเซชันทำให้ไม่เกิดปัญหามีฟองอากาศในชิ้นงาน รวมทั้งเกิดปฏิกิริยาเชื่อมโยงโดยใช้เพียงความร้อน นอกจากนี้การพัฒนาวิธีการสังเคราะห์เบนซอกซาซีนเรซินชนิดต่างๆ โดยไม่ต้องใช้ตัวทำละลายดังที่ได้มีการเปิดเผยใน US Patent 5,543,516 หรือ US Patent 6,160,079 ทำให้ได้มอนอเมอร์ที่มีความบริสุทธิ์สูง ซึ่งถือเป็นก้าวสำคัญในการนำเรซิน

ดังกล่าวมาใช้งานในเชิงการค้าเนื่องจากทำให้ลดต้นทุนการผลิตได้มาก นอกเหนือจากการลดผลกระทบต่อสภาวะแวดล้อมจากการใช้ตัวทำลาย เบนซอกซาซีนเรซินยังมีสมบัติเด่นที่สามารถทำพอลิเมอร์อัลลอยร่วมกับเรซินประเภทอื่นเพื่อเพิ่มสมบัติของเมตริกลูกผสมให้กว้างขวางและหลากหลายมากขึ้น ในการประดิษฐ์นี้ได้พัฒนาสมบัติของเบนซอกซาซีนอัลลอยเมตริกเพื่อให้มีสมบัติทางกลในช่วงที่กว้างตั้งแต่การใช้งานในรูปพลาสติกแข็งของพอลิเบนซอกซาซีนที่ไม่ได้ผ่านการดัดแปรจนเป็นเมตริกที่มีความยืดหยุ่นสูงขึ้นของพอลิเบนซอกซาซีนที่อัลลอยกับยูรีเทนอิลาสโตเมอร์ ทำให้ได้พอลิเมอร์ลูกผสมที่คงความสามารถในการขึ้นรูปและเสถียรภาพทางความร้อนของพอลิเบนซอกซาซีน ให้สมบัติทางกลที่กว้างและสามารถปรับให้เหมาะสมกับการใช้งานเฉพาะ

คำอธิบายรูปเขียนโดยย่อ

รูปที่ 1 แสดงการขึ้นรูปพรีเพรกซ์จากผืนเส้นใยทนแรงขีปนะและเมตริกชนิดเบนซอกซาซีน-ยูรีเทนพอลิเมอร์อัลลอย

รูปที่ 2 แสดงการขึ้นรูปแผ่นเกราะกันกระสุนพอลิเมอร์คอมพอสิทจากเส้นใยทนแรงขีปนะและเบนซอกซาซีน-ยูรีเทนพอลิเมอร์อัลลอย

รูปที่ 3 กราฟแสดงความสัมพันธ์ระหว่างค่ามอดูลัสของพอลิเมอร์อัลลอยระหว่างพอลิเบนซอกซาซีนกับยูรีเทนอิลาสโตเมอร์

รูปที่ 4 กราฟแสดงความสัมพันธ์ระหว่างอุณหภูมิการเปลี่ยนสถานะคล้ายแก้วของพอลิเมอร์อัลลอยระหว่างพอลิเบนซอกซาซีนกับยูรีเทนอิลาสโตเมอร์เป็นฟังก์ชันขององค์ประกอบในอัลลอย

รูปที่ 5 แสดงตัวอย่างการจัดเรียงตัวของแผ่นพอลิเมอร์คอมพอสิทในชิ้นงานเกราะที่ใช้ป้องกันกระสุนที่ระดับ IIA ตามมาตราฐาน NIJ

รูปที่ 6 แสดงตัวอย่างการจัดเรียงตัวของแผ่นพอลิเมอร์คอมพอสิทในชิ้นงานเกราะที่ใช้ป้องกันกระสุนที่ระดับ IIIA ตามมาตราฐาน NIJ

การเปิดเผยการประดิษฐ์โดยสมบูรณ์

การประดิษฐ์นี้เป็นการประดิษฐ์เกราะกันกระสุนพอลิเมอร์คอมพอสิทที่มีการเสริมแรงด้วยเส้นใยหรือผืนเส้นใยที่ทนแรงขีปนะ และมีเมตริกเป็นอัลลอยของพอลิเบนซอกซาซีนกับยูรีเทนอิลาสโตเมอร์ที่ใช้เส้นใยความแข็งแรงสูง โดยเลือกได้จากเส้นใยอะรามิด หรือ เส้นใยไซลอน หรือเส้นใยพอลิเมอร์ผลึกเหลว หรือเส้นใยผสมจากเส้นใยเหล่านี้ โดยมีเส้นใยอย่างน้อยหนึ่งชนิดที่มีค่ามอดูลัสอย่างน้อย 60 กิกะปาสคาลและมีจุดหลอมเหลวอย่างน้อย 180 องศาเซลเซียส ซึ่งเส้นใยทนแรงขีปนะดังกล่าวมีการ

เรียงตัวทิศใดทิศหนึ่งหรือหลายทิศ หรือ ใช้เส้นใยชนิดที่ผ่านการทอเป็นผืน ซึ่งเกราะกันกระสุนพอลิเมอร์ คอมพอสิทที่จำนวนชั้นรวมของผืนเส้นใยเกิดจากการซ้อนกันของแผ่นคอมพอสิทหลายแผ่นให้ผลการต้านการเจาะทะลุดีกว่าการใช้แผ่นคอมพอสิทแผ่นเดียวที่มีจำนวนชั้นรวมของ ผืนเส้นใยเท่ากัน

รูปที่ 1 แสดงการทำเกราะกันกระสุนพอลิเมอร์คอมพอสิทในการประดิษฐ์นี้ เรซินผสมที่ใช้คือเบนซอกซาซีนเรซินกับยูรีเทนอิลาสโตเมอร์ [1] ซึ่งเบนซอกซาซีนเรซิน สังเคราะห์มาจากสารตั้งต้นฟีนอล (phenol) ทำปฏิกิริยากับฟอร์มาลดีไฮด์ (formaldehyde) และเอมีนปฐมภูมิ (primary amine) อาจสังเคราะห์ในตัวทำละลายหรือด้วยเทคนิคที่ไม่ต้องใช้ตัวทำละลาย (solvent-less synthesis) โดยเบนซอกซาซีนเรซินที่ใช้ในการประดิษฐ์นี้อาจเป็นทั้งชนิดที่เป็นโมโนฟังก์ชันหรือไบฟังก์ชัน ขึ้นอยู่กับชนิดของฟีนอลที่นำมาสังเคราะห์

เบนซอกซาซีนเรซินเป็นเรซินที่สามารถสังเคราะห์ได้จากฟีนอล (phenol) ทำปฏิกิริยากับฟอร์มาลดีไฮด์ (formaldehyde) และเอมีนปฐมภูมิ (primary amine) ที่อุณหภูมิประมาณ 110 องศาเซลเซียส โดยเบนซอกซาซีนเรซินที่ใช้ในงานประดิษฐ์นี้อาจเป็นทั้งชนิดที่เป็นมอนอฟังก์ชันหรืออาจเป็นชนิดไบฟังก์ชัน เช่นเบนซอกซาซีนเรซินที่เกิดจากอะลิฟาติกเอมีน หรือเบนซอกซาซีนเรซินที่เกิดจากอะโรมาติกส์เอมีน หรือเบนซอกซาซีนเรซินที่สังเคราะห์จากไดฟีนอลโครงสร้างต่างๆ เช่น บิสฟีนอลเอ หรือบิสฟีนอลเอฟ

ในส่วนของยูรีเทนอิลาสโตเมอร์สามารถสังเคราะห์ได้จากไอโซไซยาเนตทำปฏิกิริยากับไดออลทั้งประเภทอีเทอร์หรือเอสเทอร์ที่มีน้ำหนักโมเลกุลต่างๆ ตั้งแต่ 1000-5000 โดยมวลโมเลกุลที่เหมาะสมที่สุดอยู่ที่ระดับ 2000 ถึง3000 ซึ่งไอโซไซยาเนตที่ใช้มีได้หลายชนิด เช่น ไอโซโฟโรนไดไอโซไซยาเนต (IPDI), เมททิลีนไดไอโซไซยาเนต (MDI), ทูโลอีนไดไอโซไซยาเนต (TDI) และไดออลหรือพอลิออลกลุ่มเอสเทอร์หรืออีเทอร์ เช่นพอลิพรอพิลีนไกลคอล โดยจะทำการผสมเรซินทั้ง 2 ชนิดที่อัตราส่วนของเบนซอกซาซีนเรซิน 50-95 เปอร์เซนต์โดยน้ำหนักต่อยูรีเทนเรซิน 5-50 เปอร์เซ็นต์โดยน้ำหนัก ซึ่งอัตราส่วนที่ดีที่สุดของเบนซอกซาซีนเรซิน 80 เปอร์เซนต์โดยน้ำหนักต่อยูรีเทนเรซิน 20 เปอร์เซ็นต์โดยน้ำหนักและจะทำการผสมเข้าด้วยกันที่อุณหภูมิประมาณ 60-150 องศาเซลเซียส ทำการกวนผสมให้เป็นเนื้อเดียวกัน หลังจากนั้นนำเรซินผสมระหว่างเบนซอกซาซีนเรซินและยูรีเทนเรซิน [1] มาอาบบนเส้นใยทนแรงขีปนะ เช่น เคฟลาร์ 29 [2] หรืออาจจะใช้เส้นใยความแข็งแรงสูงอื่นๆ เช่น เส้นใยเคฟลาร์ 49, เคฟลาร์ 119, เคฟลาร์ 129, เคฟลาร์ 149, เส้นใย โนเมกซ์ หรือเส้นใยอะรามิดลูกผสมต่างๆ, เส้นใยไซลอน, หรือเส้นใยทนแรงขีปนะอื่นๆ ที่มีขั้วในระดับเดียวกับเส้นใยเคฟลาร์ รวมทั้งการนำเส้นใยเหล่านี้มาผสมรวมกัน (mixed fibers) การทาเรซินลงบนผืนเส้นใยจะทาจนทั่วผืนเส้นใยทีละชั้น จนได้จำนวนชั้นตามที่ต้องการในรูปพรีเพรกซ์ที่พร้อมจะนำไปขึ้นรูปเป็นชิ้นงานเกราะ [3]

ยูรีเทนอิลาสโตเมอร์สังเคราะห์ได้จากไอโซไซยาเนตทำปฏิกิริยากับไดออลหรือพอลิออลทั้งชนิดเอสเทอร์หรืออีเทอร์ โดยไอโซโซไซยาเนตที่ใช้อาจเป็นชนิดไอโซฟอโรนไดไอโซไซยาเนต (IPDI) ซึ่งให้ยูรีเทนมอนอเมอร์ที่มีโครงสร้างดังรูป (I)

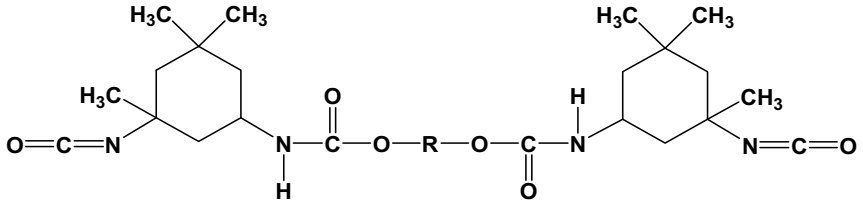

(I)

หรือไอโซไซยาเนตชนิด (MDI) ซึ่งให้ยูรีเทนมอนอเมอร์ที่มีโครงสร้างดังรูป (II)

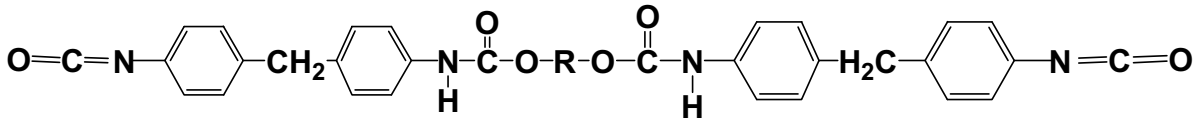

(II)

หรือไอโซโซไซยาเนตชนิด (TDI) ซึ่งให้ยูรีเทนมอนอเมอร์ที่มีโครงสร้างดังรูป (III)

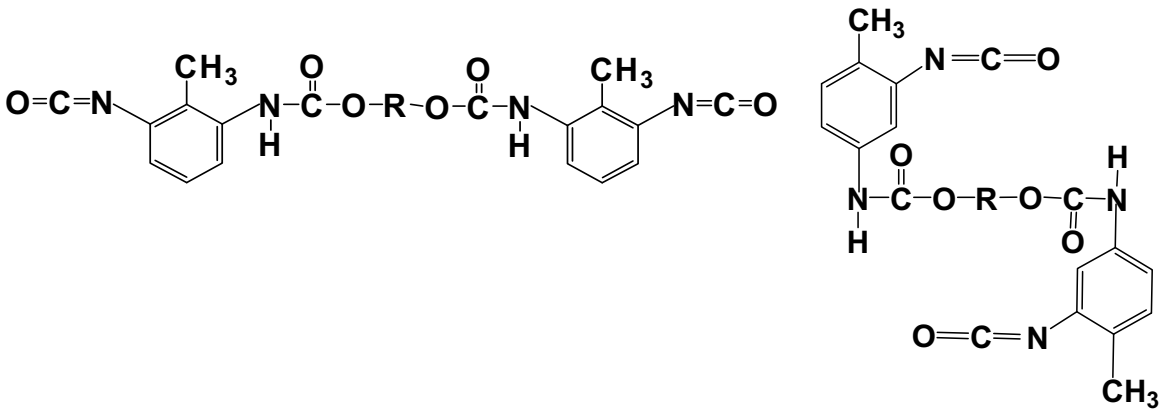

(III)

หรือไอโซไซยาเนตชนิดอื่นๆ ที่สามารถใช้สังเคราะห์ยูเรเทนอิลาสโตเมอร์ได้

รูปที่ 2 แสดงการขึ้นรูปเกราะกันกระสุนพอลิเมอร์คอมพอสิท ซึ่งหลังจากได้พรีเพรกซ์ ตามวิธีทำดังรูปที่ 1 แล้ว นำพรีเพร็กซ์มาทำการขึ้นรูปเป็นคอมพอสิทโดยใช้เครื่องอัดความร้อน โดยใช้อุณหภูมิที่ 160 องศาเซลเซียส และ ใช้ความดันประมาณ 0.1 เมกกะปลาสคาล (MPa) เป็นเวลาอย่างน้อย 1 ชั่วโมง จากนั้นจึงนำมาให้ความร้อนขั้นสุดท้าย (post cure) ในเตาอบที่อุณหภูมิไม่ต่ำกว่า 180 องศาเซสเซียส เป็นเวลาอย่างน้อย 1 ชั่วโมง หรือจนได้ชิ้นงานที่บ่มตัวอย่างสมบูรณ์ จะได้เกราะพอลิเมอร์คอมพอสิทที่มีปริมาณเส้นใยในคอมพอสิทประมาณ 70-85 เปอร์เซ็นต์โดยน้ำหนัก

รูปที่ 3 แสดงให้เห็นว่าการใช้เบนซอกซาซีนเพื่อทำอัลลอยร่วมกับยูรีเทนเรซิน จะให้สมบัติทางกลแบบไดนามิกส์ (dynamic mechanical properties) ของเมตริกลูกผสมมีสมบัติที่กว้างขวางและหลากหลายมากขึ้น โดยจะเห็นว่าเมตริกลูกผสมจะมีสมบัติทางกลในช่วงที่กว้างตั้งแต่การใช้งานในรูปพลาสติกแข็งของพอลิเบนซอกซาซีน จนเป็นเมตริกที่มีความยืดหยุ่นสูงขึ้นมากในเมตริกลูกผสม

รูปที่ 4 แสดงความสัมพันธ์ระหว่างอุณหภูมิการเปลี่ยนสถานะคล้ายแก้วของพอลิเมอร์อัลลอยระหว่างพอลิเบนซอกซาซีนกับยูรีเทนอิลาสโตเมอร์เป็นฟังก์ชันกับปริมาณยูรีเทนที่เปลี่ยนไปในเมตริกอัลลอย ซึ่งจะเห็นว่าเมื่อปริมาณยูรีเทนในพอลิเมอร์อัลลอยเพิ่มขึ้นอุณหภูมิการเปลี่ยนสถานะคล้ายแก้วของพอลิเมอร์อัลลอยจะเพิ่มขึ้นตามไปด้วย ดังนั้นพอลิเมอร์อัลลอยระหว่างพอลิเบนซอกซาซีนกับยูรีเทนอิลาสโตเมอร์จะทำให้ได้พอลิเมอร์ลูกผสมที่นอกจากจะมีสมบัติทางกลที่กว้างขึ้นแล้ว อัลลอยที่ได้ยังมีเสถียรภาพทางความร้อนที่สูงขึ้นด้วยและแสดงถึงจุดเด่นสำคัญอีกอย่างหนึ่งของพอลิเมอร์อัลลอยระหว่างพอลิเบนซอกซาซีนกับยูรีเทนอิลาสโตเมอร์คือจะให้ค่าอุณหภูมิเปลี่ยนสถานะคล้ายแก้วที่สูงกว่าเรซินเริ่มต้นทั้งคู่ซึ่งเป็นลักษณะของการเกิดงานร่วม (synergy) ของเสถียรภาพทางความร้อนของพอลิเมอร์อัลลอยที่ได้

รูปที่ 5 แสดงตัวอย่างการจัดเรียงตัวของแผ่นพอลิเมอร์คอมพอสิทจากเบนซอกซาซีนอัลลอยและผ้าทอจากเส้นใยเคฟลาร์ ในชิ้นงานเกราะกันกระสุนที่มีประสิทธิภาพที่ดีที่สุด เพื่อป้องกันปืนพกขนาด 9 มม. ที่มีลูกกระสุนเป็นหัวทองแดง โดยมีน้ำหนักของหัวกระสุนอยู่ที่ 124 เกรน และมีความเร็วในการตกกระทบ 340 เมตรต่อวินาที ซึ่งสอดคล้องกับมาตราฐาน NIJ ในระดับ IIA โดยจัดเรียงแผ่นพอลิเมอร์คอมพอสิท ที่มีความหนาอย่างน้อย 20 ชั้น [4] ซึ่งมีความหนาแน่นเชิงพื้นที่ไม่เกิน 0.50 กรัมต่อตารางเซนติเมตร ไว้ด้านหน้า และวางซ้อนทับด้วยแผ่นคอมพอสิทหนา 10 ชั้น [6] ซึ่งมีความหนาแน่นเชิงพื้นที่ไม่เกิน 0.25 กรัมต่อตารางเซนติเมตร โดยมีการจัดเรียงตัวของแผ่นคอมพอสิทที่มีความหนา 20 ชั้นไว้ด้านหน้าและ วางซ้อนทับด้วยแผ่น 10 ชั้นอย่างน้อยหนึ่งแผ่นไว้ด้านหลัง โดยระหว่างคอมพอสิทแผ่นหน้าและแผ่นหลัง [5] อาจเป็นเพียงการซ้อนทับโดยไม่ต้องมีตัวประสานหรือโดยมีการยึดติดกันด้วยตัวประสานหรือเรซินที่มีสมบัติเป็นอิลาสโตเมอร์ คือ ยูรีเทนเรซิน, ซิลิโคนเรซิน, ยางธรรมชาติ หรือ

อีพอกซี เรซินชนิดยืดหยุ่น เป็นต้น ตัวอย่างการจัดเรียงตัวแบบอื่นที่มีประสิทธิภาพรองลงมาอาจใช้แผ่นพอลิเมอร์คอมพอสิทข้างต้น ที่ความหนาอย่างน้อย 30 ชั้นเพียงแผ่นเดียว การวางทั้งสองแบบให้ค่าความหนาแน่นเชิงพื้นที่ไม่เกิน 0.80 กรัมต่อตารางเซนติเมตร อย่างไรก็ตามพบว่าการเรียงแบบแรกให้ผลการต้านแรงขีปนะที่สูงกว่า

รูปที่ 6 แสดงตัวอย่างการจัดเรียงตัวของแผ่นพอลิเมอร์คอมพอสิท เพื่อป้องกันกระสุนขนาด 9 มม. ความเร็วสูงที่ใช้กับปืนกลมือ ที่มีลูกกระสุนเป็นหัวทองแดง โดยมีน้ำหนักของหัวกระสุนอยู่ที่ 124 เกรน และมีความเร็วในการตกกระทบ 430 เมตรต่อวินาที ซึ่งสอดคล้องกับมาตราฐาน NIJ ในระดับ IIIA โดยการจัดเรียงของแผ่นพอลิเมอร์คอมพอสิทนี้ต้องวางแผ่นหน้า [7] ที่มีความหนาอย่างน้อย 30 ชั้นของผืนเส้นใย เพื่อให้ผลการต้านการเจาะทะลุและการรับแรงขีปนะที่สูง ส่วนแผ่นหลัง [8] สามารถนำแผ่นพอลิเมอร์คอมพอสิทที่มีความหนา 10 ชั้นมาซ้อนด้านหลังอย่างน้อย 2 แผ่น หรือ นำแผ่นพอลิเมอร์คอมพอสิทที่มีความหนา 20 ชั้นมาวางซ้อนอีกหนึ่งแผ่น ทั้งนี้เพื่อให้ได้จำนวนชั้นรวมของผืนเส้นใยที่หนาอย่างน้อย 50 ชั้นหรือมีความหนาแน่นเชิงพื้นที่ไม่เกิน 1.10 กรัมต่อตารางเซนติเมตร

เกราะกันกระสุนพอลิเมอร์คอมพอสิท ซึ่งมีการจัดเรียงแผ่นเกราะกันกระสุนพอลิเมอร์คอมพอสิทระหว่างแผ่นคอมพอสิตต่างๆอาจซ้อนกันโดยไม่มีสารยึดหรือยึดติดกันด้วยสารหรือเรซินที่มีสมบัติเป็นอิลาสโตเมอร์ คือ ยูรีเทนเรซิน, ซิลิโคนเรซิน หรือ, อีพอกซีเรซินชนิดยืดหยุ่น

วิธีในการประดิษฐ์ที่ดีที่สุด

เหมือนกับที่ได้กล่าวไว้แล้วในหัวข้อการเปิดเผยการประดิษฐ์โดยสมบูรณ์

ข้อถือสิทธิ

1. เกราะกันกระสุนพอลิเมอร์คอมพอสิท ที่ซึ่งมีการเสริมแรงด้วยเส้นใยที่ทนแรง ขีปนะ (Ballistic Impact) และมีเมตริกเป็นอัลลอยของพอลิเบนซอกซาซีนกับยูรีเทนอิลาสโตเมอร์

2. เกราะกันกระสุนพอลิเมอร์คอมพอสิท ตามข้อถือสิทธิ 1 ที่ซึ่งใช้เส้นใยความแข็งแรงสูงอย่างน้อยหนึ่งชนิดที่เลือกได้จากเส้นใยอะรามิด, เส้นใยไซลอน, เส้นใยพอลิเมอร์ผลึกเหลว หรือเส้นใยผสมจากเส้นใยข้างต้น โดยมีเส้นใยอย่างน้อยหนึ่งชนิดที่มีค่ามอดูลัสอย่างน้อย 60 กิกะปาสคาล และมีจุดหลอมเหลวอย่างน้อย 180 องศาเซลเซียส

3. เกราะกันกระสุนพอลิเมอร์คอมพอสิท ตามข้อถือสิทธิ 1 ที่ซึ่งใช้เส้นใยทนแรงขีปนะมีการเรียงตัวทิศใดทิศหนึ่งหรือหลายทิศทาง หรือ ใช้เส้นใยชนิดที่ผ่านการทอเป็นผืน

4. เกราะกันกระสุนพอลิเมอร์คอมพอสิท ตามข้อถือสิทธิ 1 ที่ซึ่งมีปริมาณเส้นใยในคอมพอสิท 70-85 เปอร์เซ็นต์โดยน้ำหนัก

5. เกราะกันกระสุนพอลิเมอร์คอมพอสิท ตามข้อถือสิทธิ 1 ที่ซึ่งใช้เมตริกเป็นอัลลอยของพอลิเบนซอกซาซีนกับยูรีเทนอิลาสโตเมอร์โดยมีอัตราส่วนของเบนซอกซาซีนเรซิน 50-95 เปอร์เซนต์โดยน้ำหนักต่อยูรีเทนเรซิน 5-50 เปอร์เซ็นต์โดยน้ำหนัก

6. เกราะกันกระสุนพอลิเมอร์คอมพอสิท ตามข้อถือสิทธิ 5 ที่ซึ่งอัตราส่วนที่ดีที่สุดของเบนซอกซาซีนเรซิน 80 เปอร์เซนต์โดยน้ำหนักต่อยูรีเทนเรซิน 20 เปอร์เซ็นต์โดยน้ำหนัก

7. เกราะกันกระสุนพอลิเมอร์คอมพอสิท ตามข้อถือสิทธิ 1 ที่ซึ่งยูรีเทนอิลาสโตเมอร์สังเคราะห์จากไอโซไซยาเนตทำปฏิกิริยากับไดออล ทั้งประเภทอีเทอร์หรือเอสเทอร์

8. เกราะกันกระสุนพอลิเมอร์คอมพอสิท ตามข้อถือสิทธิ 7 ที่ซึ่งไอโซไซยาเนตอย่างน้อยหนึ่งชนิดที่เลือกได้จากไอโซโฟโรนไดไอโซไซยาเนต (IPDI), เมททิลีนไดไอโซไซยาเนต (MDI), ทูโลอีนไดไอโซไซยาเนต (TDI)

9. เกราะกันกระสุนพอลิเมอร์คอมพอสิท ตามข้อถือสิทธิ 7 ที่ซึ่งมวลโมเลกุลของไดออล ทั้งประเภทอีเทอร์หรือเอสเทอร์ มีค่าอยู่ระหว่าง 1000 ถึง 5000

10. เกราะกันกระสุนพอลิเมอร์คอมพอสิท ตามข้อถือสิทธิ 9 ที่ซึ่งมวลโมเลกุลของไดออล ทั้งประเภทอีเทอร์หรือเอสเทอร์ที่มีค่าเหมาะสมที่สุดเท่ากับ 2000

11. เกราะกันกระสุนพอลิเมอร์คอมพอสิท ตามข้อถือสิทธิ 1 ที่มีความหนา 10 ชั้นหรือมีความหนาแน่นต่อพื้นที่ไม่เกิน 0.25 กรัมต่อตารางเซนติเมตร , ที่มีความหนา 20 ชั้นหรือมีความหนาแน่น

ต่อพื้นที่ไม่เกิน 0.50 กรัมต่อตารางเซนติเมตร, ที่มีความหนา 30 ชั้นหรือมีความหนาแน่นต่อพื้นที่ไม่เกิน 0.80 กรัมต่อตารางเซนติเมตร และที่มีความหนา 50 ชั้นหรือมีความหนาแน่นต่อพื้นที่ไม่เกิน 1.10 กรัมต่อตารางเซนติเมตร

12. เกราะกันกระสุนพอลิเมอร์คอมพอสิท ตามข้อถือสิทธิ 1 ที่ใช้ป้องกันการเจาะทะลุของกระสุนในระดับ IIIA ตามมาตรฐาน NIJ โดยมีจำนวนชั้นรวมของผืนเส้นใยอย่างน้อย 50 ชั้น และมีความหนาแน่นต่อพื้นที่ไม่เกิน 1.10 กรัมต่อตารางเซนติเมตร โดยมีแผ่นด้านหน้าที่รับกระสุนมีความหนาอย่างน้อย 30 ชั้นของผืนเส้นใย

13. เกราะกันกระสุนพอลิเมอร์คอมพอสิท ตามข้อถือสิทธิ 1 ที่ใช้ป้องกันการเจาะทะลุของกระสุนในระดับ IIA ตามมาตรฐาน NIJ โดยมีจำนวนชั้นรวมของผืนเส้นใยอย่างน้อย 30 ชั้น โดยมีการจัดเรียงตัวของแผ่นคอมพอสิทที่มีความหนา 20 ชั้นไว้ด้านหน้าและ วางซ้อนทับด้วยแผ่น 10 ชั้นอย่างน้อยหนึ่งแผ่นไว้ด้านหลัง

14. เกราะกันกระสุนพอลิเมอร์คอมพอสิท ตามข้อถือสิทธิ 1 ที่ซึ่งมีการจัดเรียงแผ่นเกราะกันกระสุนพอลิเมอร์คอมพอสิทระหว่างแผ่นคอมพอสิตที่ซ้อนกัน โดยมีการยึดติดกันด้วยตัวประสานหรือเรซินที่มีสมบัติเป็นอิลาสโตเมอร์ คือ ยูรีเทนเรซิน, ซิลิโคนเรซิน, ยางธรรมชาติ หรือ อีพอกซีเรซินชนิดยืดหยุ่น

บทสรุปการประดิษฐ์

เกราะกันกระสุนพอลิเมอร์คอมพอสิทที่มีการเสริมแรงด้วยเส้นใยหรือผืนเส้นใยที่ทนแรงขีปนะ และมีเมตริกเป็นอัลลอยของพอลิเบนซอกซาซีนกับยูรีเทนอิลาสโตเมอร์ที่ใช้เส้นใยความแข็งแรงสูง ซึ่งเส้นใยทนแรงขีปนะดังกล่าวมีการเรียงตัวทิศใดทิศหนึ่งหรือหลายทิศ หรือใช้เส้นใยชนิดที่ผ่านการทอเป็นผืน เกราะกันกระสุนพอลิเมอร์คอมพอสิทดังกล่าวได้ถูกพัฒนาให้มีน้ำหนักเบา และมีสมรรถนะสูง